

η -Photoproduction in a gauge invariant
chiral unitary framework

Dino Ruić

η -Photoproduction in a gauge invariant chiral unitary framework

von

Dino Ruić

Diplomarbeit in Physik

angefertigt im

Helmholtz-Institut für Strahlen- und Kernphysik

vorgelegt der

Mathematisch-Naturwissenschaftlichen Fakultät

der

Rheinischen Friedrich-Wilhelms-Universität

zu Bonn

im Juni 2011

Ich versichere, dass ich diese Arbeit selbständig verfasst und keine anderen als die angegebenen Quellen und Hilfsmittel benutzt sowie Zitate kenntlich gemacht habe.

Dino Ruić

Referent: Prof. Dr. U.-G. Meißner

Koreferent: PD Dr. Akaki Rusetsky

Contents

1	Introduction	9
1.1	The S -matrix and unitarity	9
1.2	Resonances and the Bethe-Salpeter equation	11
1.3	Gauge invariance	15
1.4	Chiral perturbation theory	17
1.5	Baryon chiral perturbation theory	23
2	Meson-baryon-scattering	27
2.1	Solution of the Bethe-Salpeter equation	27
2.2	Partial Wave Analysis	30
2.3	Conclusion	38
3	η-Photoproduction off the proton	39
3.1	Construction of the amplitude	39
3.2	Results	45
3.3	Conclusion	49
4	Extension of the amplitude	51
4.1	Construction of the amplitude	51
4.2	Results	55
4.3	Conclusion	62
5	Summary and Outlook	65
A	The solution of the BSE	69
B	Loop integrals	73
B.1	Integrals for the leading order amplitude	73
B.2	Integrals for the extended amplitude	80
C	Gauge invariance of \mathcal{M}^μ	87

D	Decompositions of the amplitudes	89
D.1	Decompositions for the leading order calculation	89
D.2	Decomposition of the extended amplitude	94
E	Calculation of the differential cross section	117
F	Differential cross section plots	123
F.1	Leading order approach	123
F.2	Extended amplitude	126
	Bibliography	126

Preface

After the invention of the first bubble chambers and spark chambers in the 1950's, particle physicists discovered a rich spectrum of hadrons, which could not be explained by the physics of that time. In the following time, a classification by charge, isospin and later by strangeness occurred. Then, in 1963, Gell-Mann and Zweig noticed a pattern in this spectrum which led them to the conclusion that the hadrons consist of smaller particles that come in different flavors, which were later called quarks. However, another degree of freedom was necessary due to the Δ^{++} baryon, which consists of three up quarks with parallel spins. The existence of such a particle would violate the antisymmetry of fermion wave functions, if there were not another quantum number to restore the symmetry properties. This problem was solved in 1965 by the introduction of the color charge, which could be implemented via the $SU(3)$ color gauge group to obtain the Lagrangian of quantum chromodynamics. In the following years experiments were conducted to test properties like asymptotic freedom, confinement, the running coupling constant, and to find evidence for the gluons, which are the gauge bosons of the $SU(3)$ gauge group.

As evidence for the validation of quantum chromodynamics grew, it also became clear that any calculations in the low-energy regime with the usual perturbative expansion are futile due to the large coupling constant at low energies. Though, when Weinberg introduced his approach to effective field theories [1], it followed that by treating the Goldstone bosons as degrees of freedom and by introducing an appropriate power counting scheme, a perturbative low-energy expansion of quantum chromodynamics would yield meaningful results.

However, the rich hadron spectrum is still not understood well. If those hadron resonances, as they appear in the cross sections, are not included explicitly in the Lagrangian, a perturbative expansion can not describe that cross section adequately in the vicinity of the resonance.

But new possibilities open when using unitarized amplitudes. The concept of unitarization is to resum Feynman diagrams in a geometric series, in which case the amplitude will always be exactly unitary. Among the uni-

tarized models some methods have become popular, as e.g. the K -matrix approach, which was first introduced by Wigner [2], and Wigner and Eisenbud [3], and the inverse amplitude method, as e.g. in [4]. Both are so-called on-shell approaches, where the off-shell contribution of loops is neglected. More recently, Borasoy, Bruns, Meißner and Nißler used a model that also incorporates off-shell contributions by means of solving the Bethe-Salpeter equation. The off-shell contributions were discovered to be non-negligible and thus such a full off-shell approach, although more involved, should in principle be superior to the on-shell approaches.

This diploma thesis is based on the model developed by Borasoy, Bruns, Meißner and Nißler which was already used to calculate the kaon-electroproduction amplitude [5]. In the following that model will be used to calculate the pion-nucleon scattering and the η -photoproduction off protons, whereas the last chapter deals with an extension for that model.

Chapter 1

Introduction

This chapter shall introduce the formalism of this thesis, as well as some basic knowledge about quantum field theory which is necessary to understand the following chapters.

The introduction will be dealing with the S -Matrix, followed by the concept of unitarity and hence the Bethe-Salpeter equation. Afterwards, there is a section about gauge invariance and sections about chiral perturbation theory and baryon chiral perturbation theory.

1.1 The S -matrix and unitarity

In 1943 W. Heisenberg set the foundations for S -matrix theory [6, 7] and until the 1960's it was believed that S -matrix theory could be an alternative for the conventional quantum field theory. However, S -matrix theory has its limitations, i.e. nowadays the S -matrix and its properties are used alongside quantum field theory as a theoretical tool rather than standing on its own.

The S -matrix describes the probability amplitude of a transition between abstract 'in' and 'out' states at times $t_{in} \rightarrow -\infty$ and $t_{out} \rightarrow \infty$, respectively (see e.g. section 3.1 in [8]):

$$S_{\beta\alpha} = \langle \beta; \text{out} | \alpha; \text{in} \rangle, \quad (1.1)$$

where β and α represent any quantum numbers necessary to describe the multiparticle states (e.g.: momenta, masses, spins, etc.). Such states are, in good approximation, prepared by experimentalists, since the usual interaction time is significantly smaller than the time of flight from the reaction-vertex to the detector. And since those states are the only observables, they form the basis of S -matrix theory.

The S -matrix has some important properties that can be derived using the principles of quantum mechanics: It is known that the superposition prin-

principle and energy-momentum conservation for particles are valid and hence they are employed in S -matrix theory. Lorentz invariance is necessary, for when changing the frame of reference the elements of the S -matrix should remain the same. The cluster decomposition law ensures that two sets of particles at a sufficiently large distance to each other do not influence their respective scattering processes. Crossing symmetry implements the symmetry between particles and their corresponding anti-particles. Maximal analyticity guarantees that the S -matrix has no other singularities than required by unitarity and crossing (for an introduction to S -Matrix theory, see e.g. [9]).

Lastly, the key property for this work is the unitarity of the S -Matrix. The unitarity condition for the S -Matrix of eq. (1.1) can be evaluated using (see e.g. section 3.2 of [8]):

$$\int d\gamma S_{\gamma\beta}^* S_{\gamma\alpha} = \int d\gamma \langle \beta; \text{in} | \gamma; \text{out} \rangle \langle \gamma; \text{out} | \alpha; \text{in} \rangle = \langle \beta; \text{in} | \alpha; \text{in} \rangle,$$

where the integration is over intermediate particle states and completeness of the states was used. Because of the orthogonality relation

$$\langle \beta; \text{in} | \alpha; \text{in} \rangle = \langle \beta; \text{out} | \alpha; \text{out} \rangle = \langle \beta | \alpha \rangle = \delta_{\beta\alpha},$$

where $|\beta\rangle$ and $|\alpha\rangle$ are ordinary free states of the underlying theory, the unitarity condition simplifies to

$$\int d\gamma S_{\gamma\beta}^* S_{\gamma\alpha} = \delta_{\beta\alpha}. \quad (1.2)$$

In other words, unitarity ensures the proper normalization of the in and out states of the S -Matrix, which can be interpreted as a conservation of probability: If an initial state is normalized to '1', a unitary S -Matrix leads to final states whose sum is also normalized to '1'.

In order to bring the unitarity condition in a more practical form, the \mathcal{S} -operator will be introduced, which links the in and out states to free states $|\alpha\rangle$ and $|\beta\rangle$ of the underlying theory,

$$S_{\beta\alpha} = \langle \beta; \text{out} | \alpha; \text{in} \rangle = \langle \beta | \mathcal{S} | \alpha \rangle.$$

Then, the unitarity condition of eq. (1.2) can be rewritten as

$$\delta_{\beta\alpha} = \int d\gamma \langle \beta | \mathcal{S}^\dagger | \gamma \rangle \langle \gamma | \mathcal{S} | \alpha \rangle = \langle \beta | \mathcal{S}^\dagger \mathcal{S} | \alpha \rangle,$$

or equivalently

$$\mathcal{S}^\dagger \mathcal{S} = 1. \quad (1.3)$$

A convenient choice to express the \mathcal{S} -operator is to split it into two parts:

$$\mathcal{S} = 1 + iT. \quad (1.4)$$

The '1' represents processes where the particles do not interact, which in terms of Feynman diagrams would be represented as disconnected lines, and the reaction matrix \mathcal{T} describes all possible interactions. Inserting eq. (1.4) into eq. (1.3) leads to the common unitarity condition for the reaction matrix:

$$-i(\mathcal{T} - \mathcal{T}^\dagger) = \mathcal{T}^\dagger \mathcal{T}. \quad (1.5)$$

This can be transferred to a physical basis by multiplying states from left and right and by inserting a basis in between \mathcal{T}^\dagger and \mathcal{T} on the right hand side:

$$-i \left[\langle \beta | \mathcal{T} | \alpha \rangle - \langle \alpha | \mathcal{T} | \beta \rangle^* \right] = \int d\gamma \langle \gamma | \mathcal{T} | \beta \rangle^* \langle \gamma | \mathcal{T} | \alpha \rangle. \quad (1.6)$$

1.2 Resonances and the Bethe-Salpeter equation

Consider a scattering process as illustrated in fig. 1.1, where an intermediate bound state (or resonance) forms out of the particles of the underlying theory.

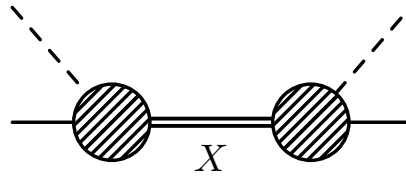


Figure 1.1: A scattering process of two particles (dashed and solid lines), forming an intermediate state (double solid line) that is called X . The shaded areas represent arbitrary interactions.

Such resonances should somehow be accounted for by the theoretical approach as their appearance in cross sections from experiments is often dominant. One ansatz is to explicitly introduce these resonances as new particles in a model. The particle X in fig. 1.1 would then be represented by a propagator with bare mass M_X . However, in this work another ansatz will be considered, in which it is possible to generate resonances dynamically by means of a resummation of Feynman diagrams, and which allows a deeper insight into the nature of the resonances. The necessity of a resummation method is due to the fact that the resonance is *not* explicitly included in the model. Thus, in a model where the resonance is generated dynamically, the squared mass M_X^2 appearing in the propagator has to be a function $f(m, \mu, g)$ of the model parameters, i.e. masses m , renormalization constants μ and couplings g . Note, that the function $f(m, \mu, g)$, and hence the pole position of the resonance X , is only μ -dependent due to the particular ansatz of a non-perturbative model like a resummation. Then, an expansion of the propagator as a power series in the squared center-of-mass energy s in the

vicinity of the closest threshold $s_{thr} < M_X^2$ leads to

$$\frac{1}{s - M_X^2} = \frac{1}{s - f(m, \mu, g)} = \frac{1}{s_{thr} - f(m, \mu, g)} - \frac{s - s_{thr}}{(s_{thr} - f(m, \mu, g))^2} + \frac{(s - s_{thr})^2}{(s_{thr} - f(m, \mu, g))^3} + O\left((s - s_{thr})^3\right),$$

where $s > s_{thr}$. The terms on the r.h.s. are equivalent to a series of local couplings in the Lagrangian, i.e. including the resonance explicitly as a particle in the Lagrangian and then integrating the resonance out by means of the path integral method will introduce these local couplings. If s approaches M_X^2 , higher order terms of the series become increasingly important and thus a perturbative low-energy expansion becomes useless, as it is only possible to sum a limited number of Feynman diagrams. However, with an adequate resummation method such a power series can be generated without the necessity for explicit inclusions of resonances.

In general, there are infinitely many ways how to resum Feynman diagrams, but as a resummation does not follow the pertinent rules of perturbation theory, the properties of perturbation theory are different from what resummation methods yield. An arbitrary resummation will in general not fulfill any requirements of S -matrix theory. Therefore a prescription has to be used that ensures certain properties. However, currently there is no resummation prescription that ensures all requirements of S -matrix theory.

The most common resummation method is to use the solution of the Bethe-Salpeter equation (BSE), which is a relativistic two-particle equation [10]. In operator form, the BSE is given by

$$\mathcal{T} = \mathcal{V} + \mathcal{V} \mathcal{G} \mathcal{T},$$

where \mathcal{T} is the reaction operator, \mathcal{V} represents a real two-particle irreducible potential and \mathcal{G} is a two-particle propagator in operator form. Multiplying by an initial state $|\alpha\rangle$ from the right and by a final state $\langle\beta|$ from the left, and inserting a basis $\int d\gamma|\gamma\rangle\langle\gamma|$ between \mathcal{V} and \mathcal{G} and a basis $\int d\sigma|\sigma\rangle\langle\sigma|$ between \mathcal{G} and \mathcal{T} leads to

$$T_{\beta\alpha} = V_{\beta\alpha} + \int \int d\gamma d\sigma V_{\beta\gamma} G_{\gamma\sigma} T_{\sigma\alpha}, \quad (1.7)$$

where the shorthand notation $O_{\beta\alpha} = \langle\beta|\mathcal{O}|\alpha\rangle$ for an arbitrary operator \mathcal{O} was used. Here, each state consists of two particles described by a set of quantum numbers, however, different states may contain different particles if the potential $V_{\beta\alpha}$ allows for those transitions. In the following, a two-particle state consisting of two specified particles is referred to as a channel. Note, that e.g. $O_{\beta\alpha}$ are the components of a matrix O in channel space.

Furthermore, the integral indicates integration over loop momenta of the intermediate states, but a summation over equal indices is also implied in order to include all possible intermediate channels.

Since $G_{\gamma\sigma}$ is an ordinary two-particle propagator, it can not change the particle states, or in other words: it contains a delta function $\delta(\gamma - \sigma)$. Therefore eq. (1.7) can be reduced to

$$\begin{aligned} T_{\beta\alpha} &= V_{\beta\alpha} + \int d\gamma V_{\beta\gamma} G_{\gamma\gamma} T_{\gamma\alpha} \\ &= V_{\beta\alpha} + \int d\gamma T_{\beta\gamma} G_{\gamma\gamma} V_{\gamma\alpha}, \end{aligned} \quad (1.8)$$

where in the second step a symmetry relation for the BSE was used, which can be proven by explicitly considering a kernel and the two-particle propagator. Then, if the integral is iterated, one can easily see that the symmetry relation is fulfilled.

The great advantage of the BSE is that any solution T leads to a unitary S -matrix. To see this, the BSE can be inserted into the unitarity condition of eq. (1.6), but as $T_{\beta\alpha}$ and $G_{\gamma\gamma}$ are potentially elements of the Clifford algebra, the adjoint shall be denoted by $\bar{O}_{\beta\alpha} = \gamma_0 O_{\beta\alpha}^\dagger \gamma_0$, where the $O_{\beta\alpha}^\dagger$ also implies transposition in channel space. Furthermore, using $\bar{V}_{\alpha\beta} = V_{\beta\alpha}$, which is a necessary condition for the BSE to yield unitary solutions [10], leads to

$$\begin{aligned} T_{\beta\alpha} - \bar{T}_{\alpha\beta} &= V_{\beta\alpha} + \int d\gamma V_{\beta\gamma} G_{\gamma\gamma} T_{\gamma\alpha} - \bar{T}_{\alpha\beta} \\ &= \bar{V}_{\alpha\beta} + \int d\gamma \bar{V}_{\gamma\beta} G_{\gamma\gamma} T_{\gamma\alpha} - \bar{T}_{\alpha\beta} + \int d\gamma \bar{T}_{\gamma\beta} G_{\gamma\gamma} T_{\gamma\alpha} \\ &\quad - \int d\gamma \bar{T}_{\gamma\beta} G_{\gamma\gamma} T_{\gamma\alpha} \\ &= -(\bar{T}_{\alpha\beta} - \bar{V}_{\alpha\beta}) + \int d\gamma \bar{T}_{\gamma\beta} G_{\gamma\gamma} T_{\gamma\alpha} - \int d\gamma (\bar{T}_{\gamma\beta} - \bar{V}_{\gamma\beta}) G_{\gamma\gamma} T_{\gamma\alpha} \\ &= - \int d\sigma \underbrace{\bar{V}_{\alpha\sigma} \bar{G}_{\sigma\sigma} \bar{T}_{\sigma\beta}}_{\bar{T}_{\sigma\beta} \bar{G}_{\sigma\sigma} V_{\sigma\alpha}} + \int d\gamma \bar{T}_{\gamma\beta} G_{\gamma\gamma} T_{\gamma\alpha} \\ &\quad - \int d\gamma \int d\sigma \underbrace{\bar{V}_{\gamma\sigma} \bar{G}_{\sigma\sigma} \bar{T}_{\sigma\beta}}_{\bar{T}_{\sigma\beta} \bar{G}_{\sigma\sigma} V_{\sigma\gamma}} G_{\gamma\gamma} T_{\gamma\alpha} \\ &= \int d\gamma \bar{T}_{\gamma\beta} G_{\gamma\gamma} T_{\gamma\alpha} - \int d\sigma \bar{T}_{\sigma\beta} \bar{G}_{\sigma\sigma} \left(V_{\sigma\alpha} + \int d\gamma V_{\sigma\gamma} G_{\gamma\gamma} T_{\gamma\alpha} \right) \\ &= \int d\gamma \bar{T}_{\gamma\beta} G_{\gamma\gamma} T_{\gamma\alpha} - \int d\sigma \bar{T}_{\sigma\beta} \bar{G}_{\sigma\sigma} T_{\sigma\alpha} \\ &= \int d\gamma \bar{T}_{\gamma\beta} (G_{\gamma\gamma} - \bar{G}_{\gamma\gamma}) T_{\gamma\alpha}, \end{aligned}$$

where extensive use of eq. (1.8) and its adjoint was made. The quantity $G_{\gamma\gamma} - \bar{G}_{\gamma\gamma}$ is equivalent to setting the intermediate particles on shell (see e.g. section 7.3 of [11]), and thus, at least for energies below the lowest three-particle threshold, the above unitarity condition is equivalent to eq. (1.6).

Later in this work, amplitudes with one initial particle and two final particles will occur. In that case, the BSE can not be used as above. However, unitarity can still be achieved in the 'subspace' of meson-baryon scattering¹: Consider a scattering amplitude T that solves the BSE with a potential V , like above. Then, the amplitude

$$M_{\beta\alpha} = M_{\beta\alpha}^0 + \int d\gamma T_{\beta\gamma} G_{\gamma\gamma} M_{\gamma\alpha}^0$$

is unitary in the sense that any process described by the real kernel M^0 will be accompanied by an exactly unitary final state interaction. In that sense M contains the full information, i.e. any dynamically generated resonance, of the scattering process T . In the remainder of this work, this property will be referred to as 'partial unitarity'. Note, that M^0 in this work will be a process with one initial particle and two final particles, but in general M^0 could have an arbitrary number of initial states. Though, M^0 has to have two final particles due to the definition of the scattering amplitude T .

As mentioned earlier, the great advantage of solutions of the BSE is that they can generate resonances dynamically and every solution is exactly unitary, therefore such approaches are also called 'unitarized'. In contrast to that, perturbative approaches can only satisfy unitarity order by order and resonances must be included explicitly to obtain meaningful results in the vicinity of such resonances.

However, the solution of the BSE also has some drawbacks: Crossing symmetry can not be maintained by this approach. Even if the interaction kernel is crossing symmetric, the solution of the BSE is not. Maximal analyticity can also not be guaranteed ab initio as solutions of the BSE contain, among the dynamically generated resonances, unphysical poles on the first Riemann sheet as well as resonances that appear without any correspondents in experiments and shadow poles, i.e. resonances that appear on multiple sheets (see [12] for a discussion on the nature of resonances). Nevertheless, when restricted to a certain process, the BSE yields good results in the physical region of this process, especially when there are resonances that can be generated dynamically by the BSE.

¹The word 'subspace' does not refer to a subspace in the mathematical sense, but rather to the part of the corresponding Feynman diagram that has two initial and two final particles, which in this case is the scattering amplitude T .

Note, that the BSE contains divergences of the loop integrations which have to be renormalized. Throughout this work, the dimensional regularization scheme will be employed, where the limit $d \rightarrow 4$ is taken after the divergent terms were subtracted in each integral. However, the divergences can not be absorbed by a finite number of counter terms in the Lagrangian, since this would spoil the solution of the BSE. In fact, any counter term in the Lagrangian would be crossing symmetric while solutions of the BSE violate crossing symmetry (see e.g. [15] for a thorough treatment of renormalization in that case). The usual framework for these divergences is to absorb them into the coupling constants appearing in the interaction kernel, which renders the amplitudes finite. This procedure is not related to the proper field theoretical treatment of renormalization in perturbation theory, but, as of now, there is no rigorous non-perturbative renormalization scheme for the solutions of the BSE.

1.3 Gauge invariance

Formulating quantum theories of massless vector particles needs a specific treatment. It is not possible to simply consider the limit of zero mass of a theory with massive vector particles as this would render the corresponding propagators to be infinite, which reflects the fact that there is no way to construct a four-vector, in the sense of Lorentz transformations, for massless particles out of creation and annihilation operators of helicity ± 1 . In general, massless fields constructed with creation and annihilation operators of helicity ± 1 can only transform as a four-vector up to an additional local gauge term. This peculiar difficulty can be circumvented by demanding that the part of the action involving the massless vector field and its interactions with other fields is invariant under those gauge transformations, which then is called gauge invariance (see chapter 8 in [8]).

The more conventional or modern point of view is that gauge invariance itself is a principle and therefore the starting point when coupling massless vector particles to matter fields. For example, consider the Lagrangian density of free spin-1/2 particles: Enforcing invariance under local phase transformations, i.e. local $U(1)$ transformations, by means of the minimal coupling approach leads to a new covariant derivative which includes a new massless vector particle, a so-called gauge-boson. Of course, the kinetic term of the gauge-bosons has to be included to allow for their propagation. The result is the common quantum electrodynamics (QED) Lagrangian, where the gauge-bosons are indeed photons. Similarly, although more involved, the quantum chromodynamics (QCD) Lagrangian can be derived by enforcing local $SU(3)$ invariance. The main difference to the QED case is that $SU(3)$ invariance demands a total of eight gauge-bosons – the number of gauge-bosons necessary to accomplish invariance under a gauge-group is the

number of generators of said gauge-group. Therefore the QCD Lagrangian is far more complicated and involves severely different physics than the QED Lagrangian.

In this work, one of the main goals is to couple a photon in a gauge-invariant manner to a non-perturbatively evaluated model amplitude, i.e. the main concern of the remainder of this section is to deal with local $U(1)$ -invariance as found in the QED Lagrangian. Recall, that gauge invariance in perturbation theory is achieved by simply including all possible Feynman-diagrams up to a given order. In a visual way, this means that the photon must be coupled to *any* charged particle in the diagram², also if it is off-shell, reflecting the charge conservation principle. Following this notion, gauge invariance in a non-perturbative model, like the resummation method of the BSE, can be implemented by adding up the Feynman diagrams where the photon couples to the external lines as well as the diagrams where the photon couples to internal lines. However, as the solution of the BSE is in fact an infinite series of Feynman diagrams, there are also infinitely many internal lines. To see how this problem can be solved, consider the BSE of eq. (1.8) in terms of Feynman diagrams:

where the shaded circle represents the amplitude T and the white square represents the interaction kernel V . The dashed and solid lines may be any pair of particles, that interact with each other or that are taken to another pair of particles via the potential V . Iterating the BSE leads to:

where the so-called bubble-chain on the r.h.s. is an infinite geometric series of loops, i.e. the ellipsis stands for any diagrams obtained by an iteration of the BSE that are of higher order in the potential V . For brevity, consider a theory where the photon only interacts with the particles represented by the solid lines. Then, coupling a photon to every internal line of the bubble-chain

²This is the case in QED, but later in this work a coupling of the photon to certain neutral particles will emerge from the next-to-leading order meson-baryon chiral Lagrangian, where the photon also has to be coupled to these particles.

and adding all those Feynman diagrams can be simplified to

where the ellipsis stands for any diagrams obtained from the iteration of the BSE with photons coupled to any possible solid internal line. Furthermore, the shaded circle represents the solution T of the BSE. The Feynman diagram on the r.h.s. apparently involves all possible couplings of a photon to internal lines. Moreover, for theories with other photon couplings, an analogous Feynman diagram has to be computed for each interaction. Note, that in addition to the photon coupling to internal lines, every diagram where the photon couples to *external* lines has to be considered, too. But this is trivial, since there are only a finite number of external lines.

To be sure that gauge invariance is indeed satisfied, the Ward-Takahashi identity can be used (see section 7.4 in [11]), i.e. any gauge-invariant amplitude $\epsilon_\mu(k)\mathcal{M}^\mu(k)$ of a QED process involving an external photon with momentum k satisfies

$$k_\mu \mathcal{M}^\mu(k) = 0.$$

This identity will be verified in later chapters to prove that the above approach for implementing gauge invariance succeeds.

1.4 Chiral perturbation theory

Chiral perturbation theory (ChPT) was developed in order to circumvent the large coupling of quantum chromodynamics (QCD) at low energies which renders any perturbative approach useless. It is based on the knowledge that the QCD Lagrangian exhibits a chiral symmetry in the chiral limit, i.e. in the limit of zero quark masses. This symmetry can then be used to construct an effective low-energy Lagrangian by enforcing the chiral symmetry and introducing an appropriate power-counting scheme to put the terms in an order of the importance of the arising terms [1].

The QCD Lagrangian reads³

$$\mathcal{L}_{QCD} = \bar{q}_f^i (i\gamma^\mu D_{\mu,ij} - \delta_{ij} m_f) q_f^j - \frac{1}{4} G_{\mu\nu}^a G^{a,\mu\nu}, \quad (1.9)$$

³Sometimes an additional term is included in the QCD Lagrangian that is proportional to the so-called vacuum angle θ . However, this term would be responsible for CP violations, but as there is now evidence from experiments for such violations, the term is usually set to zero.

where summation over repeated indices is implied, q_f^i denotes a quark field with color $i \in \{\text{red, green, blue}\}$ and with flavor $f \in \{\text{up, down, charm, strange, top, bottom}\}$, the covariant derivative is given by

$$D_{\mu,ij} = \delta_{ij}\partial_{\mu} + igt_{ij}^a A_{\mu}^a$$

and the field strength tensor reads

$$G_{\mu\nu}^a = \partial_{\mu}A_{\nu}^a - \partial_{\nu}A_{\mu}^a - gf^{abc}A_{\mu}^b A_{\nu}^c.$$

Here, g is the coupling constant of QCD, A_{μ}^a are the eight gluon fields, and t^a and f^{abc} are the generators and structure constants of the $SU(3)$ gauge group of QCD, respectively. QCD earns its complicated nature mostly through the particular form of the field strength tensor $G_{\mu\nu}^a$: The term $-gf^{abc}A_{\mu}^b A_{\nu}^c$ is responsible for a three-gluon vertex and a four-gluon vertex. Those vertices contribute to the calculation of the running coupling constant by means of the renormalization group theory in that they increase the coupling at low-energies, also called confinement, whereas at high energies the coupling decreases and reaches eventually zero, also known as asymptotic freedom.

In the limit of vanishing quark masses, $m_f \rightarrow 0$, the QCD Lagrangian becomes

$$\mathcal{L}_{QCD} \xrightarrow{m_f \rightarrow 0} i\bar{q}_f^i \gamma^{\mu} D_{\mu,ij} q_f^j - \frac{1}{4} G_{\mu\nu}^a G^{a,\mu\nu}. \quad (1.10)$$

This limit is called the 'chiral limit', but it is only reasonable if the quark masses that are set to zero are small compared to the characteristic scale of the interaction. As a consequence, the six flavors of quarks can be divided into the three light quarks u , d and s , whose masses are well below 1 GeV, and the three heavy quarks c , b and t , whose masses are above 1 GeV. The scale of 1 GeV is associated with the masses of the lightest hadrons containing light quarks⁴, e.g. the ρ with its mass being $m_{\rho} = 770$ MeV. In this work, only the three light quarks are taken into account, since their mass is negligible compared to the center-of-mass energy encountered in the η -photoproduction process. Hence from now on, flavor sums, e.g. in eq. (1.10), only involve the flavors u , d and s (up, down and strange).

In the chiral limit, the Lagrangian of eq. (1.10) can be rewritten as

$$\mathcal{L}_{QCD}^0 = i\bar{q}_L \gamma^{\mu} D_{\mu} q_L + i\bar{q}_R \gamma^{\mu} D_{\mu} q_R - \frac{1}{4} G_{\mu\nu}^a G^{a,\mu\nu}, \quad (1.11)$$

where color and flavor indices were omitted for brevity and

$$q_L = P_L q = \frac{1}{2}(1 - \gamma_5)q, \quad q_R = P_R q = \frac{1}{2}(1 + \gamma_5)q.$$

⁴Excluding Goldstone bosons. Those will be introduced later in this section.

P_L and P_R are projection operators that project the quark fields q to their chiral components q_L and q_R , respectively. This leads to the new global symmetry

$$U(3)_L \times U(3)_R$$

of the chiral QCD Lagrangian in flavor space, i.e. \mathcal{L}_{QCD}^0 is invariant under independent global unitary transformations

$$q_L \rightarrow Lq_L, \quad q_R \rightarrow Rq_R,$$

where $L \in U(3)_L$ and $R \in U(3)_R$. This global symmetry can be decomposed according to

$$U(3)_L \times U(3)_R = SU(3)_V \times SU(3)_A \times U(1)_V \times U(1)_A,$$

where the subscript V stands for vector transformations defined by $R = L$, and the subscript A stands for axial transformations defined by $R = L^\dagger$.

However, the above decomposition of the symmetry of \mathcal{L}_{QCD}^0 is not realized in nature, at least not in this way. The axial group $U(1)_A$ is known to be broken by an anomaly [13, 14], whereas $U(1)_V$ can be associated with the quark or baryon number conservation. In fact, $U(1)_V$ is also a symmetry of \mathcal{L}_{QCD} of eq. (1.9), i.e. for non-vanishing quark masses.

As for the remaining symmetry groups $SU(3)_L \times SU(3)_R$, there is ample evidence that those are broken down to only the vectorial subgroup $SU(3)_V$ [16]. If $SU(3)_L \times SU(3)_R$ were a symmetry of QCD, the hadron spectrum would be parity-doubled, but this is not observed. Therefore the symmetry of QCD is realized in the well-known Nambu-Goldstone mode [17, 18, 19], which states that the symmetry of the Lagrangian is not the same as the symmetry of the vacuum. Furthermore, because the symmetry group is broken down to its vectorial subgroup, there are in total eight massless Goldstone bosons introduced by means of the Goldstone theorem and these Goldstone bosons share the quantum numbers of the generators of the $SU(3)_A$, i.e. the Goldstone bosons form an octet of pseudoscalar mesons. However, since the chiral symmetry is only approximate, the particles associated with these Goldstone bosons are not massless, but still are significantly lighter than typical hadrons, which have masses in the GeV range. In fact, there are eight pseudoscalar mesons π^\pm , π^0 , K^\pm , K^0 , \bar{K}^0 and η which are all lighter than the lowest-lying hadron that is not a Goldstone boson, i.e. the ρ -resonance.

The explicit symmetry breaking due to the non-vanishing quark masses is impairing the convergence of a perturbation theory around the chiral limit. Especially comparing the two-flavor case to the three-flavor case, where in the two-flavor case the QCD Lagrangian includes the u - and d -quark⁵ and in the three-flavor case the s -quark is included as well. Due to the fact that the

⁵All heavier quarks are integrated out by means of the path integral formalism.

mass of the s -quark is significantly larger than the masses of either u - or d -quark, the additional Goldstone bosons of the $SU(3)$ -flavor case, compared to $SU(2)$ -flavor, have also significantly larger masses. In the $SU(3)$ case the suppression factor of higher order terms of a perturbation theory is, in a pessimistic estimate, approximately $M_\eta/M_\rho \approx 0.71$. For higher energies the suppression factors become even worse and especially in the vicinity of resonances ChPT breaks down, which is why the BSE, a non-perturbative approach, will be used in this work.

The chirally symmetric Lagrangian of eq. (1.11) can be used to formulate an effective field theory that contains the Goldstone bosons as degrees of freedom [1]. According to [20, 21], the eight Goldstone bosons in the $SU(3)$ -flavor case can be described by continuous real functions $\phi(x)$ on Minkowski space and there exists an isomorphic mapping between the quotient $(SU(3)_V \times SU(3)_A)/SU(3)_V$ and the Goldstone boson fields. But the quotient can be uniquely characterized through a $SU(3)$ matrix $U(x)$, which is invariant under *local* $SU(3)_V$ just as the vacuum. Therefore the effective Lagrangian can be chosen to be a function of $U(x)$, which can be expressed in terms of the Goldstone boson fields:

$$U(x) = \exp\left(\frac{i\phi(x)}{f}\right), \quad (1.12)$$

where the Goldstone boson fields are collected in the hermitean matrix

$$\phi = \phi^a \lambda^a = \sqrt{2} \begin{pmatrix} \frac{1}{\sqrt{2}}\pi^0 + \frac{1}{\sqrt{6}}\eta & \pi^+ & K^+ \\ \pi^- & -\frac{1}{\sqrt{2}}\pi^0 + \frac{1}{\sqrt{6}}\eta & K^0 \\ K^- & \bar{K}^0 & -\frac{2}{\sqrt{6}}\eta \end{pmatrix} \quad (1.13)$$

with the generators λ^a of the $SU(3)$ Lie-algebra in the particle basis, and the constant f will turn out to be the pion decay constant in the chiral limit.

Thus, an effective Lagrangian can be written down by implementing all symmetries of the full QCD Lagrangian, i.e. Lorentz invariance and invariance under C , P and T transformations as well as local chiral transformations as e.g. applied to $U(x)$. Furthermore, external sources can be included to account e.g. for external vector fields, which will be introduced later in this work.

To see how that works, consider first the QCD Lagrangian \mathcal{L}_0 and include external sources as

$$\mathcal{L}_{QCD} = \mathcal{L}_0 + \mathcal{L}^{ext}$$

with

$$\mathcal{L}^{ext} = \bar{q}(\gamma^\mu(v_\mu + \gamma_5 a_\mu) - (s - i\gamma_5 p))q,$$

where v_μ , a_μ , s and p are hermitian matrices in flavor space and they represent vector, axial-vector, scalar and pseudo-scalar external sources, respectively. Moreover, v_μ and a_μ do not contain singlet components, i.e. their

trace in flavor space vanishes. Note, that the quark mass term is included in the scalar external field $s = \text{diag}(m_u, m_d, m_s) + \dots$, where m_u , m_d and m_s are the masses of the up, down and strange quark, respectively.

Now, the generating functional Z defined by

$$\exp(iZ(v, a, s, p)) = \langle 0|T \exp\left(i \int d^4x \mathcal{L}^{ext}(v, a, s, p)\right)|0\rangle$$

should be invariant under local $SU(3)_V \times SU(3)_A = SU(3)_L \times SU(3)_R$ transformations, since the Lagrangian \mathcal{L}_{QCD} should be invariant, just as \mathcal{L}_0 . This can be achieved by demanding particular transformation properties for the external fields:

$$\begin{aligned} v_\mu + a_\mu &\rightarrow R(v_\mu + a_\mu)R^\dagger + iR\partial_\mu R^\dagger, \\ v_\mu - a_\mu &\rightarrow L(v_\mu - a_\mu)L^\dagger + iL\partial_\mu L^\dagger, \\ s &\rightarrow RsL^\dagger, \\ p &\rightarrow RpL^\dagger, \end{aligned}$$

where $L \in SU(3)_L$ and $R \in SU(3)_R$.

Then, the corresponding effective field theory with Goldstone bosons as degrees of freedom can be expressed as

$$\exp(iZ(v, a, s, p)) = \int \mathcal{D}U \exp\left(i \int d^4x \mathcal{L}_{\text{eff}}(U, v, a, s, p)\right).$$

The measure $\mathcal{D}U$ of this path integral contains only Goldstone bosons and thus this formulation is based on the assumption that the degrees of freedom of the theory *are* the Goldstone bosons, which means that this approach is only suited for the low-energy or long-range region of QCD where the interaction through Goldstone bosons is dominant. High-energy degrees of freedom have been integrated out, but their effect is still contained in the local interactions of \mathcal{L}_{eff} .

Now that the groundwork has been done, the remainder of this section will deal with the construction of the chiral effective Lagrangian.

The effective Lagrangian contains an infinite series of local couplings which have to be invariant under the same symmetry groups as the QCD Lagrangian. The basic building blocks are the matrix U containing the Goldstone boson fields, the external fields v_μ , a_μ , s and p and derivatives of those quantities. Of course, only a finite number of terms of the effective Lagrangian can be used in calculations, therefore an ordering of these terms has to occur, which is now widely known as power counting: As it turns out, higher order terms are suppressed by factors of $q/4\pi f$, where $4\pi f$ is about 1 GeV in size which is approximately the size of the hadronic scale. But the Goldstone boson momenta q in the low-energy regime of QCD are

small compared to the hadronic scale and thus an expansion in powers of q leads to a suppression of higher order terms. Correspondingly the effective Lagrangian has to be expanded in derivatives. Omitting the external fields for a moment, the effective Lagrangian can only contain an even number of derivatives, due to the fact that the Lagrangian has to be a Lorentz scalar. This leads to a constant term with no derivatives $U^\dagger U = 1$, which can simply be omitted. The subsequent term contains two derivatives and reads

$$\mathcal{L}_{\text{eff}}^{(2)} = \frac{f^2}{4} \langle \partial_\mu U^\dagger \partial^\mu U \rangle,$$

where the brackets $\langle \dots \rangle$ denote the trace in flavor space. The coefficient is chosen such that the expansion of U leads to the standard kinetic term for a real scalar field:

$$\mathcal{L}_{\text{eff}}^{(2)} = \frac{1}{2} \partial_\mu \phi^a \partial^\mu \phi^a + \mathcal{O}(\phi^4).$$

Including the external fields again, the partial derivatives have to be replaced by covariant derivatives

$$\nabla_\mu U = \partial_\mu U - i(v_\mu + a_\mu)U + iU(v_\mu - a_\mu) \quad (1.14)$$

in order to make the Lagrangian invariant under chiral transformations. As $\partial_\mu U$ is of order $\mathcal{O}(q)$, the same should be valid for the covariant derivative $\nabla_\mu U$ and thus, for consistency, the fields v_μ and a_μ are also of order $\mathcal{O}(q)$.

A mass term can be included via the scalar external field s :

$$\mathcal{L}_{\text{eff}}^{(2)} = \frac{f^2}{4} \langle \nabla_\mu U^\dagger \nabla^\mu U \rangle + \frac{f^2}{2} B_0 \langle s U^\dagger + U s^\dagger \rangle,$$

where B_0 is a constant related to the scalar quark condensate in the chiral limit and the external field s can be set to the quark mass matrix $s = \text{diag}(m_u, m_d, m_s)$. But this implies that s is $\mathcal{O}(q^2)$, which can be justified by expanding the mass term in powers of Goldstone bosons [22]:

$$M_{\pi^\pm}^2 = B_0(m_u + m_d),$$

$$M_{\pi^0}^2 = B_0(m_u + m_d) + \mathcal{O}\left(\frac{(m_u - m_d)^2}{m_s - \frac{1}{2}(m_u + m_d)}\right),$$

$$M_{K^\pm}^2 = B_0(m_u + m_s),$$

$$M_{K^0}^2 = B_0(m_d + m_s),$$

$$M_\eta^2 = \frac{1}{3} B_0(m_u + m_d + 4m_s) + \mathcal{O}\left(\frac{(m_u - m_d)^2}{m_s - \frac{1}{2}(m_u + m_d)}\right).$$

Since on-shell Goldstone boson momenta satisfy $q^2 = M_\phi^2$ and because, in leading order, *squared* meson masses are proportional to quark masses, the

external field s is $\mathcal{O}(q^2)$.

In this manner the higher order terms of the effective Lagrangian can be derived, leading to an infinite series of local terms

$$\mathcal{L}_{\text{eff}} = \mathcal{L}_{\text{eff}}^{(2)} + \mathcal{L}_{\text{eff}}^{(4)} + \mathcal{L}_{\text{eff}}^{(6)} + \dots ,$$

which of course are more involved the higher the order. Moreover, expanding the \mathcal{L}_{eff} in that way, leads to the necessity of an ordering for Feynman diagrams that are calculated with the vertices and propagators arising in \mathcal{L}_{eff} . In particular, at leading order only the tree graphs of $\mathcal{L}_{\text{eff}}^{(2)}$ have to be considered. At next-to-leading order, tree graphs *and* one-loop diagrams with vertices from $\mathcal{L}_{\text{eff}}^{(2)}$ as well as tree graphs with vertices from $\mathcal{L}_{\text{eff}}^{(4)}$ have to be considered, and so on. This ordering arises by virtue of the loop integrals, which introduce additional orders of q in a diagram, and thus they have to be included in the power counting scheme.

To summarize, the construction of a Lagrangian with Goldstone bosons as degrees of freedom and implementing the symmetries of the underlying theory leads to an infinite series of local terms which can be ordered by their importance with an appropriate power counting scheme for the Goldstone boson momenta.

1.5 Baryon chiral perturbation theory

The goal of this section is to introduce the baryon chiral perturbation theory (BChPT) and in particular to construct an effective Lagrangian for the single baryon sector, i.e. only one baryon is involved and therefore processes that involve baryon-baryon interactions are not considered. To this end, the flavor $SU(3)$ ground-state octet of baryon fields can be introduced in analogy to the meson fields:

$$B = B^a \lambda^a = \begin{pmatrix} \frac{1}{\sqrt{2}}\Sigma^0 + \frac{1}{\sqrt{6}}\Lambda & \Sigma^+ & p \\ \Sigma^- & -\frac{1}{\sqrt{2}}\Sigma^0 + \frac{1}{\sqrt{6}}\Lambda & n \\ \Xi^- & \Xi^0 & -\frac{2}{\sqrt{6}}\Lambda \end{pmatrix}, \quad (1.15)$$

which accordingly transforms as an octet under the subgroup $SU(3)_V$. Note, that the corresponding antiparticles form an analogous octet. The corresponding transformation law under $SU(3)_L \times SU(3)_R$ can be chosen as

$$B \rightarrow K B K^\dagger,$$

where K depends on $L \in SU(3)_L$, $R \in SU(3)_R$ and U . It can be derived from the transformation property of a quantity often called u , which is the positive square root of U , i.e. $u = \sqrt{U}$:

$$u \rightarrow R u K^\dagger = K u L^\dagger.$$

It is then possible to define the chiral vielbein

$$u_\mu = iu^\dagger \nabla_\mu U u^\dagger, \quad (1.16)$$

which transforms, just like B , as $u_\mu \rightarrow K u_\mu K^\dagger$ and is of order $\mathcal{O}(q)$ due to the covariant derivative in its definition. B and u_μ can be used as building blocks for the effective meson-baryon Lagrangian to arrive at [23, 24]:

$$\mathcal{L}_{B\phi}^{(1)} = \langle \bar{B}(i\gamma^\mu D_\mu - m_0)B \rangle - \frac{D}{2} \langle \bar{B}\gamma^\mu \gamma_5 \{u_\mu, B\} \rangle - \frac{F}{2} \langle \bar{B}\gamma^\mu \gamma_5 [u_\mu, B] \rangle, \quad (1.17)$$

where external fields are included within the covariant derivative

$$\begin{aligned} D_\mu B &= \partial_\mu B + [\Gamma_\mu, B], \\ \Gamma_\mu &= \frac{1}{2} \left(u^\dagger [\partial_\mu - i(v_\mu + a_\mu)] u + u [\partial_\mu - i(v_\mu - a_\mu)] u^\dagger \right). \end{aligned} \quad (1.18)$$

The quantity m_0 denotes the mass of the particles in the baryon octet in the chiral limit and D and F are constants, whose sum is equal to the axial-vector coupling g_A in the chiral limit. Their values can be determined from semileptonic baryon decays [26, 27] and throughout this work they are set to

$$D = 0.8, \quad F = 0.46.$$

The construction of a meson-baryon effective Lagrangian deserves some comments on the power counting scheme. The leading order Lagrangian of eq. (1.17) is of order $\mathcal{O}(q)$, due to the kinetic term. However, in contrast to the Goldstone boson masses, the baryon mass m_0 is not small and therefore counted as $\mathcal{O}(1)$. Furthermore, the baryon field B and its adjoint \bar{B} are also counted as $\mathcal{O}(1)$. Other counting rules are given by

$$D_\mu B = \mathcal{O}(1), \quad \bar{B}\gamma_5 B = \mathcal{O}(q), \quad \bar{B}\gamma_\mu B = \mathcal{O}(1), \quad \bar{B}\gamma_\mu \gamma_5 B = \mathcal{O}(1).$$

In this spirit the next-to-leading order meson-baryon effective Lagrangian can be constructed [24, 25]:

$$\begin{aligned} \mathcal{L}_{B\phi}^{(2)} &= b_{D/F} \langle \bar{B}[\chi_+, B]_\pm \rangle + b_0 \langle \bar{B}B \rangle \langle \chi_+ \rangle \\ &+ b_{1/2} \langle \bar{B}[u_\mu, [u^\mu, B]_\mp] \rangle + b_3 \langle \bar{B}\{u_\mu, \{u^\mu, B\}\} \rangle + b_4 \langle \bar{B}B \rangle \langle u_\mu u^\mu \rangle \\ &+ ib_{5/6} \langle \bar{B}\sigma^{\mu\nu}[u_\mu, u_\nu], B \rangle_\mp + ib_7 \langle \bar{B}\sigma^{\mu\nu} u_\mu \rangle \langle u_\nu B \rangle \\ &+ \frac{ib_{8/9}}{2m_0} \left(\langle \bar{B}\gamma^\mu [u_\mu, [u_\nu, [D^\nu, B]]_\mp] \rangle + \langle \bar{B}\gamma^\mu [D_\nu, [u^\nu, [u_\mu, B]]_\mp] \rangle \right) \\ &+ \frac{ib_{10}}{2m_0} \left(\langle \bar{B}\gamma^\mu \{u_\mu, \{u_\nu, [D^\nu, B]\}\} \rangle + \langle \bar{B}\gamma^\mu [D_\nu, \{u^\nu, \{u_\mu, B\}\}] \rangle \right) \\ &+ \frac{ib_{11}}{2m_0} \left(2 \langle \bar{B}\gamma^\mu [D_\nu, B] \rangle \langle u_\mu u^\nu \rangle \right. \\ &\quad \left. + \langle \bar{B}\gamma^\mu B \rangle \langle [D_\nu, u_\mu] u^\nu + u_\mu [D_\nu, u^\nu] \rangle \right) \end{aligned}$$

$$+ b_{12/13} \langle \bar{B} \sigma^{\mu\nu} [F_{\mu\nu}^+, B]_{\pm} \rangle \quad (1.19)$$

where

$$\begin{aligned} F_{\mu\nu}^+ &= u^\dagger F_{\mu\nu}^L u + u F_{\mu\nu}^R u^\dagger, \\ F_{\mu\nu}^L &= \partial_\mu r_\nu - \partial_\nu r_\mu - i[r_\mu, r_\nu], \\ F_{\mu\nu}^R &= \partial_\mu l_\nu - \partial_\nu l_\mu - i[l_\mu, l_\nu], \\ l_\mu &= v_\mu - a_\mu, \\ r_\mu &= v_\mu + a_\mu, \\ \chi_\pm &= u^\dagger \chi u^\dagger \pm u \chi^\dagger u, \\ \chi &= 2B_0 s. \end{aligned}$$

Here, the coefficients b_i are called low-energy constants (LEC). They cannot be determined from chiral symmetry itself, but must be obtained from experiments. Note, that each term containing a pair of indices in the subscript of the LECs is actually a sum of two terms: the first one containing the left index and the upper sign of the respective commutator, and similarly the second one containing the right index and the lower sign of the commutator.

The Lagrangian derived in the framework of baryon chiral perturbation theory will be the basic Lagrangian used throughout this work and will be used to derive almost all the interactions necessary for evaluating the η -photoproduction amplitude later on.

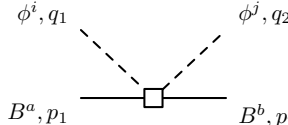
eq. (1.12), the chiral connection can be expanded in powers of meson fields ϕ to the desired order of external meson legs:

$$\begin{aligned}\Gamma_\mu &= \frac{1}{2} \left(u^\dagger \partial_\mu u + u \partial_\mu u^\dagger \right) \\ &= \frac{1}{2} \left(\left[1 - \frac{i\phi}{\sqrt{2}f} \right] \partial_\mu \left[\frac{i\phi}{\sqrt{2}f} - \frac{\phi^2}{4f^2} \right] \right. \\ &\quad \left. + \left[1 + \frac{i\phi}{\sqrt{2}f} \right] \partial_\mu \left[-\frac{i\phi}{\sqrt{2}f} - \frac{\phi^2}{4f^2} \right] \right) + \mathcal{O}(\phi^4) \\ &= \frac{1}{4f^2} [\phi, \partial_\mu \phi] + \mathcal{O}(\phi^4),\end{aligned}$$

where the external fields v_μ and a_μ have been set to zero for now. Inserting Γ_μ into the Lagrangian gives

$$\langle \bar{B} (i\gamma^\mu [\Gamma_\mu, B]) \rangle = \frac{i}{4f^2} \langle \bar{B} [[\phi, \not{\partial}\phi], B] \rangle$$

Then, using the pertinent Feynman rules yields



$$\begin{aligned} &= i \left(\frac{i}{4f_i f_j} (-i\not{q}_1) \langle (\lambda^b)^\dagger [(\lambda^j)^\dagger, \lambda^i], \lambda^a \rangle \right. \\ &\quad \left. + \frac{i}{4f_i f_j} (i\not{q}_2) \langle (\lambda^b)^\dagger [[\lambda^i, (\lambda^j)^\dagger], \lambda^a] \rangle \right). \end{aligned} \quad (2.2)$$

Since the two mesons are indistinguishable, the Feynman rules lead to two terms, which represent that either of the mesons could be incoming or outgoing. The λ^i are the generators of the $SU(3)$ Lie-Algebra in the particle basis, appearing in the definitions of ϕ and B in eq. (1.13) and (1.15), respectively. Furthermore, the f_i can take on values corresponding to the meson involved in the particular channel, i.e. f_i has the possible values f_π , f_η and f_K which are the decay-constants of the π , η and K , respectively. These decay constants are set to be at physical values throughout this work:

$$\begin{aligned} f_\pi &= 92.4 \text{ MeV}, \\ f_\eta &= 120.12 \text{ MeV}, \\ f_K &= 113 \text{ MeV}. \end{aligned} \quad (2.3)$$

Note, that in the chiral limit $f_\pi = f_\eta = f_K$. Thus, taking different values for the decay constants is equivalent to incorporating higher order terms, which, in practice, can be absorbed into a redefinition of the potential.

Combining the terms of eq. (2.2) and defining the potential V as the Weinberg-Tomozawa diagram multiplied by i gives

$$V^{bj,ai}(\not{q}_2, \not{q}_1) = g^{bj,ai}(\not{q}_1 + \not{q}_2),$$

where

$$g^{bj,ai} = -\frac{1}{4f_j f_i} \langle (\lambda^b)^\dagger [(\lambda^j)^\dagger, \lambda^i], \lambda^a \rangle.$$

Finally, with the propagators

$$iS^{bj,aj}(\not{p}) = \frac{i\delta^{ba}\delta^{ji}}{\not{p} - m_a}$$

and

$$i\Delta^{bj,aj}(p) = \frac{i\delta^{ba}\delta^{ji}}{p^2 - M_j^2},$$

the BSE for the meson-baryon scattering amplitude can be written down in matrix form:

$$T(\not{q}_2, \not{q}_1; p) = V(\not{q}_2, \not{q}_1) + \int \frac{d^d l}{(2\pi)^d} V(\not{q}_2, l) iS(\not{p} - l) \Delta(l) T(l, \not{q}_1; p). \quad (2.4)$$

In principle, eq. (2.4) could be solved numerically, but it is by far more convenient to use the analytic solution as was shown in [28, 31]:

$$T(\not{q}_2, \not{q}_1; p) = W(\not{q}_2, \not{q}_1; p) + W(\not{q}_2, \not{p} - m; p) G(p) [1 - W(\not{p} - m, \not{p} - m; p) G(p)]^{-1} W(\not{p} - m, \not{q}_1; p),$$

where

$$W(\not{q}_2, \not{q}_1; p) = \not{q}_2 g \frac{1}{1 + I_M g} + \frac{1}{1 + g I_M} g \not{q}_1 - g \frac{1}{1 + I_M g} I_M (\not{p} - m) \frac{1}{1 + g I_M} g$$

and

$$m^{bj,ai} = m_a \delta^{ba} \delta^{ji} \quad (2.5)$$

is the baryon mass matrix, furthermore $p = p_1 + q_1$ is the total incoming momentum. Since the former equations are matrix-like in channel space, the '1' has to be the unit matrix in channel space. Moreover, the loop integrals are given by

$$I_M^{bj,ai} = \int \frac{d^d l}{(2\pi)^d} i\Delta^{bj,aj}(l) \quad (2.6)$$

and

$$G^{bj,ai}(p) = \int \frac{d^d l}{(2\pi)^d} i[\Delta(l) S(\not{p} - l)]^{bj,ai}. \quad (2.7)$$

Throughout this work, the divergent integrals will be regularized using the dimensional regularization. At first sight, it is not clear whether the additional terms appearing in the renormalization scheme will alter the appearance of T . But as described in [28], a shift in the integrals I_M and G can always be absorbed by modifying the interaction kernel V . Therefore, in practice these

terms can simply be omitted. In contrast, using a perturbative renormalization procedure and thus including counter terms in the Lagrangian would spoil the solution of the BSE.

Now T can be reduced to 8 independent Dirac-structures:

$$\begin{aligned} T(\not{q}_2, \not{q}_1; p) = & \not{q}_2 \not{p} \not{q}_1 T_1(p) + \not{q}_2 \not{q}_1 T_2(p) + \not{p} \not{q}_1 T_3(p) + \not{q}_2 \not{p} T_4(p) \\ & + \not{q}_1 T_5(p) + \not{q}_2 T_6(p) + \not{p} T_7(p) + T_8(p). \end{aligned} \quad (2.8)$$

The explicit form of the T_i structures and the loop integrals I_M and G can be found in appendices A and B, respectively.

2.2 Partial Wave Analysis

As an intermediate result, the partial waves of πN - scattering, more precisely $\pi^0 p$ - and $\pi^+ n$ - scattering, will be presented in this section.

The first step in this approach is to restrict the channels. Any open channels, other than $\pi^0 p$ and $\pi^+ n$, must have the same charge and strangeness quantum numbers. In this work the only particles considered are the ground-state octets of mesons and baryons. Hence, there are six channels in total:

$$(B\phi) = (p\pi^0, n\pi^+, p\eta, \Lambda K^+, \Sigma^0 K^+, \Sigma^+ K^0). \quad (2.9)$$

For calculating the partial waves, T from eq. (2.8) must be set on shell, which can be achieved by the substitutions $\not{q}_1, \not{q}_2 \rightarrow \not{p} - m$, where m is the diagonal baryon mass matrix whose diagonal entries are given by eq. (2.5). Then T simplifies to

$$T_{on} = \not{p} T_{on}^{(1)} + T_{on}^{(0)}$$

where

$$T_{on}^{(1)} = p^2 T_1 + m T_1 m - m T_2 - T_2 m - T_3 m - m T_4 + T_5 + T_6 + T_7$$

and

$$T_{on}^{(0)} = p^2 (T_2 + T_3 + T_4 - T_1 m - m T_1) + m T_2 m - T_5 m - m T_6 + T_8$$

only depend on p^2 . Here, the abbreviation $T_i = T_i(p)$ was used.

Now T_{on} can be rewritten in order to make the chiral ordering manifest:

$$T_{on} = \not{p} T_{on}^{(1)} + T_{on}^{(0)} = A + \frac{1}{2} (\not{q}_2 + \not{q}_1) B,$$

where \not{q}_1 and \not{q}_2 of course must be taken on-shell. Replacing again $\not{q}_1, \not{q}_2 \rightarrow \not{p} - m$, keeping in mind that this is a matrix equation and the ordering of m and B matters, a comparison of coefficients yields

$$A_{on} = T_{on}^{(0)} + \frac{1}{2} (m T_{on}^{(1)} + T_{on}^{(1)} m)$$

and

$$B_{on} = T_{on}^{(1)}.$$

The decomposition of the angular dependence of the amplitudes is given as usual in the basis of the Legendre polynomials P_l :

$$A_{on}(s, z) = \frac{1}{2} \sum_{l=0}^{\infty} (2l+1) A_l(s) P_l(z),$$

where $z = \cos \theta$ is the angular dependence of A_{on} and $s = p^2$ is a Mandelstam variable. Multiplying by $P_m(z)$, integrating over $z \in [-1, 1]$ and using the orthogonality relation $\int_{-1}^1 dz P_l(z) P_m(z) = \frac{2}{2l+1} \delta_{lm}$ leads to

$$A_l(s) = \int_{-1}^1 dz P_l(z) A_{on}(s, z),$$

and equivalently

$$B_l(s) = \int_{-1}^1 dz P_l(z) B_{on}(s, z).$$

However, since $T_{on}^{(1)}$ and $T_{on}^{(0)}$ have no angular dependence, neither have A_{on} nor B_{on} . Hence, the only non-vanishing contributions come from

$$A_0(s) = 2A_{on}(s)$$

and

$$B_0(s) = 2B_{on}(s).$$

Theses results can now be applied to partial wave amplitudes (see [32], eq. (A.3.7)) which read

$$\begin{aligned} -16\pi\sqrt{s}f_{l\pm} &= \sqrt{E_{\text{cm}} + m} \left(A_l + \frac{1}{2}((\sqrt{s} - m)B_l + B_l(\sqrt{s} - m)) \right) \sqrt{E_{\text{cm}} + m} \\ &+ \sqrt{E_{\text{cm}} - m} \left(-A_{l\pm 1} + \frac{1}{2}((\sqrt{s} + m)B_{l\pm 1} + B_{l\pm 1}(\sqrt{s} + m)) \right) \sqrt{E_{\text{cm}} - m}, \end{aligned} \quad (2.10)$$

where the center-of-mass energy E_{cm} is a matrix in channel space with components

$$E_{\text{cm}}^{bj, ai} = \delta^{ba} \delta^{ji} \sqrt{q_{ai}^2 + m_a^2}$$

and

$$q_{ai} = \frac{\sqrt{(s - (m_a + M_i)^2)(s - (m_a - M_i)^2)}}{2\sqrt{s}} \quad (2.11)$$

are the components of the center-of-mass three-momentum for a baryon a and a meson i . A partial wave amplitude such as $f_{l\pm}$ indicates that the total angular momentum is $j = l \pm \frac{1}{2}$.

Being aware of that the only contribution comes from A_0 and B_0 , eq. (2.10) reduces, for the $l = 0$ partial wave, to

$$-16\pi\sqrt{s}f_{0+} = \sqrt{E_{\text{cm}} + m} \left(A_0 + \frac{1}{2}((\sqrt{s} - m)B_0 + B_0(\sqrt{s} - m)) \right) \sqrt{E_{\text{cm}} + m}.$$

The other non-vanishing partial wave, f_{1-} , will be omitted, since there should be a considerable contribution from higher angular momentum waves, in which case the current approach does not apply – the Weinberg-Tomozawa vertex contributes only to the s-wave amplitude.

Finally, the T -Matrix for this decomposition reads

$$T_{0+} = \sqrt{q_{\text{cm}}}f_{0+}\sqrt{q_{\text{cm}}}, \quad (2.12)$$

where the components of q_{cm} read

$$q_{\text{cm}}^{bj,ai} = \delta^{ba}\delta^{ji}q_{ai}\theta(s - (m_a + M_i)^2).$$

Note, that eq. (2.12) obtains this particular symmetric form due to its matrix character in channel space.

For a comparison with other data of πN - scattering, the isospin channels $\frac{1}{2}$ and $\frac{3}{2}$ have to be extracted. The pertinent rules for Clebsch-Gordan coefficients lead to

$$\begin{aligned} S_{11} &= 2(T_{0+})^{\pi^+n} - (T_{0+})^{\pi^0p}, \\ S_{31} &= 2(T_{0+})^{\pi^0p} - (T_{0+})^{\pi^+n}, \end{aligned} \quad (2.13)$$

where $(T_{0+})^{\pi^0p}$ and $(T_{0+})^{\pi^+n}$ indicate the component in channel space of the 6×6 -matrix T_{0+} representing π^0p - and π^+n -scattering, respectively. Furthermore, S_{11} and S_{31} correspond to the common notation $L_{2I,2J}$, where L is the angular momentum, I is the isospin and $J = L + S$, where S is the spin. In this step, the violation of the isospin-symmetry due to the inclusion of higher orders in the amplitude is neglected. However, the isospin violation through the hadron masses is still included.

Before fitting the partial waves to data, it has to be clarified which fit-parameters should be used. Unlike in perturbation theory, in coupled-channel models it is common practice to take *different* renormalization constants for each channel. The argumentation behind that is, that by omitting all other Feynman-diagrams, such as higher order terms, and by only iterating one kind of a graph, there has to be a compensation for the loss of amplitudes. Nevertheless, the isospin-symmetry forbids to take different renormalization

constants for one multiplet, resulting in a total of four independent renormalization constants $\mu_{B\phi}$ for the six channels in eq. (2.9):

$$\begin{aligned}
(p\pi^0, n\pi^+) &\rightarrow \mu_{N\pi} \\
(p\eta) &\rightarrow \mu_{p\eta} \\
(\Lambda K^+) &\rightarrow \mu_{\Lambda K} \\
(\Sigma^0 K^+, \Sigma^+ K^0) &\rightarrow \mu_{\Sigma K}
\end{aligned} \tag{2.14}$$

It is now possible to fit the model to the data from the SAID group at GWU [33]. For all calculations throughout this work the masses of the involved particles are taken from the particle data group [34] to be

$$\begin{aligned}
m_p &= 0.9383 \text{ GeV}, & M_{\pi^0} &= 0.1350 \text{ GeV}, \\
m_n &= 0.9396 \text{ GeV}, & M_{\pi^+} &= 0.1396 \text{ GeV}, \\
m_\Lambda &= 1.1157 \text{ GeV}, & M_\eta &= 0.5475 \text{ GeV}, \\
m_{\Sigma^0} &= 1.1926 \text{ GeV}, & M_{K^+} &= 0.4937 \text{ GeV}, \\
m_{\Sigma^+} &= 1.1894 \text{ GeV}, & M_{K^0} &= 0.4976 \text{ GeV},
\end{aligned} \tag{2.15}$$

which means that higher order contributions from ChPT are included in the masses.

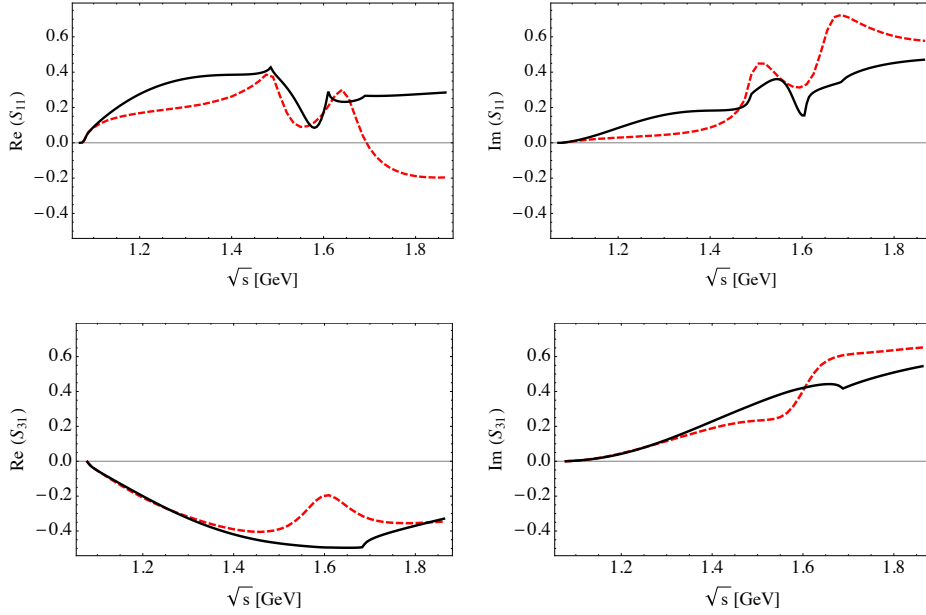


Figure 2.1: S_{11} and S_{31} partial waves for a fit to data of the SAID group [33] from 1100 MeV up to 1655 MeV. The dashed lines represent the partial waves obtained by the SAID group, the solid lines represent the best fit.

The best fit to both, the S_{11} and S_{31} partial waves, at energies between 1100 MeV and 1655 MeV is illustrated in fig 2.1. This particular energy region

is not mandatory to the outcome of the fitting procedure, the region may be varied by approximately 50 MeV to 100 MeV without changing the outcome drastically. The obtained renormalization constants are¹

$$\begin{aligned}
\log(\mu_{N\pi}^{(1)}/\text{GeV}) &= -1.04479, \\
\log(\mu_{p\eta}^{(1)}/\text{GeV}) &= -1.03018, \\
\log(\mu_{\Lambda K}^{(1)}/\text{GeV}) &= -1.83275, \\
\log(\mu_{\Sigma K}^{(1)}/\text{GeV}) &= 1.59499,
\end{aligned}
\tag{2.16}$$

where a logarithmic representation was chosen, as the renormalization constants enter the loop integrals in that manner (see appendix B).

As can be seen, the model does not match well to the data. Nevertheless there is a qualitative agreement up to approximately 1550 MeV, which resembles somewhat the behaviour already found in [35].

To further analyze the model, the partial waves can be continued analytically to the second Riemann sheet. To do so, the correct analytic continuation of the two-point functions I_{MB} , originating from the integral G in eq. (2.7) (see appendix B), to their complex planes must be assured. When crossing the branch cut in the complex s -plane from above, i.e. from positive values of $\text{Re}(s)$, in order to get to the second Riemann sheet, the logarithm appearing in I_{MB} collects an additional term due to its ambiguity as an inverse function. For I_{MB} this term manifests in precisely twice its imaginary part (which is the discontinuity) just above the branch cut on the first Riemann sheet. Hence, for a numeric computation the substitution

$$I_{MB}^{bj,ai} \rightarrow I_{MB}^{bj,ai} - \frac{i q_{ai}}{4\pi\sqrt{s}} \delta_{ba} \delta_{ji} \theta(\text{Re}(s) - (m_a + M_i)^2)
\tag{2.17}$$

has to be made. The step function $\theta(\text{Re}(s) - (m_a + M_i)^2)$ enters the equation due to the differing two-particle thresholds of the various channels. The step function also has a side effect: The Riemann sheets that are reached by trespassing the real s -axis above the various two-particle thresholds are effectively 'glued' together, making it possible to visualize all sheets in one image. Because of the step function, there will be artificial cuts in the plots that are perpendicular to the real axis starting at each threshold.

In this energy regime, the S_{11} and S_{31} partial waves should reveal three resonances on the second Riemann sheet: The $S_{11}(1535)$, the $S_{11}(1650)$ and the $S_{31}(1620)$. However, in the sheets of the model amplitude, shown in fig. 2.2, only one resonance at

$$(\sqrt{s_{\text{res}}})^{(1)} \approx [1590 - 48i] \text{ MeV}$$

¹For later reference, the results of this fit are indexed with a '(1)'.

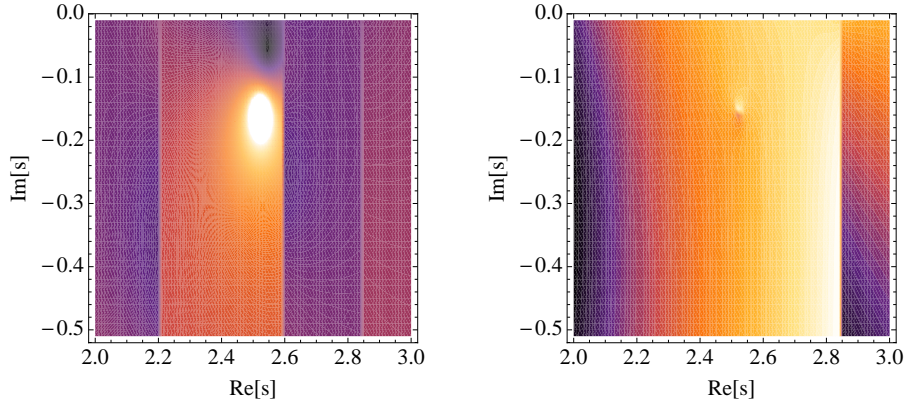


Figure 2.2: Second Riemann sheets of $|S_{11}|$ (left) and $|S_{31}|$ (right) model partial waves for a fit to the data of [33] from 1100 MeV up to 1655 MeV. Brighter means higher values.

appears in the S_{11} partial wave. This resonance seems to be the $S_{11}(1535)$, although its real part is slightly larger than the analyses collected in [34]:

$$(\sqrt{s_{\text{res}}})^{\text{data}} = [(1490\dots1530) - (45\dots125)i] \text{ MeV}. \quad (2.18)$$

Apparently, the model with only the Weinberg-Tomozawa coupling can not generate the $S_{11}(1650)$ and the $S_{31}(1620)$ dynamically². As a matter of fact, the structure in the $\text{Re}(S_{11})$ diagram in fig. 2.1 at about 1600 MeV up to 1700 MeV is a mere cusp effect, although it might look like a resonance. Thus, the previous fitting attempt to the partial wave data is indeed inadequate. A good agreement between model and data can only occur if the resonances evident from the data also occur in the model. To avoid the futile fitting of resonances which are not dynamically generated, the region of the input data must be modified as to only contain the low-energy regime and the $S_{11}(1535)$ resonance.

The diagrams in fig. 2.3 illustrate the simultaneous fit to the S_{11} data from 1100 MeV up to 1565 MeV, in order to avoid the $S_{11}(1650)$, and the S_{31} data from 1100 MeV up to 1400 MeV avoiding the $S_{31}(1620)$. Again the exact range of the fit is not mandatory to the outcome of the fitting procedure, the energy range may be varied a little without a substantial change. The

²In [36] it is stated that by replacing the divergent integrals by finite constants and fitting them to experimental data, it is possible to generate the $S_{11}(1535)$ and the $S_{11}(1650)$ (besides an unphysical pole). However, this amounts to a total of 12 fitting parameters (not including masses and decay constants), which may obscure the actual physical content of the model.

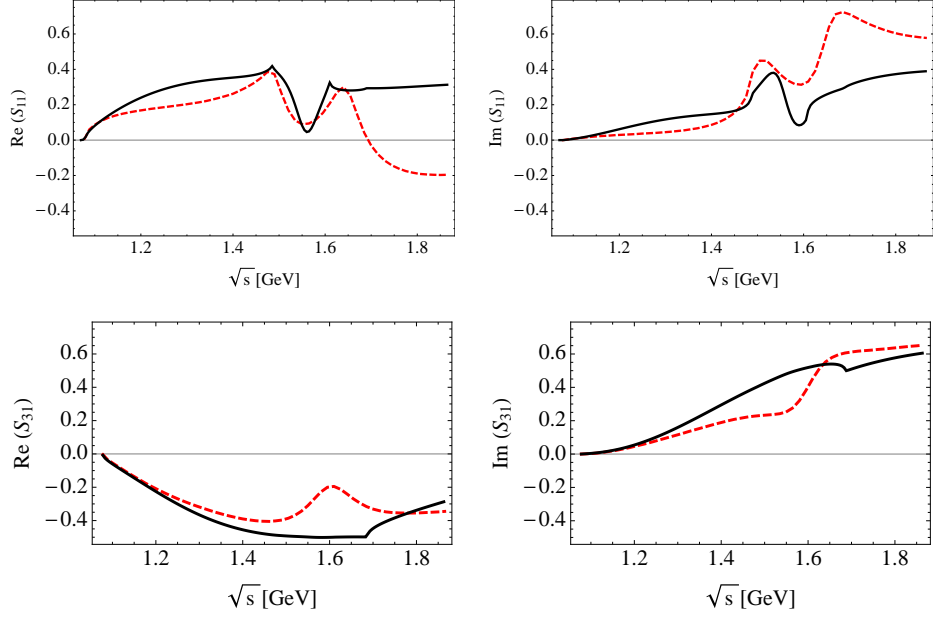


Figure 2.3: S_{11} and S_{31} partial waves for a fit to the data of [33] from 1100 MeV up to 1565 MeV for the S_{11} and from 1100 MeV up to 1400 MeV for the S_{31} . The dashed lines are the data, the solid lines are the best fit.

obtained renormalisation constants are

$$\begin{aligned}
 \log(\mu_{N\pi}^{(2)}/\text{GeV}) &= -1.43904, \\
 \log(\mu_{p\eta}^{(2)}/\text{GeV}) &= -0.791079, \\
 \log(\mu_{\Lambda K}^{(2)}/\text{GeV}) &= -1.81753, \\
 \log(\mu_{\Sigma K}^{(2)}/\text{GeV}) &= 1.88101.
 \end{aligned}
 \tag{2.19}$$

As can be seen, there is a slight improvement in the low-energy regime for the S_{11} partial wave as well as in the shape of the imaginary part around the $S_{11}(1535)$ resonance. The enhancement can be expressed via the quantity³

$$\begin{aligned}
 \chi^2(\mu^{(i)}) &= \sum_{E_{\text{cm}} < 1565 \text{ MeV}} \frac{(\text{data}_{11}(E_{\text{cm}}) - S_{11}(E_{\text{cm}}, \mu^{(i)}))^2}{S_{11}(E_{\text{cm}}, \mu^{(i)})} \\
 &+ \sum_{E_{\text{cm}} > 1100 \text{ MeV}} \frac{(\text{data}_{31}(E_{\text{cm}}) - S_{31}(E_{\text{cm}}, \mu^{(i)}))^2}{S_{31}(E_{\text{cm}}, \mu^{(i)})},
 \end{aligned}
 \tag{2.20}$$

where $\mu^{(i)} = (\mu_{\pi N}^{(i)}, \mu_{\eta p}^{(i)}, \mu_{K\Lambda}^{(i)}, \mu_{K\Sigma}^{(i)})$ is an abbreviation for the renormalization

³This quantity was used to find the best fits, however with different summation constraints for the first fit.

constants of eq. (2.16) and eq. (2.19). The data points at the center-of-mass energy $E_{\text{cm}} = \sqrt{s}$ are denoted by $\text{data}_{11}(E_{\text{cm}})$ and $\text{data}_{31}(E_{\text{cm}})$, and lastly, the functions S_{11} and S_{31} are the model partial wave amplitudes from eq. (2.13). The quantity of eq. (2.20) looks like the test statistic of the common chi-square test. However, since there is neither an assumption about errors nor their distribution, the χ^2 of eq. (2.20) is a mere measure of how close the model matches the data points.

Comparing the results of both fits yields

$$\frac{\chi^2(\mu^{(2)})}{\chi^2(\mu^{(1)})} = 0.739291,$$

i.e. the fitting procedure avoiding the resonances, that are not dynamically generated by the model, results in an improvement of about 26% in the low-energy regime.

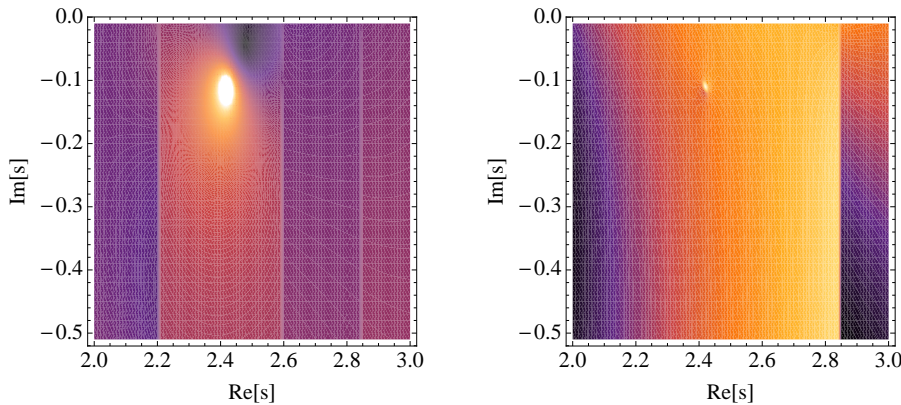


Figure 2.4: Second Riemann sheets of $|S_{11}|$ (left) and $|S_{31}|$ (right) partial waves for a fit to the data of [33] from 1100 MeV up to 1565 MeV for the S_{11} and from 1100 MeV up to 1400 MeV for the S_{31} . Brighter means higher values.

Extracting the resonance position of the second Riemann sheets in fig. 2.4 yields

$$(\sqrt{s_{\text{res}}})^{(2)} \approx [1556 - 35i] \text{ MeV}, \quad (2.21)$$

where the real part is closer to the estimate provided by the particle data group [34] (see eq. (2.18)), but the imaginary part is now lower than the estimate.

2.3 Conclusion

It is possible to find an analytic solution for the Bethe-Salpeter equation using solely the Weinberg-Tomozawa vertex as the interaction kernel. However, by this approach only the $S_{11}(1535)$ can be generated dynamically. Therefore a complete fit to energies where the $S_{31}(1620)$ and the $S_{11}(1650)$ contribute significantly is impossible⁴ and results in a displacement of the $S_{11}(1535)$ position in the model. However, even by indentifying the resonances that are not dynamically generated and by choosing the fitting region to avoid these resonances, the prediction for the position of the $S_{11}(1535)$ could not be improved.

Although the Weinberg-Tomozawa vertex has a significant contribution to the S_{11} and S_{31} partial waves, it is not possible to achieve a decent fit to the data from threshold to about the $S_{11}(1535)$, where the resonance appears at the correct position. The problem lies within the interaction kernel itself, i.e. the model for the scattering amplitude presented in this chapter is the minimal way to describe πN -scattering in an off-shell coupled channel approach. An extension of the interaction kernel is possible and yields superior results, but is also by far more involved. By incorporating the contact interactions from the next-to-leading order Lagrangian, the low-energy behaviour can be improved and the $S_{11}(1650)$ can be generated dynamically (see [28]). A more severe problem lies within the generation of the $S_{31}(1620)$. There is currently no model⁵ that produces such a resonance. It seems likely that it has at most a small dynamically generated component, which means that it has to be incorporated as an explicit field.

⁴As seen in fig. 2.1, it is possible that by coincidence a cusp effect mimics somewhat the behaviour of a resonance.

⁵Including also the on-shell approaches.

Chapter 3

η -Photoproduction off the proton

The goal of this chapter is the construction of a unitary and gauge-invariant photoproduction amplitude off protons as well as a fit to data. The upcoming treatment will proceed in analogy to previous work of Borasoy, Bruns, Meißner and Nißler [5] on Kaon photo- and electroproduction. Therefore the following evaluation leads to the η -electroproduction amplitude, where, in the end, the photon virtuality will be taken to zero in order to retrieve the photoproduction amplitude.

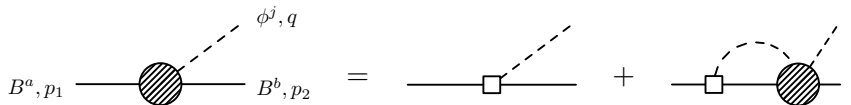
3.1 Construction of the amplitude

As described in sections 1.2 and 1.3 it is possible to construct a unitarized *and* gauge-invariant amplitude. However, for the construction it is necessary to find a unitary 'skeleton'-amplitude, to which the photon can be coupled in a gauge-invariant manner. The virtual process $p \rightarrow B\phi$ is suited for this purpose, since coupling of an incoming photon to this would render the process to be $\gamma p \rightarrow B\phi$, where B is a baryon and ϕ is a meson.

As seen in section 1.2, a 'skeleton'-amplitude Γ for the virtual process $p \rightarrow B\phi$ that is unitary in the subspace of meson-baryon scattering has to fulfill the equation

$$\Gamma(\not{q}, \not{p}) = \hat{V}(\not{q}, \not{p}) + \int \frac{d^d l}{(2\pi)^d} T(\not{q}, l; p) iS(\not{p} - l) \Delta(l) \hat{V}(l, \not{p}), \quad (3.1)$$

or diagrammatically



where $p = p_2 + q$ is the total four-momentum and T is the solution of the BSE for meson-baryon scattering from section 2.1. Note, that with this particular ansatz crossing symmetry is violated. Furthermore,

$$\hat{V}(\not{q}, \not{p}) = \begin{array}{c} \phi^j, q \\ \diagup \\ \text{---} \square \text{---} \\ \text{---} B^a, p_1 \quad \quad B^b, p_2 \end{array}$$

is a real kernel. This vertex comes from the chiral vielbein u_μ of eq. (1.16) appearing in the leading order meson-baryon Lagrangian of eq. (1.17). Expanding u_μ up to $\mathcal{O}(\phi)$ gives

$$u_\mu = iu^\dagger \nabla_\mu U u^\dagger = -\frac{\sqrt{2}}{f} \partial_\mu \phi + \mathcal{O}(\phi^2).$$

Here, U is given by eq. (1.12), $u = \sqrt{U}$ and the covariant derivative ∇_μ is given by eq. (1.14), where the external fields v_μ and a_μ are set to zero for now. Inserting u_μ into the last two terms on the right hand side of the chiral Lagrangian of eq. (1.17) leads to

$$\begin{aligned} & -\frac{D}{2} \langle \bar{B} \gamma^\mu \gamma_5 \{u_\mu, B\} \rangle - \frac{F}{2} \langle \bar{B} \gamma^\mu \gamma_5 [u_\mu, B] \rangle \\ & = +\frac{D}{\sqrt{2}f} \langle \bar{B} \gamma^\mu \gamma_5 \{\partial_\mu \phi, B\} \rangle + \frac{F}{\sqrt{2}f} \langle \bar{B} \gamma^\mu \gamma_5 [\partial_\mu \phi, B] \rangle \end{aligned}$$

The corresponding potential is then given by

$$\hat{V}^{bj,a}(\not{q}) = \not{q} \gamma_5 \hat{g}^{bj,a},$$

where

$$\hat{g}^{bj,a} = -\frac{D}{\sqrt{2}f_j} \langle (\lambda^b)^\dagger \{(\lambda^j)^\dagger, \lambda^a\} \rangle - \frac{F}{\sqrt{2}f_j} \langle (\lambda^b)^\dagger [(\lambda^j)^\dagger, \lambda^a] \rangle.$$

Inserting \hat{V} and T into eq. (3.1) and replacing $l \rightarrow (\not{p} - m) - (\not{p} - l - m)$, the integration simplifies via cancellations of the fermion propagator and yields

$$\Gamma(\not{q}, \not{p}) = \not{q} \gamma_5 \hat{g} + T(\not{q}, \not{p} - m; p) [(\not{p} - m)G(p) - I_M] \gamma_5 \hat{g}.$$

Collecting the Dirac-structures leads to

$$\Gamma(\not{q}, \not{p}) = [\not{q} \not{p} \Gamma_1(p) + \not{q} \Gamma_2(p) + \not{p} \Gamma_3(p) + \Gamma_4(p)] \gamma_5. \quad (3.2)$$

With the abbreviation $T_i(p) = T_i$, the Γ_i are given by

$$\begin{aligned} \Gamma_1(p) &= T_1(p^2 H_1 - m H_0) + T_2(H_0 - m H_1) + T_4 H_0 + T_6 H_1, \\ \Gamma_2(p) &= \hat{g} + p^2 T_1(H_0 - m H_1) + T_2(p^2 H_1 - m H_0) + p^2 T_4 H_1 + T_6 H_0, \\ \Gamma_3(p) &= T_3(p^2 H_1 - m H_0) + T_5(H_0 - m H_1) + T_7 H_0 + T_8 H_1, \\ \Gamma_4(p) &= p^2 T_3(H_0 - m H_1) + T_5(p^2 H_1 - m H_0) + p^2 T_7 H_1 + T_8 H_0, \end{aligned}$$

with

$$\begin{aligned} H_1 &= (G_0(p) - mG_1(p))\hat{g}, \\ H_0 &= (p^2G_1(p) - mG_0(p) - I_M)\hat{g}, \end{aligned}$$

where I_M is given by eq. (B.1), and G_1 and G_0 are given by eq. (B.5).

Before coupling the photon to the 'skeleton'-amplitude, the channels can be restricted once again due to charge and strangeness conservation. Using only the groundstate meson and baryon octets, the process $\gamma p \rightarrow MB$ renders the possible intermediate and final particles to be the same as in eq. (2.9). Note, that by choosing the initial baryon to be fixed as a proton, the potential \hat{V} , and hence the amplitude Γ , become six-dimensional vectors in channel-space.

Now the photon can be coupled to the 'skeleton'-amplitude. Gauge invariance can be obtained by taking *all* possible Feynman diagrams into account, where the photon couples to any external and internal lines as well as to any vertices. The vertex rules for the latter can be derived from the chiral Lagrangian by inclusion of a vector field, i.e. $v_\mu \neq 0$. However, the amplitude for the process $\gamma p \rightarrow B\phi$ must fulfill the partial unitarity condition as well, i.e. the photoproduction amplitude \mathcal{M} obeys the equation

$$\mathcal{M}^\mu(\not{q}, \not{k}; p) = \mathcal{M}_0^\mu(\not{q}, \not{k}; p) + \int \frac{d^d l}{(2\pi)^d} T(\not{q}, l; p) iS(\not{p} - l) \Delta(l) \mathcal{M}_0^\mu(l, \not{k}; p), \quad (3.3)$$

where \mathcal{M}_0^μ is a real kernel. Note that for the present case, the photoproduction amplitude \mathcal{M} is a six-dimensional vector in channel space and likewise all of the following amplitudes.

In total, there are five different classes of photoproduction amplitudes that are described by eq. (3.3), where each class obeys the partial unitarity condition by itself. The first one consists of the diagrams:

$$S_s^\mu = \begin{array}{c} \begin{array}{c} \gamma, k \\ \text{wavy line} \\ \bullet \\ B^a, p_1 \end{array} \text{---} \begin{array}{c} \square \\ \text{vertex} \end{array} \text{---} \begin{array}{c} \phi^j, q \\ \text{dashed line} \\ B^b, p_2 \end{array} \\ + \\ \begin{array}{c} \gamma, k \\ \text{wavy line} \\ \bullet \\ B^a, p_1 \end{array} \text{---} \begin{array}{c} \square \\ \text{vertex} \end{array} \text{---} \begin{array}{c} \text{shaded circle} \\ \text{kernel} \end{array} \text{---} \begin{array}{c} \phi^j, q \\ \text{dashed line} \\ B^b, p_2 \end{array} \end{array},$$

where the kernel is the tree graph on the right hand side. The coupling of the photon occurs via the common quantum electrodynamics vertex $ieQ\gamma^\mu$, which is the coupling of v_μ to the baryons and mesons. Here, Q is the charge of the involved particle, which in this case is a proton¹, s.t. $Q = 1$. Using the pertinent Feynman rules, keeping in mind that Γ already contains the tree graph, yields

$$S_s^\mu = \Gamma(\not{q}, \not{p}) iS(\not{p}) (ie\gamma^\mu), \quad (3.4)$$

¹The notation for the initial baryon state B^a was left in the Feynman diagrams to avoid confusion of the abbreviation 'p' for protons with the total four-momentum. Keep in mind, that from here on the initial state baryon is always a proton.

where $p = p_1 + k = p_2 + q$ is the total four-momentum.

The second class contains the u-channel diagram and a diagram where the photon couples to an intermediate baryon:

$$S_u^\mu + S_B^\mu = \begin{array}{c} \text{Diagram 1: } B^a, p_1 \text{ (solid line) enters a shaded vertex. A wavy line } \gamma, k \text{ enters from below. A dashed line } \phi^j, q \text{ exits to the right. A solid line } B^b, p_2 \text{ exits to the right.} \\ \text{Diagram 2: } B^a, p_1 \text{ (solid line) enters a shaded vertex. A wavy line } \gamma, k \text{ enters from below. A dashed line } \phi^j, q \text{ exits to the right. A solid line goes to a second shaded vertex. A wavy line } \gamma, k \text{ enters from below. A solid line } B^b, p_2 \text{ exits to the right.} \end{array} +$$

Since S_u^μ is real in the physical region for the photoproduction process, it can constitute the kernel for this class. Again, using Feynman rules leads to

$$S_u^\mu = (ieQ_B \gamma^\mu) iS(\not{p}_1 - \not{q}) \Gamma(\not{q}, \not{p}_1), \quad (3.5)$$

$$S_B^\mu = -i \int \frac{d^d l}{(2\pi)^d} T(\not{q}, \not{l}; p) S(\not{p} - \not{l}) \Delta(l) (eQ_B \gamma^\mu) S(\not{p}_1 - \not{l}) \Gamma(\not{l}, \not{p}_1), \quad (3.6)$$

where the baryon charge matrix

$$Q_B = \text{diag}(1, 0, 1, 0, 0, 1)$$

in channel space was introduced to account for the various charges appearing in the six channels in intermediate and final states.

Likewise, the third class consists of the t-channel diagram and a diagram where the photon couples to an intermediate meson:

$$S_t^\mu + S_M^\mu = \begin{array}{c} \text{Diagram 1: } B^a, p_1 \text{ (solid line) enters a shaded vertex. A wavy line } \gamma, k \text{ enters from above. A dashed line } \phi^j, q \text{ exits to the right. A solid line } B^b, p_2 \text{ exits to the right.} \\ \text{Diagram 2: } B^a, p_1 \text{ (solid line) enters a shaded vertex. A wavy line } \gamma, k \text{ enters from above. A dashed line } \phi^j, q \text{ exits to the right. A solid line goes to a second shaded vertex. A wavy line } \gamma, k \text{ enters from above. A solid line } B^b, p_2 \text{ exits to the right.} \end{array} +$$

where S_t^μ is also real in the physical region for the photoproduction process and constitutes the kernel for this class. Using the vertex rule $ieQ_M(2q - k)^\mu$ from scalar quantum electrodynamics one arrives at

$$S_t^\mu = (ieQ_M(2q - k)^\mu) i\Delta(q - k) \Gamma(\not{q} - \not{k}, \not{p}_1), \quad (3.7)$$

$$S_M^\mu = -i \int \frac{d^d l}{(2\pi)^d} T(\not{q}, \not{p} - \not{l}; p) S(\not{l}) \Delta(p - l) (eQ_M(2(p_1 - l) + k)^\mu) \\ \times \Delta(p_1 - l) \Gamma(\not{p}_1 - \not{l}, \not{p}_1), \quad (3.8)$$

where

$$Q_M = \text{diag}(0, 1, 0, 1, 1, 0)$$

is the meson charge matrix for intermediate and final state particles in channel space.

The fourth class arises solely due to the 'Kroll-Ruderman' (KR) interaction contained in the meson-baryon chiral Lagrangian of eq. (1.17):

$$S_{KR}^\mu = \begin{array}{c} \begin{array}{c} \gamma, k \\ \text{---} \end{array} \begin{array}{c} \phi^j, q \\ \text{---} \end{array} \\ \begin{array}{c} B^a, p_1 \\ \text{---} \end{array} \begin{array}{c} \square \\ \text{---} \end{array} \begin{array}{c} B^b, p_2 \\ \text{---} \end{array} + \begin{array}{c} \gamma, k \\ \text{---} \end{array} \begin{array}{c} \phi^j, q \\ \text{---} \end{array} \\ \begin{array}{c} B^a, p_1 \\ \text{---} \end{array} \begin{array}{c} \square \\ \text{---} \end{array} \begin{array}{c} \text{---} \\ \text{---} \end{array} \begin{array}{c} B^b, p_2 \\ \text{---} \end{array} \end{array}.$$

The vertex stems from the covariant derivative ∇_μ in the chiral vielbein u_μ of eq. (1.16). Expanding u_μ and keeping only terms including the vector field $v_\mu = -ieQ_q A_\mu$, where $Q_q = \frac{1}{3} \text{diag}(2, -1, -1)$ is the quark charge matrix in $SU(3)$, and accounting for the terms with one meson leg amounts to

$$u_\mu = i u^\dagger \nabla_\mu U u^\dagger = i \frac{\sqrt{2} e}{f} A_\mu [Q_q, \phi] + \mathcal{O}(\phi^2)$$

Inserting this into the last two terms of the chiral Lagrangian of eq. (1.17) gives

$$\begin{aligned} & -\frac{D}{2} \langle \bar{B} \gamma^\mu \gamma_5 \{u_\mu, B\} \rangle - \frac{F}{2} \langle \bar{B} \gamma^\mu \gamma_5 [u_\mu, B] \rangle \\ &= -i \frac{eD}{\sqrt{2}f} \langle \bar{B} \gamma^\mu \gamma_5 \{A_\mu [Q_q, \phi], B\} \rangle - i \frac{eF}{\sqrt{2}f} \langle \bar{B} \gamma^\mu \gamma_5 [A_\mu [Q_q, \phi], B] \rangle + \mathcal{O}(\phi^2) \\ &= -i \frac{eD}{\sqrt{2}f} Q_\phi \langle \bar{B} \gamma^\mu \gamma_5 A_\mu \{\phi, B\} \rangle - i \frac{eF}{\sqrt{2}f} Q_\phi \langle \bar{B} \gamma^\mu \gamma_5 A_\mu [\phi, B] \rangle + \mathcal{O}(\phi^2), \end{aligned}$$

where it was used that for a meson ϕ of a specified type, $[Q_q, \phi] = Q_\phi \phi$ is valid, where Q_ϕ is the charge of the meson ϕ . Note that Q_ϕ is not a matrix, but a mere number. However, evaluating the corresponding vertex rule for all six channels, it is straightforward to see that the potential reads

$$V_{KR}^\mu = eQ_M \hat{g} \gamma^\mu \gamma_5,$$

where Q_M is the meson charge matrix in channel space. Thus, the amplitude for the fourth class is given by

$$S_{KR}^\mu = V_{KR}^\mu + \int \frac{d^d l}{(2\pi)^d} T(\not{q}, \not{l}; p) iS(\not{p} - \not{l}) \Delta(l) V_{KR}^\mu. \quad (3.9)$$

Finally, the Feynman diagrams for the fifth class emerge from the chiral connection Γ^μ by the inclusion of an external vector field v_μ , giving rise to a $\bar{B}B\phi\phi\gamma$ interaction:

$$S_{WT1}^\mu + S_{WT2}^\mu = \begin{array}{c} \begin{array}{c} \phi^j, q \\ \text{---} \end{array} \\ \begin{array}{c} B^a, p_1 \\ \text{---} \end{array} \begin{array}{c} \text{---} \\ \text{---} \end{array} \begin{array}{c} \square \\ \text{---} \end{array} \begin{array}{c} B^b, p_2 \\ \text{---} \end{array} \\ \begin{array}{c} \gamma, k \\ \text{---} \end{array} \end{array} + \begin{array}{c} \begin{array}{c} \phi^j, q \\ \text{---} \end{array} \\ \begin{array}{c} B^a, p_1 \\ \text{---} \end{array} \begin{array}{c} \text{---} \\ \text{---} \end{array} \begin{array}{c} \square \\ \text{---} \end{array} \begin{array}{c} \text{---} \\ \text{---} \end{array} \begin{array}{c} B^b, p_2 \\ \text{---} \end{array} \\ \begin{array}{c} \gamma, k \\ \text{---} \end{array} \end{array}.$$

The vertex rule can be obtained by expanding the Γ^μ with a vector field $v_\mu = -ieQ_q A_\mu$ up to $\mathcal{O}(\phi^2)$, which leads to

$$\begin{aligned}\Gamma_\mu &= \frac{1}{2} \left(u^\dagger (\partial_\mu - iv_\mu) u + u (\partial_\mu - iv_\mu) u^\dagger \right) \\ &= -\frac{i}{2} \left(\left[1 - \frac{i\phi}{\sqrt{2}f} - \frac{\phi^2}{4f^2} \right] v_\mu \left[1 + \frac{i\phi}{\sqrt{2}f} - \frac{\phi^2}{4f^2} \right] \right. \\ &\quad \left. + \left[1 + \frac{i\phi}{\sqrt{2}f} - \frac{\phi^2}{4f^2} \right] v_\mu \left[1 - \frac{i\phi}{\sqrt{2}f} - \frac{\phi^2}{4f^2} \right] \right) + \dots \\ &= \frac{i}{4f^2} (-2\phi v_\mu \phi + v_\mu \phi^2 + \phi^2 v_\mu) + \dots \\ &= \frac{e}{4f^2} A_\mu [[Q_q, \phi], \phi] + \dots,\end{aligned}$$

where the ellipsis stands for higher order terms in ϕ and for terms that do not contain the vector field v_μ . Inserting this into the Lagrangian gives

$$\langle \bar{B} \gamma^\mu i [\Gamma_\mu, B] \rangle = \frac{ie}{4f^2} \langle \bar{B} \gamma^\mu A_\mu [[Q_q, \phi], \phi], B \rangle$$

Since each of the ϕ can be either an incoming or an outgoing particle, the corresponding vertex contains two terms that account for different charges of the incoming and outgoing mesons. Therefore the potential in matrix form reads

$$V_{WT\gamma}^\mu = e\gamma^\mu \{Q_M, g\}.$$

Consequently, the amplitudes of the fifth class are given by

$$S_{WT1}^\mu = V_{WT\gamma}^\mu \int \frac{d^d l}{(2\pi)^d} iS(\not{p}_1 - \not{l}) \Delta(l) \Gamma(\not{l}, \not{p}_1), \quad (3.10)$$

$$S_{WT2}^\mu = \int \frac{d^d \tilde{l}}{(2\pi)^d} T(\not{q}, \not{\tilde{l}}; p) iS(\not{p} - \not{\tilde{l}}) \Delta(\tilde{l}) S_{WT1}^\mu. \quad (3.11)$$

As mentioned earlier, each of the five classes is unitary in the subspace of meson-baryon scattering by itself. Due to the linearity of eq. (3.3) in \mathcal{M}_0 , the total photoproduction amplitude

$$\mathcal{M}^\mu = S_s^\mu + S_u^\mu + S_t^\mu + S_B^\mu + S_M^\mu + S_{KR}^\mu + S_{WT1}^\mu + S_{WT2}^\mu$$

also obeys eq. (3.3) and thus is unitary in that sense. However, only the sum of the amplitudes of *all* five classes yields a gauge-invariant amplitude. This can be seen from evaluating the contraction $k_\mu \mathcal{M}^\mu$ while setting the external particles on-shell. The explicit but lengthy evaluation is provided in appendix C.

For the upcoming numeric computation it is convenient to decompose the amplitudes into independent Lorentz-structures which is carried out in

appendix D. The corresponding unpolarized differential cross sections can be calculated by using the operator basis \mathcal{N}_k^μ commonly used for photoproduction processes and then evaluating the CGLN-amplitudes, which is provided in appendix E.

3.2 Results

In this section the results of a fit to differential cross section data of the above photoproduction model will be presented. The fitting parameters will be the four renormalization constants $\mu_{N\pi}$, $\mu_{p\eta}$, $\mu_{\Lambda K}$ and $\mu_{\Sigma K}$ appearing in the six channels as described by eq. (2.14). Masses and decay constants are again set to physical values, which are quantified by eq. (2.15) and eq. (2.3), respectively.

Since the goal is to calculate the photoproduction amplitude, the photon has to be real, i.e. $k^2 = 0$. But due to k^2 appearing in various denominators (see appendix B) it is numerically not possible to simply set k^2 to zero. However, since there can not be a physical singularity at $k^2 = 0$, because the photoproduction process is a boundary case of electroproduction, the limit $k^2 \rightarrow 0^-$ from below can be taken. In practice, k^2 can be set to any sufficiently small negative value.

As a measure of the goodness of the fit, the common

$$\chi^2/\text{d.o.f.} = \frac{N}{\sigma N - \delta} \sum_E \frac{1}{n(E)} \left(\sum_z \frac{(\text{data}(E, z) - \frac{d\sigma}{d\Omega}(E, z, \mu))^2}{(\text{err}(E, z))^2} \right)$$

will be used, where $\text{data}(E, z)$ is the data point at energy E and angle $z = \cos(\theta)$ and $\text{err}(E, z)$ is its corresponding error estimate. The prediction of the differential cross section from the model is given by $\frac{d\sigma}{d\Omega}(E, z, \mu)$ at energy E , angle z and at specific values of the four renormalization constants which are collectively called μ . Furthermore, $n(E)$ is the number of data points at energy E , σ is the number of distinct energies E , δ is the number of degrees of freedom and N is the total number of data points, i.e. $N = \sum_E n(E)$.

For the upcoming fit, experimental differential cross section data for the η -photoproduction off the proton is taken from McNicoll et al. [29]. The goal was to find a fit that describes the data within the largest possible range, where $\chi^2/\text{d.o.f.} < 1$ is fulfilled. This is achieved by the center-of-mass energy range $1487.8 \text{ MeV} < E_{\text{cm}} < 1609.0 \text{ MeV}$, which results in

$$\begin{aligned} \log(\mu_{N\pi}/\text{GeV}) &= -0.610537 \pm \begin{matrix} 0.000355 \\ 0.000506 \end{matrix}, \\ \log(\mu_{p\eta}/\text{GeV}) &= -0.511596 \pm \begin{matrix} 0.056634 \\ 0.051671 \end{matrix}, \\ \log(\mu_{\Lambda K}/\text{GeV}) &= -5.11206 \pm \begin{matrix} 0.40299 \\ 0.31200 \end{matrix}, \\ \log(\mu_{\Sigma K}/\text{GeV}) &= 1.84511 \pm \begin{matrix} 0.00029 \\ 0.00041 \end{matrix} \end{aligned} \quad (3.12)$$

with

$$\chi^2/\text{d.o.f.} = 0.999645. \quad (3.13)$$

The errors were obtained by varying each parameter separately to higher and lower values until $\chi^2/\text{d.o.f.}$ increased by 1. Strictly speaking, the values found with that procedure are not errors, but rather a measure of how sensitive the model amplitude is to a change in a certain parameter. From eq. (3.12) it is clear that the parameter set has to be very fine tuned to achieve the current fit.

Some of the differential cross section data including the fitted model is shown in fig. 3.1 – the complete set is provided in appendix F. The error bounds were illustrated by computing the envelope function of all cross sections that are obtained when each parameter is varied separately to its error boundaries. Then, the shaded area indicates maximum and minimum values for the cross sections with separately varied parameters.

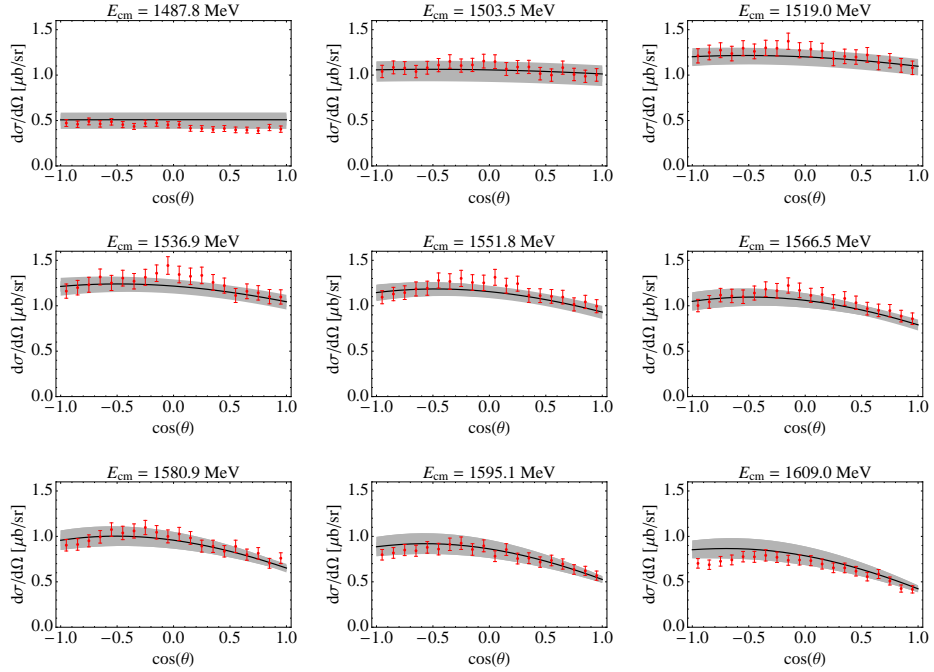


Figure 3.1: Parts of the differential cross section data from McNicoll et al. [29] (red symbols) with the corresponding best fit of the model evaluated in this chapter (black line) at various center-of-mass energies E_{cm} chosen from within the fitting range. The shaded area represents the errors.

Fig. 3.1 shows a good agreement between the experiment and the model, even more than 100 MeV away from threshold. The corresponding total cross section is displayed in fig. 3.2. Of course, the total cross section matches in

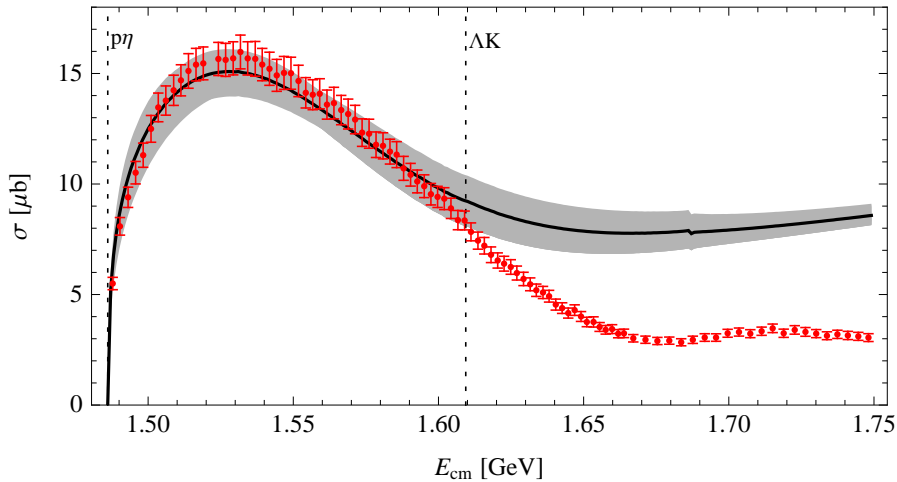


Figure 3.2: Total cross section data from McNicoll et al. [29] (red symbols) with the model amplitude fitted to this differential cross section data (black line). The errors are given by the shaded area and the vertical dashed lines represent the $p\eta$ - and the ΛK -threshold.

the fitted energy range, but at higher energies the cross section exceeds the data.

It is likely that the problem of the excess lies within the simple nature of the interaction kernel used for this model. The Weinberg-Tomozawa vertex generates only the $S_{11}(1535)$, which is said to saturate the cross section close to threshold [30]. As will be seen in the next chapter, the Weinberg-Tomozawa vertex, although generating a good portion of the $S_{11}(1535)$, is likely not to include the complete information of the resonance in leading order. However, the lacking parts can be compensated by an adequate choice of the renormalization parameters, which in return leads to an excess at higher energies.

As a last step, the prediction about the position of the $S_{11}(1535)$ shall be extracted from the model. Thus, the analytic continuation to the second Riemann sheet has to be calculated, as was done in section 2.2 for meson-baryon scattering. The substitution for the two-point function can be read off eq. (2.17). However, the photoproduction amplitude involves three-point integrals whose analytic structure contains, similarly to the two-point functions, branch cuts at each two-particle threshold along the positive real s axis.

Hence, the second Riemann sheet is reached numerically by replacing each two-point function as in eq. (2.17) and each three-point function $I_{M\bar{B}B}$ as

$$I_{M\bar{B}B}^{bj,ai}(s) \rightarrow I_{M\bar{B}B}^{bj,ai}(s) + \text{Disc}(I_{M\bar{B}B}^{bj,ai}(s)) \theta(\text{Re}(s) - (m_b + M_j)^2) \quad (3.14)$$

and analogously for I_{MMB} . The appearing two-point and three-point functions and the discontinuities of the three-point functions are evaluated in appendix B.

The function visualized in the following is the magnitude of the multipole E_{0+} which can be obtained using the CGLN-amplitudes (see appendix E for an explicit form of the CGLN-amplitudes):

$$E_{0+} = \int_{-1}^1 dz \left(\frac{1}{2} P_0(z) \mathcal{F}_1 - \frac{1}{2} P_1(z) \mathcal{F}_2 + \frac{1}{6} (P_0(z) - P_2(z)) \mathcal{F}_4 \right), \quad (3.15)$$

where the P_l , with $l = 0, 1, 2$, are the Legendre polynomials; \mathcal{F}_1 , \mathcal{F}_2 and \mathcal{F}_4 are CGLN-amplitudes and $z = \cos(\theta)$ is the scattering angle.

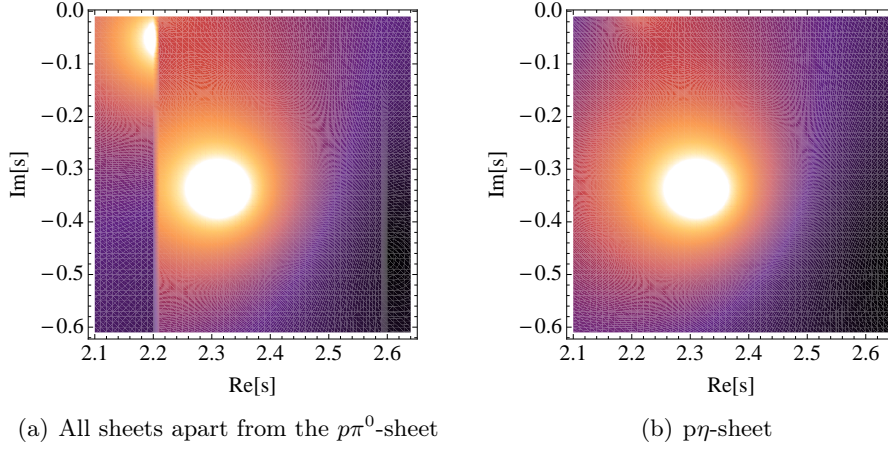


Figure 3.3: Visualization of the second Riemann sheets of $|E_{0+}|$: higher values are brighter, lower values are darker. (a) Composition of Riemann sheets, the cuts at $\text{Re}(s) \approx 2.2 \text{ GeV}^2$ and $\text{Re}(s) \approx 2.6 \text{ GeV}^2$ are due to the step functions θ in eq. (2.17) and eq. (3.14). (b) Analytic continuation of the $p\eta$ -sheet.

The resulting Riemann sheet is illustrated in fig. 3.3(a). As in section 2.2, the step function θ in the analytic continuations of the two-point and three-point functions amounts to cuts perpendicular to the real s -axis, starting at each two-particle threshold, however, those cuts are artificial and are of no physical relevance. The Riemann sheets in fig. 3.3(a) exhibit the only two resonances in the vicinity of the η -photoproduction regime, of which the one at lower $\text{Re}(s)$ lies fairly close to the real axis on the $n\pi^+$ -sheet. There is no known particle that would result in such a resonance, it is merely an artifact of the BSE on a sheet that is below the η -photoproduction threshold. As mentioned in section 1.2, such artifacts are the sacrifice that have to be made in order to obtain an exactly unitary amplitude. From a variation of

the parameters it seems, that this resonance is a shadow pole, since it moves in a correlated manner with the resonance on the $p\eta$ -sheet. Shadow poles are copies of a resonance that appear on other sheets and, unfortunately, it is not exactly determinable where this pole comes from or what its nature is. Therefore, this pole will be regarded as unphysical in the following.

To further illustrate the sheet of the η -photoproduction process in the physical photoproduction energy region, the analytic continuation of the $p\eta$ -sheet can be calculated. As mentioned above, fig. 3.3(a) displays Riemann sheets that are glued together at each threshold. This can be overcome by redefining the prescriptions of the analytic continuation in the integrals of eq. (2.17) and eq. (3.14) such that the step functions θ are set to the values they would have when crossing the real s -axis between the $p\eta$ -threshold and the ΛK^+ -threshold, i.e.

$$\theta(\text{Re}(s) - (m_b + M_j)^2) \stackrel{p\eta\text{-sheet}}{\equiv} \begin{cases} 1, & \text{for } (m_b + M_j)^2 \leq (m_p + M_\eta)^2 \\ 0, & \text{for } (m_b + M_j)^2 > (m_p + M_\eta)^2 \end{cases}.$$

To be clear, the step functions have to be replaced by the values on the r.h.s. independently of the value of $\text{Re}(s)$. The resulting analytic continuation of the $p\eta$ -sheet is shown in fig. 3.3(b). The position of the resonance on this sheet is

$$\sqrt{s_{\text{res}}} \approx [1527 - 111i] \text{ MeV},$$

which lies within the boundaries determined by analyses collected in [34], see eq. (2.18), and can therefore be identified with the $S_{11}(1535)$. As can be seen in fig. 3.3(b) the physical region of the η -photoproduction process seems unbiased by the shadow pole. And by observing that the fitting procedure correctly predicted the position of the $S_{11}(1535)$ it is evident that the contribution from the shadow pole is, at most, marginal.

3.3 Conclusion

A gauge-invariant unitary model amplitude has been fitted to differential cross section data of the η -photoproduction process off protons. The $S_{11}(1535)$ could be generated dynamically from the interaction kernel containing the Weinberg-Tomozawa vertex and its position lies within the error estimates of experimental analyses from the particle data group [34]. There appeared another resonance on the $n\pi^+$ -sheet, which is an artifact of the construction of the model, but its presence leaves the physical region of the η -photoproduction process apparently mostly unbiased and can therefore be ignored.

As expected, the validity of the model amplitude is extensive due to unitarization, which generates the $S_{11}(1535)$ dynamically, and due to the

enforcement of gauge invariance in a quantum field theoretical manner. Nevertheless, at energies beyond the ΛK -threshold the model exceeds the experimental data. A possible explanation is that the interaction kernel does not generate the 'whole' $S_{11}(1535)$, which has to be compensated by an adequate choice of the renormalization constants. But by choosing the renormalization constants to broaden and heighten the resonance in order to fit the data, the behavior of the model at higher energies will be elevated, too. However, this will be inspected more thoroughly in the next chapter.

Chapter 4

Extension of the amplitude

The goal of this chapter is to evaluate the gauge-invariant and unitarized photoproduction amplitude including the terms containing photon interactions from the next-to-leading order (NLO) meson-baryon Lagrangian of eq. (1.19). While doing so, one encounters some difficulties, which will be discussed in the following.

4.1 Construction of the amplitude

The groundwork for the extended amplitude was done in the previous chapter where the five unitarity classes were introduced which were unitary by themselves but only all five classes together would yield a gauge invariant amplitude. The extension of the amplitude will be entering the total amplitude in the same way: The new photon vertices that are going to be introduced in this chapter will be implemented as to obey eq. (3.3) and hence the partial unitarity requirement. Furthermore, gauge invariance has to be fulfilled for the new classes separately, as the five classes from the previous chapter already satisfy gauge invariance.

As before, the starting point will be the derivation of the vertex rules. The terms of the NLO Lagrangian of eq. (1.19) that include the photon field read

$$\mathcal{L}_{NLO}^\gamma = b_{12} \langle \bar{B} \sigma^{\mu\nu} \{F_{\mu\nu}^+, B\} \rangle + b_{13} \langle \bar{B} \sigma^{\mu\nu} [F_{\mu\nu}^+, B] \rangle, \quad (4.1)$$

where

$$F_{\mu\nu}^+ = u F_{\mu\nu}^L u^\dagger + u^\dagger F_{\mu\nu}^R u \quad (4.2)$$

with $F_{\mu\nu}^{L/R} = -e Q_q F_{\mu\nu}$ in the present case and $F_{\mu\nu} = \partial_\mu A_\nu - \partial_\nu A_\mu$ is the electromagnetic field strength tensor with the photon field A_μ . Furthermore, $Q_q = \frac{1}{3} \text{diag}(2, -1, -1)$ is the quark charge matrix and lastly the abbreviation $\sigma^{\mu\nu} = \frac{i}{2} [\gamma^\mu, \gamma^\nu]$ was used.

From the terms of the NLO Lagrangian proportional to b_{12} and b_{13} appearing in eq. (4.1) a $\bar{B}B\gamma$ -vertex rule can be derived. To this end, the u 's,

where terms of lower and higher order than $\mathcal{O}(\phi^2)$ were abbreviated by $\mathcal{O}(\phi^0)$ and $\mathcal{O}(\phi^4)$, respectively. Inserting $F_{\mu\nu}^+$ into the Lagrangian \mathcal{L}_{NLO}^γ of eq. (4.1), the corresponding potential can be read off:

$$\hat{V}_b^\mu = [k, \gamma^\mu] \hat{g}_b,$$

where

$$\begin{aligned} \hat{g}_b = & -\frac{e}{2f_i f_j} \left(b_{12} \langle (\lambda^b)^\dagger \{ [[Q_q, \lambda^i], (\lambda^j)^\dagger] + [[Q_q, (\lambda^j)^\dagger], \lambda^i], \lambda^a \} \rangle \right. \\ & \left. + b_{13} \langle (\lambda^b)^\dagger [[Q_q, \lambda^i], (\lambda^j)^\dagger] + [[Q_q, (\lambda^j)^\dagger], \lambda^i], \lambda^a \rangle \right). \end{aligned}$$

With this vertex the last class can be evaluated. The representation via Feynman diagrams is given by

$$\begin{aligned} S_{b,WT1}^\mu + S_{b,WT2}^\mu = & \text{Diagram 1} \\ & + \text{Diagram 2} \end{aligned}$$

where $S_{b,WT1}^\mu$ constitutes the real kernel of the corresponding integral equation of eq. (3.3). Symbolically the class can be expressed as

$$S_{b,WT1}^\mu = \hat{V}_b^\mu \int \frac{d^d l}{(2\pi)^d} iS(\not{p}_1 - l) \Delta(l) \Gamma(l, \not{p}_1), \quad (4.6)$$

$$S_{b,WT2}^\mu = \int \frac{d^d \tilde{l}}{(2\pi)^d} T(\not{q}, \tilde{l}; p) iS(\not{p} - \tilde{l}) \Delta(\tilde{l}) S_{WT1}^\mu. \quad (4.7)$$

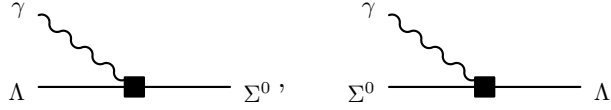
The decompositions into independent Dirac structures of the above amplitudes are provided in appendix D. Furthermore, the total amplitude is given by the sum of all eight unitarity classes, i.e. the sum of the five classes described in section 3.1 and the three classes described above:

$$\begin{aligned} \mathcal{M}_b^\mu = & S_s^\mu + S_u^\mu + S_t^\mu + S_B^\mu + S_M^\mu + S_{KR}^\mu + S_{WT1}^\mu + S_{WT2}^\mu \\ & + S_{b,s}^\mu + S_{b,u}^\mu + S_{b,B}^\mu + S_{b,WT1}^\mu + S_{b,WT2}^\mu. \end{aligned}$$

As mentioned earlier, each class is unitary by itself, whereas gauge invariance for the first five classes described in section 3.1 is only achieved by including *all* these five classes. In contrast, the three classes of this section are all gauge-invariant by themselves. This can be proved trivially by noting

that both the vertices, V_b^μ and \hat{V}_b^μ , are proportional to $[\not{k}, \gamma^\mu]$, which vanishes upon a contraction with k_μ . As in the previous chapter, the differential cross section can be obtained via the CGLN-amplitudes (see appendix E).

The amplitudes considered in this section lead to complications which have to be resolved before an actual numerical computation can be attempted. These issues can be traced back to the potential V_b^μ : In contrast to the interaction from quantum electrodynamics, the V_b^μ interaction arising from the NLO Lagrangian of eq. (4.1) is not diagonal in channel space. Therefore the vertices



are included in V_b^μ , which means a photon may induce transitions between Λ and Σ^0 baryons. The consequences of this are that the loop appearing in the amplitude $S_{b,B}$ of eq. (4.5) consists of baryon propagators with potentially unequal masses. Such a loop contains a three-point function with a tensor structure in the numerator (see eq. (B.13) of appendix B) and it can be decomposed into four Lorentz scalars (see eq. (B.14)) which, among others, contain the tadpole integral \mathcal{I}_M of eq. (B.9). However, the off-diagonal matrix elements of \mathcal{I}_M that arise due to the $\Lambda \leftrightarrow \Sigma^0$ transitions in V_b^μ , i.e. the elements linking the ΛK^+ and $\Sigma^0 K^+$ channels, contain no information on what baryon is involved in this particular transition, since \mathcal{I}_M only depends on the meson mass of a particular channel. But the ΛK^+ and $\Sigma^0 K^+$ share the same meson and hence it is not determinable whether the renormalization constant $\mu_{B\phi}$, which sets the scale for a channel containing the baryon B and the meson ϕ , is the renormalization constant of the channel ΛK^+ or of the channel $\Sigma^0 K^+$. Therefore, in the following

$$\mu_{\Lambda K} \equiv \mu_{\Sigma K}$$

has to be assumed in order to avoid this complication.

Another implication follows directly from the unequal baryon masses in the loop of $S_{b,B}^\mu$. The decomposition of the three-point function with a tensor structure in the numerator (again, see eq. (B.14) of appendix B) contains baryon two-point functions $[\mathcal{I}_{BB}^{(1)}(k^2)]^{bj,ai}$ defined by

$$k^\mu [\mathcal{I}_{BB}^{(1)}(k^2)]^{bj,ai} = \int \frac{d^d l}{(2\pi)^d} \frac{i\delta^{ji} l^\mu}{[(k-l)^2 - m_b^2][l^2 - m_a^2]},$$

which can be evaluated to yield (compare to eq. B.12)

$$[\mathcal{I}_{BB}^{(1)}(k^2)]^{bj,ai} = \frac{1}{2k^2} \left[(k^2 + m_a^2 - m_b^2) \mathcal{I}_{BB}^{bj,ai}(k^2) + \mathcal{I}_B^{bj,ai} - \mathcal{I}_B^{ai,bj} \right].$$

But considering the photoproduction limit $k^2 \rightarrow 0^-$, it is easily seen that the term proportional to $m_a^2 - m_b^2$ is infinite for the off-diagonal channels, where $m_b \neq m_a$. Also, inspecting the tadpole integrals $\mathcal{I}_B^{bj,ai}$ and $\mathcal{I}_B^{ai,bj}$ on the r.h.s., which are defined in analogy to the meson tadpole integral of eq. B.9, one finds that¹:

$$\lim_{k^2 \rightarrow 0^-} \frac{1}{k^2} (\mathcal{I}_B^{bj,ai} - \mathcal{I}_B^{ai,bj}) \longrightarrow \begin{cases} +\infty, & \text{for } bj, ai = \Lambda K^+, \Sigma^0 K^+ \\ -\infty, & \text{for } bj, ai = \Sigma^0 K^+, \Lambda K^+ \\ 0, & \text{else} \end{cases} .$$

The divergence of the off-diagonal elements of $[\mathcal{I}_{BB}^{(1)}(k^2)]^{bj,ai}$ leads to a divergence of the photoproduction amplitude, which is certainly unphysical, as photoproduction is a boundary case of electroproduction for photons of infinitely small virtuality k^2 .

To handle this, a new regularization scheme can be employed. According to Becher and Leutwyler [37], BChPT can be infrared regularized in a Lorentz invariant manner while also preserving the power counting rules. In this approach one identifies the infrared divergent parts of the integrals in the chiral limit, which can then be absorbed into counter terms. Moreover, all pure baryon integrals, like \mathcal{I}_B and \mathcal{I}_{BB} , are infrared finite due to the non-vanishing baryon masses in the chiral limit and thus the pure baryon integrals vanish based on the introduction of appropriate counter terms in the Lagrangian. In this spirit, the pure baryon integrals shall be set to zero, i.e.

$$\mathcal{I}_B^{bj,ai} \equiv 0, \quad \mathcal{I}_{BB}^{bj,ai} \equiv 0.$$

However, in order to control the ultraviolet divergences of the meson tadpole integral and all other ultraviolet divergent two-point functions, the usual dimensional regularization scheme shall be employed for all other integrals. Furthermore, as mentioned at the end of the section 1.2, the solution of the BSE is spoiled by the introduction of counter terms in the Lagrangian, but still, the BSE can be renormalized by modifying the interaction kernel of the BSE appropriately as to absorb the upcoming divergences [28].

4.2 Results

For the numeric computation of the differential cross section, three renormalization constants $\mu_{N\pi}$, $\mu_{p\eta}$ and $\mu_K \equiv \mu_{\Lambda K} = \mu_{\Sigma K}$, and in addition the

¹The sign of the infinities depends on the actual definition of the baryon tadpole integrals. In this case, the integral $\mathcal{I}_B^{bj,ai}$ depends solely on the final state baryon mass m_b , in analogy to the definition of the meson tadpole of eq. (B.9). However, the baryon tadpole could in principle be defined as depending on the initial state baryon mass m_a , which would result in slightly different formulae for the amplitudes.

two LECs b_{12} and b_{13} will be used as degrees of freedom for the fitting procedure. As mentioned in the previous section, the integrals \mathcal{I}_{BB} and \mathcal{I}_B will be set to zero as for the specific renormalization procedure that is used.

Unfortunately, the restriction $\mu_{\Lambda K} = \mu_{\Sigma K}$ for the renormalization constants is also a severe restriction for the photoproduction amplitude. As seen in eq. (3.12) of chapter 3, the renormalization constants $\mu_{\Lambda K}$ and $\mu_{\Sigma K}$ are quite different for a decent fit in the leading order approach. And since the renormalization constants enter the photoproduction amplitude in a fairly involved way, the LECs b_{12} and b_{13} , which enter linearly, can not compensate for that. As for the constraint on the renormalization constants and the particular renormalization scheme used in this chapter, this model can not be compared directly to the leading order approach of chapter 3. Therefore the current section is about a comparison of the amplitude *including* the NLO potentials V_b^μ and \hat{V}_b^μ on the one hand, with the amplitude *excluding* the NLO potentials on the other hand. Of course, the particular renormalization scheme will be used in both cases.

The restrictions on the renormalization constants render a fitting procedure, like the one for the leading order approach, useless. It is impossible to find a set of renormalization constants and LECs that describe the differential cross section adequately for an energy range that includes the $S_{11}(1535)$ completely. Hence, the following numerical computations are more of a *qualitative* comparison as to how the amplitude changes when including the NLO potentials.

For the fitting procedure the same data points as for the leading order approach from the previous chapter were taken from McNicoll et al. [29] and thus the model was fitted to differential cross section data. The energy range of the fit was chosen to be $1487.8 \text{ MeV} < E_{\text{cm}} < 1541.8 \text{ MeV}$, i.e. from threshold up to slightly above the peak of the $S_{11}(1535)$. As in the last chapters, this particular fitting region is not mandatory for the outcome of the fitting procedure, since the energy range can be varied in a reasonable amount without changing the results significantly.

The fit results in two parameter sets:

$$\begin{aligned}
 \log(\mu_{N\pi}^{\text{NLO}}/\text{GeV}) &= 0.597548 \pm \begin{matrix} 0.626016 \\ 0.442811 \end{matrix}, \\
 \log(\mu_{p\eta}^{\text{NLO}}/\text{GeV}) &= -5.32771 \pm \begin{matrix} 0.04240 \\ 0.03806 \end{matrix}, \\
 \log(\mu_K^{\text{NLO}}/\text{GeV}) &= -0.364032 \pm \begin{matrix} 0.002398 \\ 0.002221 \end{matrix}, \\
 b_{12}^{\text{NLO}} &= 0.846209 \pm \begin{matrix} 0.016447 \\ 0.016951 \end{matrix}, \\
 b_{13}^{\text{NLO}} &= -0.397511 \pm \begin{matrix} 0.008924 \\ 0.009361 \end{matrix},
 \end{aligned} \tag{4.8}$$

and

$$\begin{aligned}
\log(\mu_{N\pi}^0/\text{GeV}) &= 0.961197 \pm \begin{matrix} 3.779000 \\ 0.368047 \end{matrix}, \\
\log(\mu_{p\eta}^0/\text{GeV}) &= -5.03681 \pm \begin{matrix} 0.02805 \\ 0.02581 \end{matrix}, \\
\log(\mu_K^0/\text{GeV}) &= -0.402429 \pm \begin{matrix} 0.002332 \\ 0.002062 \end{matrix}, \\
b_{12}^0 &= 0, \\
b_{13}^0 &= 0,
\end{aligned} \tag{4.9}$$

where the superscript 'NLO' indicates inclusion of the NLO potentials, and the subscript '0' indicates exclusion of the NLO potentials in the photoproduction amplitude. The values for the LECs b_{12}^{NLO} and b_{13}^{NLO} differ largely from the values $b_{12} \approx 0.3$ and $b_{13} \approx 0.1$ that are obtained by perturbative approaches [38]. Though, there is no reason why resummation methods should obtain the same parameters as perturbative approaches. In particular, in an infinite series of Feynman diagrams the parameter set has to compensate for the diagram topologies omitted in the series, or in other words, possible contributions from other topologies are to some extent absorbed into the parameter set.

The corresponding $\chi^2/\text{d.o.f.}$ for the above parameter sets are given by

$$\begin{aligned}
[\chi^2/\text{d.o.f.}]^{\text{NLO}} &= 1.74466, \\
[\chi^2/\text{d.o.f.}]^0 &= 3.44305.
\end{aligned} \tag{4.10}$$

The errors were obtained by the same method as previously: Each parameter is varied separately to higher and lower values until $\chi^2/\text{d.o.f.}$ has increased by 1. For both parameter sets, all values, apart from $\mu_{N\pi}^{\text{NLO}}$ and $\mu_{N\pi}^0$, are very fine tuned. The influence of the $N\pi$ renormalization constant is almost nonexistent. In particular, it is possible to find similar $\chi^2/\text{d.o.f.}$ for values of the $N\pi$ renormalization constant that are orders of magnitudes different from the ones given above, if the other parameters are refitted. However, since the model is very sensitive to the other parameters, they would only change by a small fraction of their current values.

Fig. 4.1 shows a part of the differential cross section including the data points from McNicoll et al. [29]. Fig. 4.2 and fig. 4.3 show the corresponding error bands, which were, as previously, computed as the envelope function of all differential cross sections that are obtained when each parameter is varied separately to its error boundaries. The complete set of plots is provided in appendix F. The differential cross section close to threshold is almost the same for both sets of parameters, as can be seen best in fig. 4.1. But with increasing center-of-mass energy the differential cross section of the parameter set without NLO potentials exhibits an ever-increasing slope which is not consistent with the data points. In contrast, the differential cross section

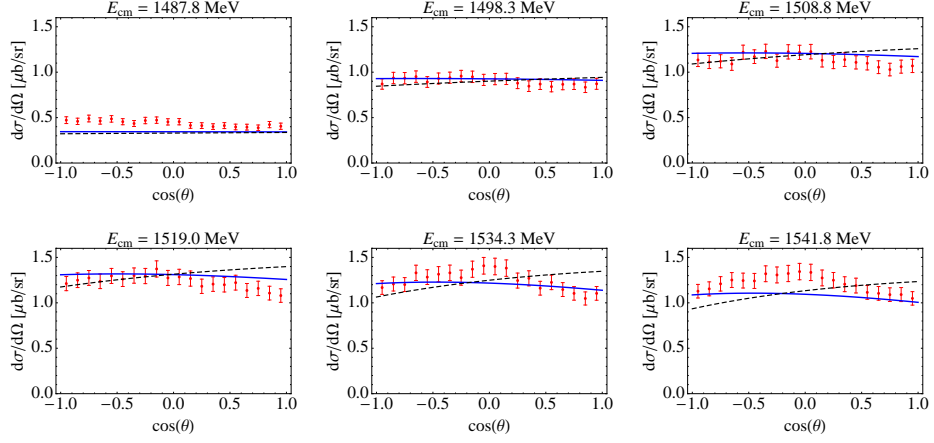


Figure 4.1: Parts of the differential cross section data from McNicoll et al. [29] (red symbols) including the best fit of the model with NLO potentials (solid blue line) and the best fit of the model without NLO potentials (dashed black line).

with NLO potentials does not exhibit such a slope and fits the data better, however, at energies beyond about 1530 MeV the model lacks the curvature of the data points.

Fig. 4.4 illustrates the corresponding total cross sections. They are almost identical for both parameter sets and exhibit a reasonable agreement to the data points about the peak position of the $S_{11}(1535)$. However, the width of the resonance is underestimated by a large fraction. As it turns out, there is no parameter set where the model generates the $S_{11}(1535)$ with the correct width².

The respective error bands of the total cross section are illustrated in fig. 4.5 and fig. 4.6. The main observation is that a variation of the parameters changes mainly the height of the resonance, whereas the width remains roughly the same. Also, those particular parameter sets seem to be fine tuned for only the resonance region, but at higher energies those variations have almost no impact.

To conclude this section, the respective amplitudes on the second Riemann sheets shall be computed in the same manner as in the leading order approach, i.e. analytically continuing the model amplitude by replacing the two point functions as in eq. (2.17) and the three-point functions as in eq. (3.14) and then calculating the multipole E_{0+} of eq. (3.15). The resulting sheets of both parameter sets are shown in fig. 4.7. The model with and the

²This, of course, can not be proven, but extensive searches in parameter space, using random walks and gradient methods, have not come to another conclusion.

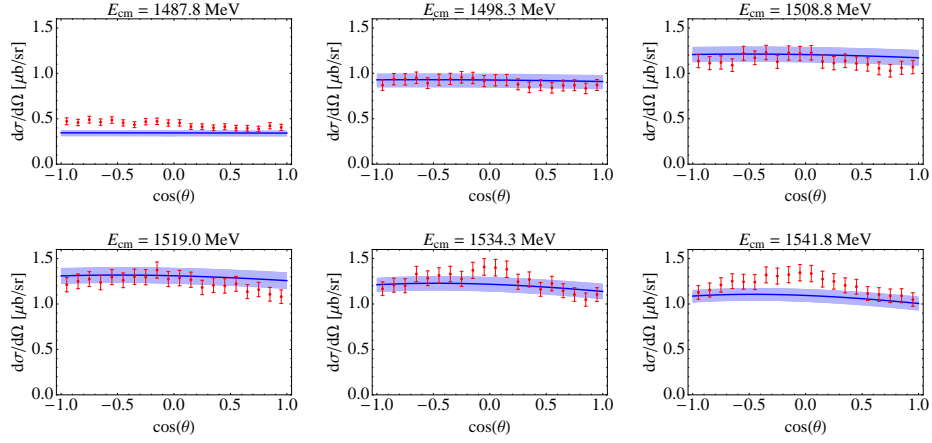


Figure 4.2: Parts of the differential cross section data from McNicoll et al. [29] (red symbols) including the best fit of the model with NLO potentials (solid blue line) and its error estimate (shaded area).

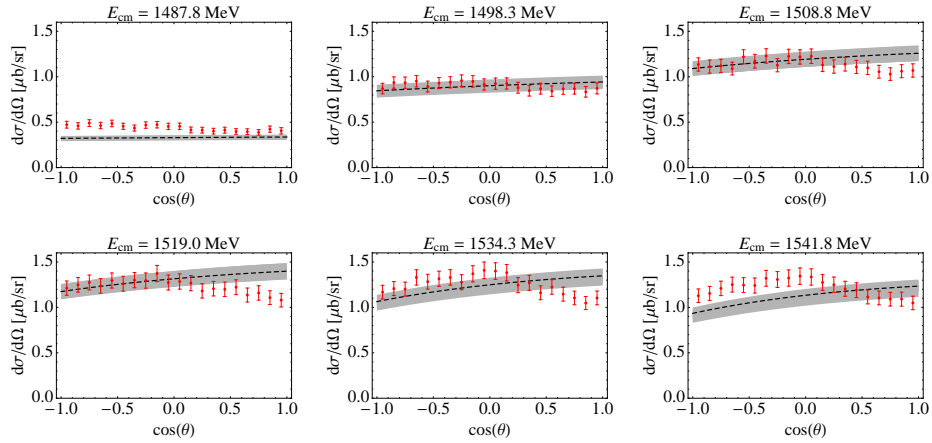


Figure 4.3: Parts of the differential cross section data from McNicoll et al. [29] (red symbols) including the best fit of the model without NLO potentials (dashed black line) and its error estimate (shaded area).

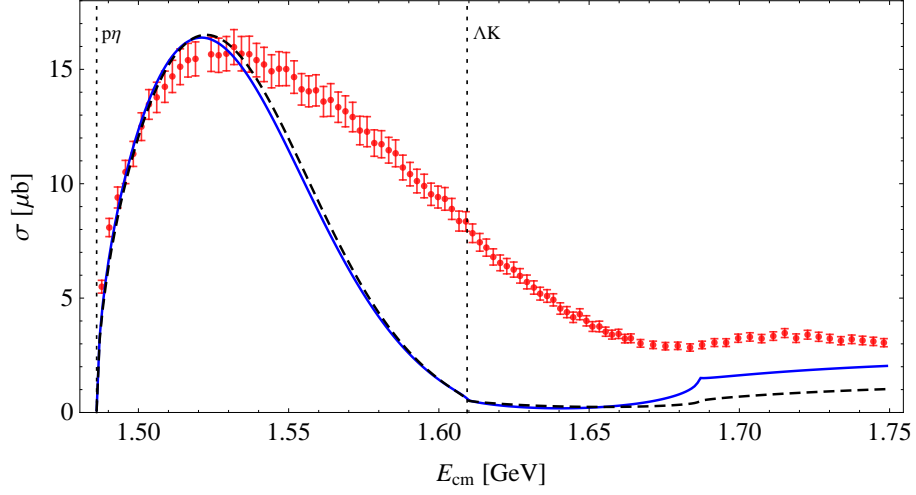


Figure 4.4: Total cross section data from McNicoll et al. [29] (red symbols) with the best fit of the model with NLO potentials (solid blue line) and without NLO potentials (dashed black line). The vertical dotted lines represent the $p\eta$ - and the ΛK -threshold.

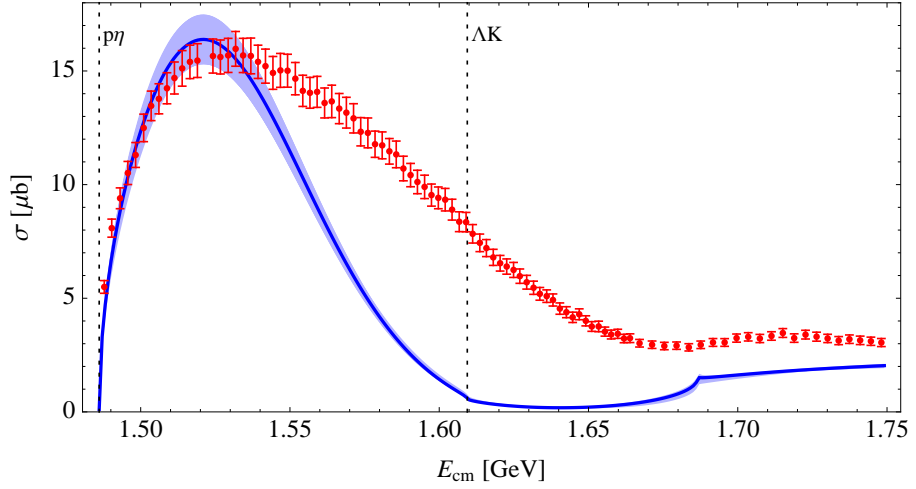


Figure 4.5: Total cross section data from McNicoll et al. [29] (red symbols) with the best fit of the model with NLO potentials (solid blue line) and its estimated error bands (shaded area). The vertical dotted lines represent the $p\eta$ - and the ΛK -threshold.

model without the NLO potentials exhibit two resonances each, of which one is below the η -photoproduction threshold and should therefore be considered as an artifact of the approach, for the same reasons that were explained in

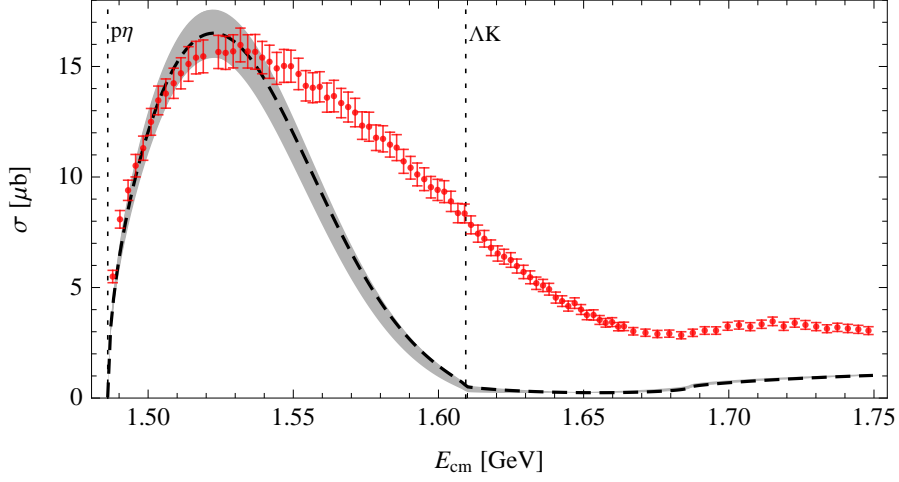


Figure 4.6: Total cross section data from McNicoll et al. [29] (red symbols) with the best fit of the model without NLO potentials (solid blue line) and its estimated error bands (shaded area). The vertical dotted lines represent the $p\eta$ - and the ΛK -threshold.

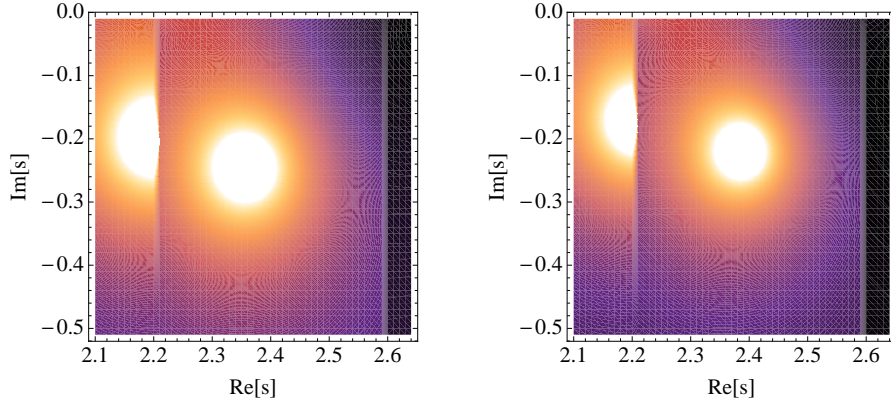


Figure 4.7: Second Riemann sheets of $|E_{0+}|$ (see eq. (3.15)) for the model with NLO potentials (left) and the model without NLO potentials (right). Brighter means higher values.

section 3.2. The other resonances, on the ηp -sheet, are positioned at

$$\begin{aligned} (\sqrt{s_{\text{res}}})^{\text{NLO}} &\approx [1539 - 81i] \text{ MeV}, \\ (\sqrt{s_{\text{res}}})^0 &\approx [1548 - 71i] \text{ MeV}. \end{aligned}$$

Both imaginary parts lie within the error bands of the resonance position of the $S_{11}(1535)$ in eq. (2.18) taken from [34]. However, the real parts of the

resonance positions exceed the error bands of eq. (2.18), where the parameter set including the NLO potentials is closer, which was to be expected as the fit is better than without NLO potentials.

4.3 Conclusion

The extension of the amplitude with terms of the NLO meson-baryon Lagrangian including the photon field leads to severe restrictions for the renormalization constants and therefore leads to the necessity of the particular renormalization scheme used in this chapter. However, these restrictions are a necessary step for an extension of the model and can not be avoided in future work on this topic. Thus, the evaluation of the extended model in this chapter should be regarded as a first step in that direction and as a comparison of how the NLO photon interactions impact the η -photoproduction cross section.

The difference between the amplitudes with and without NLO photon interactions can be seen from the fit to the differential and total cross sections. In both cases, the dynamic generation of the $S_{11}(1535)$ results in a qualitative agreement with the total cross section data and incorporating the NLO photon interactions almost does not change the outcome of the total cross section. However, the width of the resonance is underestimated and the real part of the resonance position exceeds the boundaries of the values given by the particle data group [34] in both cases. The main observation is the difference in the differential cross section: The NLO photon interactions lead to an improvement of the angular dependence of the differential cross section, thus improving the overall $\chi^2/\text{d.o.f.}$ greatly. From the construction of the photoproduction amplitude it is clear that the resonance is generated by the final state interaction, which is the meson-baryon scattering amplitude. But the LECs b_{12} and b_{13} do not contribute to the scattering amplitude and therefore the shape of the resonance in the total cross section *should not* differ largely in the two cases. Hence, the main influence of the b_{12} and b_{13} should be to change the angular dependence.

It is not possible to find a set of parameters that results in the correct width of the $S_{11}(1535)$ in the total cross section. Any fitting approaches to higher energies result in a displacement of the resonance on the second Riemann sheet, which gets worse the higher the upper boundary for the fitting region. In section 3.3, it was mentioned that the excess of the total cross section at center-of-mass energies higher than 1600 MeV is due to modification of the height and width of the resonance with the renormalization parameters. However, the extended amplitude of this chapter contains one renormalization constant less and the correct width can not be obtained anymore. As it appears, the fourth renormalization constant in the leading order approach can be used to mimic the behavior of an interaction kernel containing more

interactions than a mere Weinberg-Tomozawa vertex. Therefore the lacking width of the extended amplitude can only be overcome by including higher order terms in the interaction kernel.

The slight displacement of the real part of the resonance position on the second Riemann sheet is also an effect of the constraint on the renormalization parameters, since in the leading order approach, the correct position could be predicted. By an extension of the interaction kernel, the resonance of the extended amplitude should also lie within the error bounds given by [34].

Chapter 5

Summary and Outlook

The calculation of the meson-baryon scattering amplitude of chapter 2 reveals that the solution of the BSE, with an interaction kernel containing only the Weinberg-Tomozawa vertex, results in partial waves that are in a qualitative agreement with the partial waves deduced by the SAID group [33]. From the analytic continuation to the second Riemann sheets it becomes clear that only the $S_{11}(1535)$ resonance can be generated dynamically, although there should also be the $S_{11}(1650)$ and the $S_{31}(1620)$. However, the $S_{31}(1620)$ is an example of a resonance that has, if at all, a very small dynamically generated component and therefore has to be included explicitly in the Lagrangian.

The meson-baryon scattering amplitude was then used as the final state interaction to calculate a gauge invariant η -photoproduction amplitude in chapter 3 with interactions taken from the leading order meson-baryon chiral Lagrangian and QED. This model shows remarkable agreement with the differential cross section data from McNicoll et al. [29] up to energies more than 120 MeV higher than the $p\eta$ -threshold. The analytic continuation demonstrates that the $S_{11}(1535)$ is generated dynamically by this approach and lies within the error bounds given by the particle data group [34]. However, another pole appears below the η -photoproduction threshold, which is most likely a shadow pole, i.e. a copy of the $S_{11}(1535)$ on another sheet generated by the model. Such unphysical poles are a drawback of unitarization methods like the BSE and are generally ignored. Nevertheless, it is possible that such a sub-threshold pole influences the physical regime of the photoproduction process. But as the fit agrees well with the data and the position of the $S_{11}(1535)$ could be predicted correctly, the influence of the sub-threshold pole can at most be marginal. Furthermore, it is not possible to generate other resonances from this photoproduction amplitude as the resonances are generated within the final state interaction. In this model, the final state interaction is the meson-baryon scattering amplitude of chapter 2 which exhibits only the $S_{11}(1535)$.

In chapter 4, the photon interactions of the NLO meson-baryon chiral Lagrangian were taken into account. This resulted in difficulties which could be resolved by setting the ΛK and the ΣK renormalization constants to be equal and by employing a modified renormalization scheme. By reducing the number of independent renormalization constants from four to three, the photoproduction amplitude led to a much worse fit, and therefore chapter 4 was a direct comparison of the impact of the NLO photon interactions on the outcome of the cross sections and the resonances. The main difference can be seen in the differential cross section which was improved by the NLO potentials. The total cross section was almost the same and the dynamically generated $S_{11}(1535)$ did not change its position significantly. Thus including the NLO photon interactions leads only to a better overall fit and extends the validity of the model but does not contribute on a qualitative level.

It is worth mentioning that any extension of a photoproduction amplitude to the next-to-leading order will suffer from the difficulties seen in chapter 4 and thus discarding a renormalization constant can not be avoided by approaches as in this work. Therefore, this extended amplitude is a first step when analyzing next-to-leading order photoproduction amplitudes.

Future work is based on an extension of the interaction kernel of the BSE as well as adding higher order contributions to the photon interactions. The main concern is to enhance the final state interaction of the photoproduction amplitude which is the same as the calculation of the meson-baryon scattering amplitude, since it is clear that the dynamic generation of the $S_{11}(1650)$ depends on the choice of the interaction kernel. A first approach was made in [28], where the $S_{11}(1650)$ was successfully generated with a model that incorporates leading order and next-to-leading order contact interactions from the meson-baryon chiral Lagrangian. However, the Born terms had to be omitted, because it is not yet possible to solve the BSE with an interaction kernel containing these terms. The difficulty lies within the u-channel diagrams, since an iteration of the BSE leads to a series of overlapping four-point functions and it is not clear how these can be reduced to make them computable. In contrast, the s-channel Born graph leads only to a renormalization of the various baryon masses for the meson-baryon scattering amplitude. But for the photoproduction amplitude, the s-channel Born graph results in complications with the gauge-invariance, since the self-energies are linked to the electromagnetic baryon form factors by means of a Ward-Takahashi identity.

Thus, as a next step, the calculation of a photoproduction amplitude with a full incorporation of all leading order and next-to-leading order contact interactions would be reasonable.

Acknowledgements

I want to thank Maxim Mai and Peter Bruns for their outstanding support during this diploma thesis. For their patience in answering all of my questions, for proofreading anything that came to my mind and for discussions on any topic I can imagine. Moreover, I would like thank Ulf-G. Meißner for giving me the opportunity to work on this interesting topic and I would like to thank Akaki Rusetsky for reading my diploma thesis.

Appendix A

The solution of the BSE

As proven in [31], the BSE

$$T(\not{q}_2, \not{q}_1; p) = V(\not{q}_2, \not{q}_1) + \int \frac{d^d l}{(2\pi)^d} V(\not{q}_2, l) iS(\not{p} - l) \Delta(l) T(l, \not{q}_1; p),$$

with

$$V(\not{q}_2, \not{q}_1) = g^{bj, ai} (\not{q}_1 + \not{q}_2),$$

is solved by an amplitude of the form

$$T(\not{q}_2, \not{q}_1; p) = W(\not{q}_2, \not{q}_1; p) + W(\not{q}_2, \not{p} - m; p) G(p) [1 - W(\not{p} - m, \not{p} - m; p) G(p)]^{-1} W(\not{p} - m, \not{q}_1; p), \quad (\text{A.1})$$

with

$$W(\not{q}_2, \not{q}_1; p) = \not{q}_2 g \frac{1}{1 + I_M g} + \frac{1}{1 + g I_M} g \not{q}_1 - g \frac{1}{1 + I_M g} I_M (\not{p} - m) \frac{1}{1 + g I_M} g. \quad (\text{A.2})$$

For any further calculations it is necessary to decompose the solution into independent Dirac structures. To do so, the constituents of eq. (A.1), i.e. the functions G and W , have to be decomposed first. The integral G contains the structures

$$G(p) = G_1(p) \not{p} + G_0(p),$$

where the Lorentz scalars $G_1(p)$ and $G_0(p)$ can be read off eq. (B.5) in appendix B. Similarly the function $W(\not{p} - m, \not{p} - m; p)$ becomes

$$W(\not{p} - m, \not{p} - m; p) = W_1(p) \not{p} + W_0(p),$$

where

$$W_1(p) = g \frac{2 + I_M g}{(1 + I_M g)^2},$$

$$W_0(p) = g \frac{1}{1 + I_M g} (I_M m) \frac{1}{1 + g I_M} g - mg \frac{1}{1 + I_M g} - \frac{1}{1 + g I_M} gm$$

can be read off eq. (A.2) by using the substitutions $\not{q}_1, \not{q}_2 \rightarrow \not{p} - m$.

The crucial point of the decomposition is the inverse, appearing in eq. (A.1), where Dirac structures appear in the denominator. Since $W(\not{p} - m, \not{p} - m; p)$ and $G(p)$ only consist of one term proportional to \not{p} and a Lorentz scalar, $G(p)[1 - W(\not{p} - m, \not{p} - m; p)G(p)]^{-1}$ can also only contain these two Dirac structures. Hence it can be rewritten as

$$G(p)[1 - W(\not{p} - m, \not{p} - m; p)G(p)]^{-1} = \Omega_1(p)\not{p} + \Omega_0(p),$$

with the Lorentz scalars

$$\begin{aligned} \Omega_1 &= G_0(p) \left[p^2 \widetilde{W}_1 - \widetilde{W}_0 \widetilde{W}_1^{-1} \widetilde{W}_0 \right]^{-1} \\ &\quad - G_1(p) \widetilde{W}_1^{-1} \widetilde{W}_0 \left[p^2 \widetilde{W}_1 - \widetilde{W}_0 \widetilde{W}_1^{-1} \widetilde{W}_0 \right]^{-1}, \\ \Omega_0 &= p^2 G_1(p) \left[p^2 \widetilde{W}_1 - \widetilde{W}_0 \widetilde{W}_1^{-1} \widetilde{W}_0 \right]^{-1} \\ &\quad - G_0(p) \widetilde{W}_1^{-1} \widetilde{W}_0 \left[p^2 \widetilde{W}_1 - \widetilde{W}_0 \widetilde{W}_1^{-1} \widetilde{W}_0 \right]^{-1}, \end{aligned}$$

where

$$\begin{aligned} \widetilde{W}_1 &= -W_1(p)G_0(p) - W_0(p)G_1(p) \\ \widetilde{W}_0 &= 1 - p^2 W_1(p)G_1(p) - W_0(p)G_0(p). \end{aligned}$$

Inserting this into eq. (A.1) and collecting Dirac structures amounts to the decomposition

$$\begin{aligned} T(\not{q}_2, \not{q}_1; p) &= \not{q}_2 \not{p} \not{q}_1 T_1(p) + \not{q}_2 \not{q}_1 T_2(p) + \not{p} \not{q}_1 T_3(p) + \not{q}_2 \not{p} T_4(p) \\ &\quad + \not{q}_1 T_5(p) + \not{q}_2 T_6(p) + \not{p} T_7(p) + T_8(p), \end{aligned}$$

with eight scalar coefficients:

$$\begin{aligned} T_1(p) &= L_1 \Omega_1(p) L_1, \\ T_2(p) &= L_1 \Omega_0(p) L_1, \\ T_3(p) &= (L_2 \Omega_0(p) + L_3 \Omega_1(p)) L_1, \\ T_4(p) &= T_3^T(p), \\ T_5(p) &= (p^2 L_2 \Omega_1(p) + L_3 \Omega_0(p)) L_1 + L_1, \\ T_6(p) &= T_5^T(p), \\ T_7(p) &= (p^2 L_2 \Omega_1(p) + L_3 \Omega_0(p)) L_2 \\ &\quad + (L_2 \Omega_0(p) + L_3 \Omega_1(p)) L_3^T - g I_M L_2, \\ T_8(p) &= p^2 (L_2 \Omega_0(p) L_2 + L_3 \Omega_1(p) L_2 + L_2 \Omega_1(p) L_3^T) \\ &\quad + L_3 \Omega_0(p) L_3^T - L_3 I_M g, \end{aligned}$$

where

$$L_1 = g \frac{1}{1 + I_M g},$$

$$L_2 = \frac{1}{(1 + g I_M)^2} g,$$

$$L_3 = - \frac{1}{1 + g I_M} g m \frac{1}{1 + I_M g}$$

and the superscript ' T ' denotes transposition in channel space.

Appendix B

Loop integrals

This appendix is dedicated to the various loop integrals that appear throughout this work. Section B.1 provides the integrals necessary for the meson-baryon-scattering amplitude of chapter 2 and the leading order calculation of the η -photoproduction amplitude of chapter 3, whereas section B.2 provides the integrals for the calculation of the extended amplitude of chapter 4. All integrals are given component-by-component – the corresponding matrix form in channel space can then be deduced straightforwardly. Furthermore, no summation over multiple channel indices is understood.

B.1 Integrals for the leading order amplitude

Within this section all integrals that are necessary for the leading order calculation of chapter 3 will be evaluated. To this end, the dimensional regularization scheme will be used, where d denotes the dimension. All integrals will depend on d , which is only set to its physical value $d \rightarrow 4$ at the end of the calculation of amplitudes.

First of all, the meson tadpole integral that appeared in eq. (2.6) is given by

$$I_M^{bj,ai} = \int \frac{d^d l}{(2\pi)^d} \frac{i\delta^{ba}\delta^{ji}}{l^2 - M_j^2 + i\epsilon} = \delta^{ba}\delta^{ji} \left(2M_j^2 \bar{\lambda} + \frac{1}{8\pi^2} M_j^2 \log\left(\frac{M_j}{\mu_{bj}}\right) \right), \quad (\text{B.1})$$

where the superscripts b, j and a, i denote the final and initial baryon and meson types, respectively. Moreover, M_j is the mass of the meson of type j , μ_{bj} is the scale of the dimensional regularization scheme, ϵ is a small positive quantity and

$$\bar{\lambda} = \frac{\mu^{d-4}}{16\pi^2} \left(\frac{1}{d-4} - \frac{1}{2}(\log(4\pi) - \gamma_E + 1) \right), \quad (\text{B.2})$$

where $\gamma_E \approx 0.577$ is the Euler-Mascheroni constant. Terms of $\mathcal{O}(d-4)$ were neglected, since they vanish anyway in the limit $d \rightarrow 4$. Throughout this

work, the \overline{MS} renormalization scheme will be used, i.e. all terms proportional to $\bar{\lambda}$ will be dropped. Note, that the renormalization constant μ_{bj} varies amongst the channels, i.e. there are four independent renormalization constants (see the explanation above eq. (2.14) in section 2.2).

The corresponding baryon tadpole integral can be deduced by replacing the meson mass M_j by a mass m_a of a baryon of type a :

$$I_B^{bj,ai} = I_M^{bj,ai} \Big|_{M_j \rightarrow m_a}.$$

The next integral is the two-point function with one meson and one baryon. Here and in the remainder the ie 's in the denominator will be omitted for brevity:

$$\begin{aligned} I_{MB}^{bj,ai}(p^2) &= \int \frac{d^d l}{(2\pi)^d} \frac{i\delta^{ba}\delta^{ji}}{[(p-l)^2 - m_b^2][l^2 - M_j^2]} \\ &= \frac{\delta^{ba}\delta^{ji}}{16\pi^2} \left[-1 + \log\left(\frac{m_b^2}{\mu_{bj}^2}\right) + \frac{M_j^2 - m_b^2 + p^2}{2p^2} \log\left(\frac{M_j^2}{m_b^2}\right) \right. \\ &\quad \left. - \frac{4|\mathbf{q}|^{bj,ai}}{\sqrt{p^2}} \operatorname{artanh}\left(\frac{2|\mathbf{q}|^{bj,ai}\sqrt{p^2}}{(m_b + M_j)^2 - p^2}\right) \right], \end{aligned}$$

where

$$|\mathbf{q}|^{bj,ai} = \frac{\sqrt{(p^2 - (m_b + M_j)^2)(p^2 - (m_b - M_j)^2)}}{2\sqrt{p^2}}$$

is the center-of-mass three-momentum of a system with a center-of-mass energy of $\sqrt{p^2}$ consisting of two particles with masses m_b and M_j . Consecutively, the baryon-baryon as well as the meson-meson two-point function can be obtained by replacing

$$I_{BB}^{bj,ai}(p^2) = I_{MB}^{bj,ai}(p^2) \Big|_{M_j \rightarrow m_b}, \quad I_{MM}^{bj,ai}(p^2) = I_{MB}^{bj,ai}(p^2) \Big|_{m_b \rightarrow M_j}.$$

Up to now, everything could be calculated analytically, but the three-point function with one meson and two baryons

$$I_{M BB}^{bj,ai}(p_1^2, p_2^2) = \int \frac{d^d l}{(2\pi)^d} \frac{i\delta^{ba}\delta^{ji}}{[(p-l)^2 - m_b^2][(p_1-l)^2 - m_b^2][l^2 - M_j^2]} \quad (\text{B.3})$$

must be calculated numerically, as for which the use of dispersion relations renders useful. In the complex p^2 -plane, $I_{M BB}$ exhibits cuts along the real p^2 axis, starting at the corresponding threshold of the channel and going to positive infinity. The exclusive knowledge of the discontinuity of these

cuts is sufficient to reconstruct the real part of I_{MBB} , and hence the complete function I_{MBB} . With the pertinent Cutkosky rules (see e.g. [11]) the discontinuity of I_{MBB} can be calculated directly:

$$\text{Disc}(I_{MBB}^{bj,ai}(p_1^2, p^2)) = -\frac{i\delta^{ba}\delta^{ji}}{16\pi|\mathbf{k}|\sqrt{p^2}} \log\left(\frac{\mathcal{H}^{bj,ai} + 2|\mathbf{k}||\mathbf{q}|^{bj,ai}}{\mathcal{H}^{bj,ai} - 2|\mathbf{k}||\mathbf{q}|^{bj,ai}}\right), \quad (\text{B.4})$$

where

$$|\mathbf{k}| = \frac{\sqrt{(k^2)^2 - 2k^2(p_1^2 + p^2) + (p_1^2 - p^2)^2}}{2\sqrt{p^2}}, \quad k = p - p_1$$

and for reasons of a clear arrangement the function

$$\begin{aligned} \mathcal{H}^{bj,ai} = & -\frac{1}{2p^2} \sqrt{(k^2 - p_1^2 + p^2)^2 (-M_j^2 + m_b^2 + p^2)^2} \\ & + \sqrt{(k^2 - p_1^2 + p^2)^2 - m_a^2 + m_b^2 + p_1^2 - p^2} \end{aligned}$$

was introduced¹. The corresponding dispersion relation for the numeric computation reads

$$I_{MBB}^{bj,ai}(p_1^2, p^2) = -\frac{1}{2\pi i} \int_{(m_b+M_j)^2}^{\infty} ds' \frac{\text{Disc}(I_{MBB}^{bj,ai}(p_1^2, s'))}{p^2 - s'},$$

in which the analytic properties of I_{MBB} are manifested.

The three-point function I_{MMB} with two mesons and one baryon can be deduced from I_{MBB} by interchanging the meson and baryon masses:

$$I_{MMB}^{bj,ai}(p_1^2, p^2) = I_{MBB}^{bj,ai}(p_1^2, p^2) \Big|_{m_b \leftrightarrow M_j}.$$

Up to now, all basic integrals were evaluated. However, in the course of the calculation of the photoproduction amplitude, various loop integrals with vector or tensor structures in the numerators appear. The simplest one is the two-point function I_{MB} with a l^μ in the numerator. By using that such an integral can only be proportional to the vector, appearing in the integral, times a Lorentz scalar, one arrives at

$$\int \frac{d^d l}{(2\pi)^d} \frac{i\delta^{ba}\delta^{ji} l^\mu}{[(p-l)^2 - m_b^2][l^2 - M_j^2]} = p^\mu [I_{MB}^{(1)}(p^2)]^{bj,ai}.$$

¹For later convenience, \mathcal{H} was defined for generally differing initial and final baryon masses m_a and m_b , respectively. However, in the present case, due to the δ^{ba} in eq. (B.4), those masses are the same, i.e. $m_a = m_b$.

Contracting both sides of the equation with p_μ and completing the square on the l.h.s in order to cancel the propagators leads to

$$[I_{MB}^{(1)}(p^2)]^{bj,ai} = \frac{1}{2p^2} \left[(p^2 + M_j^2 - m_b^2) I_{MB}^{bj,ai}(p^2) + I_B^{bj,ai} - I_M^{bj,ai} \right].$$

The above results can be combined to solve the integral

$$G^{bj,ai}(p^2) = \int \frac{d^d l}{(2\pi)^d} \frac{i\delta^{ba}\delta^{ji}}{[(\not{p} - \not{l}) - m_b][l^2 - M_j^2]}$$

that appeared in eq. (2.7). Expanding the fraction of the fermion propagator leads to two independent Dirac structures that can be expressed as

$$\begin{aligned} G^{bj,ai}(p^2) &= \not{p}G_1(p^2) + G_0(p^2) \\ &= \frac{\not{p}}{2p^2} \left[(p^2 - M_j^2 + m_b^2) I_{MB}^{bj,ai}(p^2) + I_M^{bj,ai} - I_B^{bj,ai} \right] + m_b I_{MB}^{bj,ai}(p^2). \end{aligned} \quad (\text{B.5})$$

The three-point functions with vector and tensor structures are more advanced, since there have to be considered more possible Dirac structures. The three-point function with two baryons and one meson with a vector structure in the numerator can be decomposed as

$$\begin{aligned} \int \frac{d^d l}{(2\pi)^d} \frac{i\delta^{ba}\delta^{ji}\not{l}^\mu}{[(p-l)^2 - m_b^2][(p_1-l)^2 - m_b^2][l^2 - M_j^2]} &= A^{bj,ai}(p_1^2, p^2) (p_1 + p)^\mu \\ &\quad + B^{bj,ai}(p_1^2, p^2) (p_1 - p)^\mu. \end{aligned}$$

Contracting both sides of the equation with either $(p_1 + p)_\mu$ and $(p_1 - p)_\mu$ and completing the squares in order to cancel the propagators leads to two independent equations which can be solved for A and B yielding

$$\begin{aligned} A^{bj,ai}(p_1^2, p^2) &= \frac{1}{2D} \left[\left(4[\bar{M}^2]^{bj,ai} - \frac{\Delta p^4}{k^2} \right) I_{MBB}^{bj,ai}(p_1^2, p^2) + 2I_{BB}^{bj,ai}(k^2) \right. \\ &\quad \left. - \left(1 - \frac{\Delta p^2}{k^2} \right) I_{MB}^{bj,ai}(p_1^2) - \left(1 + \frac{\Delta p^2}{k^2} \right) I_{MB}^{bj,ai}(p^2) \right], \\ B^{bj,ai}(p_1^2, p^2) &= \frac{\Delta p^2}{2k^2 D} \left[(4[\bar{M}^2]^{bj,ai} + k^2 - 4\bar{p}^2) I_{MBB}^{bj,ai}(p_1^2, p^2) + 2I_{BB}^{bj,ai}(k^2) \right. \\ &\quad \left. - \left(1 - \frac{4\bar{p} - k^2}{\Delta p^2} \right) I_{MB}^{bj,ai}(p_1^2) - \left(1 + \frac{4\bar{p} - k^2}{\Delta p^2} \right) I_{MB}^{bj,ai}(p^2) \right], \end{aligned}$$

where

$$\begin{aligned}
\bar{p}^2 &= \frac{1}{2}(p_1^2 + p^2), \\
[\bar{M}^2]^{bj,ai} &= \frac{1}{2}(\bar{p}^2 + M_j^2 - m_b^2) \delta^{ba} \delta^{ji}, \\
\Delta p^2 &= p^2 - p_1^2, \\
\Delta p^4 &= (\Delta p^2)^2, \\
D &= 4\bar{p}^2 - k^2 - \frac{\Delta p^4}{k^2}.
\end{aligned}$$

Analogously the three-point function with a tensor structure in the numerator can be calculated. Its decomposition reads

$$\begin{aligned}
\int \frac{d^d l}{(2\pi)^d} \frac{i\delta^{ba} \delta^{ji} l^\mu l^\nu}{[(p-l)^2 - m_b^2][(p_1-l)^2 - m_a^2][l^2 - M_j^2]} &= C_1^{bj,ai}(p_1^2, p^2) g^{\mu\nu} \\
&+ C_2^{bj,ai}(p_1^2, p^2) (p_1 + p)^\mu (p_1 + p)^\nu \\
&+ C_3^{bj,ai}(p_1^2, p^2) (p_1 - p)^\mu (p_1 - p)^\nu \\
&+ C_4^{bj,ai}(p_1^2, p^2) ((p_1 + p)^\mu (p_1 - p)^\nu + (p_1 - p)^\mu (p_1 + p)^\nu).
\end{aligned}$$

Again, contracting separately with each Lorentz structure on the r.h.s and thus cancelling the propagators leads to four equations which can be solved for the coefficients:

$$\begin{aligned}
C_1^{bj,ai}(p_1^2, p^2) &= \frac{1}{d-2} \left[M_j^2 I_{MBB}^{bj,ai}(p_1^2, p^2) + \frac{1}{2} I_{BB}^{bj,ai}(k^2) \right. \\
&\quad \left. - 2[\bar{M}^2]^{bj,ai} A^{bj,ai}(p_1^2, p^2) + \frac{\Delta p^2}{2} B^{bj,ai}(p_1^2, p^2) \right], \quad (\text{B.6})
\end{aligned}$$

$$\begin{aligned}
C_2^{bj,ai}(p_1^2, p^2) &= \frac{1}{k^2 D} \left[k^2 (M_j^2 I_{MBB}^{bj,ai}(p_1^2, p^2) + I_{BB}^{bj,ai}(k^2)) \right. \\
&\quad + \frac{\Delta p^2}{2} (k^2 B^{bj,ai}(p_1^2, p^2) - \Delta p^2 A^{bj,ai}(p_1^2, p^2)) \\
&\quad - \frac{k^2}{4} ([I_{MB}^{(1)}(p_1^2)]^{bj,ai} + [I_{MB}^{(1)}(p^2)]^{bj,ai}) \\
&\quad + \frac{\Delta p^2}{4} ([I_{MB}^{(1)}(p_1^2)]^{bj,ai} - [I_{MB}^{(1)}(p^2)]^{bj,ai}) \\
&\quad \left. - (d-1)k^2 C_1^{bj,ai}(p_1^2, p^2) \right],
\end{aligned}$$

$$\begin{aligned}
C_3^{bj,ai}(p_1^2, p^2) &= \frac{1}{k^2 D} \left[(4\bar{p} - k^2)(M_j^2 I_{MBB}^{bj,ai}(p_1^2, p^2) + \frac{1}{2} I_{BB}^{bj,ai}(k^2)) \right. \\
&\quad - 2[\bar{M}^2]^{bj,ai}((4\bar{p}^2 - k^2)A^{bj,ai}(p_1^2, p^2) - \Delta p^2 B^{bj,ai}(p_1^2, p^2)) \\
&\quad + \frac{1}{4}(4\bar{p}^2 - \Delta p^2 - k^2)[I_{MB}^{(1)}(p_1^2)]^{bj,ai} \\
&\quad + \frac{1}{4}(4\bar{p}^2 + \Delta p^2 - k^2)[I_{MB}^{(1)}(p^2)]^{bj,ai} \\
&\quad \left. - (d-1)(4\bar{p}^2 - k^2)C_1^{bj,ai}(p_1^2, p^2) \right], \\
C_4^{bj,ai}(p_1^2, p^2) &= \frac{1}{k^2 D} \left[\Delta p^2 (M_j^2 I_{MBB}^{bj,ai}(p_1^2, p^2) + I_{BB}^{bj,ai}(k^2)) \right. \\
&\quad - \frac{\Delta p^2}{2}((4\bar{p}^2 - k^2)A^{bj,ai}(p_1^2, p^2) - \Delta p^2 B^{bj,ai}(p_1^2, p^2)) \\
&\quad + \frac{1}{4}(4\bar{p}^2 - \Delta p^2 - k^2)[I_{MB}^{(1)}(p_1^2)]^{bj,ai} \\
&\quad - \frac{1}{4}(4\bar{p}^2 + \Delta p^2 - k^2)[I_{MB}^{(1)}(p^2)]^{bj,ai} \\
&\quad \left. - (d-1)\Delta p^2 C_1^{bj,ai}(p_1^2, p^2) \right], \tag{B.7}
\end{aligned}$$

where d is the dimension stemming from the regularization scheme. Since this loop integral is divergent, the coefficient C_1 of eq. (B.6) picks up an additional term in the limit $d \rightarrow 4$. This can be quantified by assuming $\bar{\lambda}$ of eq. (B.2) was not omitted, in which case the additional appearance of the dimension d in the coefficient C_1 leads to a different expansion in powers of $d - 4$. To quantify the difference, $C_1(d = 4)$ shall be the function obtained by setting naively $d = 4$ in eq. (B.6). Then, the limit $d \rightarrow 4$ leads to the following additional constants:

$$\begin{aligned}
C_1^{bj,ai} &\rightarrow C_1^{bj,ai}(d = 4) - \delta^{ba} \delta^{ji} \frac{1}{64\pi^2}, \\
(d-1)C_1^{bj,ai} &\rightarrow 3C_1^{bj,ai}(d = 4) - \delta^{ba} \delta^{ji} \frac{1}{64\pi^2}, \tag{B.8}
\end{aligned}$$

which are all that are needed in the leading order approach.

As mentioned earlier, the results for the case of a three-point function with two mesons and one baryon can be deduced by interchanging the meson and baryon masses. The corresponding coefficients will be tagged by a tilde:

$$\begin{aligned}
\tilde{A}^{bj,ai}(p_1^2, p^2) &= A^{bj,ai}(p_1^2, p^2) \Big|_{m_b \leftrightarrow M_j}, \\
\tilde{B}^{bj,ai}(p_1^2, p^2) &= B^{bj,ai}(p_1^2, p^2) \Big|_{m_b \leftrightarrow M_j}, \\
\tilde{C}_k^{bj,ai}(p_1^2, p^2) &= C_k^{bj,ai}(p_1^2, p^2) \Big|_{m_b \leftrightarrow M_j},
\end{aligned}$$

where $k = 1, 2, 3, 4$.

The above results can be used to decompose two important loop integrals that appear during the evaluation of the leading order photoproduction amplitude. The first one reads

$$\begin{aligned} & \int \frac{d^d l}{(2\pi)^d} \delta^{ba} \delta^{ji} \frac{1}{(\not{p} - \not{l}) - m_b} i e Q_B^{bj, ai} \gamma^\mu \frac{1}{(\not{p}_1 - \not{l}) - m_b} \frac{1}{l^2 - M_j^2} \\ &= \gamma^\mu F_1^{bj, ai}(p_1^2, p^2) + \not{p} \gamma^\mu F_2^{bj, ai}(p_1^2, p^2) + \gamma^\mu \not{p}_1 F_3^{bj, ai}(p_1^2, p^2) \\ &+ \not{p} \gamma^\mu \not{p}_1 F_4^{bj, ai}(p_1^2, p^2) + p^\mu F_5^{bj, ai}(p_1^2, p^2) + p_1^\mu F_6^{bj, ai}(p_1^2, p^2) \\ &+ p^\mu \not{p} F_7^{bj, ai}(p_1^2, p^2) + p^\mu \not{p}_1 F_8^{bj, ai}(p_1^2, p^2) + p_1^\mu \not{p} F_9^{bj, ai}(p_1^2, p^2) \\ &+ p_1^\mu \not{p}_1 F_{10}^{bj, ai}(p_1^2, p^2), \end{aligned}$$

where Q_B is the baryon charge matrix which is diagonal in channel space. The ten coefficients of the Lorentz structures are given by

$$\begin{aligned} F_1^{bj, ai}(p_1^2, p^2) &= e Q_B^{bj, ai} \left[2C_1(p_1^2, p^2) + (m_b^2 - M_j^2) I_{M B B}^{bj, ai}(p_1^2, p^2) - I_{B B}^{bj, ai}(k^2) \right. \\ &\quad \left. + p_1^2 (A^{bj, ai}(p_1^2, p^2) + B^{bj, ai}(p_1^2, p^2)) \right. \\ &\quad \left. + p^2 (A^{bj, ai}(p_1^2, p^2) - B^{bj, ai}(p_1^2, p^2)) \right], \\ F_2^{bj, ai}(p_1^2, p^2) &= e Q_B^{bj, ai} m_b I_{M B B}^{bj, ai}(p_1^2, p^2), \\ F_3^{bj, ai}(p_1^2, p^2) &= F_2^{bj, ai}(p_1^2, p^2), \\ F_4^{bj, ai}(p_1^2, p^2) &= e Q_B^{bj, ai} m_b \left[I_{M B B}^{bj, ai}(p_1^2, p^2) - 2A^{bj, ai}(p_1^2, p^2) \right], \\ F_5^{bj, ai}(p_1^2, p^2) &= 2e Q_B^{bj, ai} m_b \left[B^{bj, ai}(p_1^2, p^2) - A^{bj, ai}(p_1^2, p^2) \right], \\ F_6^{bj, ai}(p_1^2, p^2) &= -2e Q_B^{bj, ai} m_b \left[B^{bj, ai}(p_1^2, p^2) + A^{bj, ai}(p_1^2, p^2) \right], \\ F_7^{bj, ai}(p_1^2, p^2) &= 2e Q_B^{bj, ai} \left[B^{bj, ai}(p_1^2, p^2) - A^{bj, ai}(p_1^2, p^2) + C_2^{bj, ai}(p_1^2, p^2) \right. \\ &\quad \left. + C_3^{bj, ai}(p_1^2, p^2) - 2C_4^{bj, ai}(p_1^2, p^2) \right], \\ F_8^{bj, ai}(p_1^2, p^2) &= 2e Q_B^{bj, ai} \left[C_2^{bj, ai}(p_1^2, p^2) - C_3^{bj, ai}(p_1^2, p^2) \right], \\ F_9^{bj, ai}(p_1^2, p^2) &= F_8^{bj, ai}(p_1^2, p^2), \\ F_{10}^{bj, ai}(p_1^2, p^2) &= 2e Q_B \left[C_2^{bj, ai}(p_1^2, p^2) + C_3^{bj, ai}(p_1^2, p^2) + 2C_4^{bj, ai}(p_1^2, p^2) \right. \\ &\quad \left. - A^{bj, ai}(p_1^2, p^2) - B^{bj, ai}(p_1^2, p^2) \right]. \end{aligned}$$

Similarly the second integral can be decomposed into Lorentz structures

as:

$$\begin{aligned}
& \int \frac{d^d l}{(2\pi)^d} \delta^{ba} \delta^{ji} \frac{1}{(p-l)^2 - M_j^2} i e Q_M^{bj,ai} (p+p_1-2l)^\mu \frac{1}{(p_1-l)^2 - M_j^2} \frac{1}{l - m_b} \\
&= \gamma^\mu \tilde{F}_1^{bj,ai}(p_1^2, p^2) + \not{p} \gamma^\mu \tilde{F}_2^{bj,ai}(p_1^2, p^2) + \gamma^\mu \not{p}_1 \tilde{F}_3^{bj,ai}(p_1^2, p^2) \\
&\quad + \not{p} \gamma^\mu \not{p}_1 \tilde{F}_4^{bj,ai}(p_1^2, p^2) + p^\mu \tilde{F}_5^{bj,ai}(p_1^2, p^2) + p_1^\mu \tilde{F}_6^{bj,ai}(p_1^2, p^2) \\
&\quad + p^\mu \not{p} \tilde{F}_7^{bj,ai}(p_1^2, p^2) + p^\mu \not{p}_1 \tilde{F}_8^{bj,ai}(p_1^2, p^2) + p_1^\mu \not{p} \tilde{F}_9^{bj,ai}(p_1^2, p^2) \\
&\quad + p_1^\mu \not{p}_1 \tilde{F}_{10}^{bj,ai}(p_1^2, p^2),
\end{aligned}$$

where Q_M is the meson charge matrix which is diagonal in channel space. The coefficients for this decomposition read

$$\begin{aligned}
\tilde{F}_1^{bj,ai}(p_1^2, p^2) &= -2eQ_M^{bj,ai} \tilde{C}_1^{bj,ai}(p_1^2, p^2), \\
\tilde{F}_2^{bj,ai}(p_1^2, p^2) &= 0, \\
\tilde{F}_3^{bj,ai}(p_1^2, p^2) &= 0, \\
\tilde{F}_4^{bj,ai}(p_1^2, p^2) &= 0, \\
\tilde{F}_5^{bj,ai}(p_1^2, p^2) &= eQ_M^{bj,ai} \left[m_b I_{MMB}^{bj,ai}(p_1^2, p^2) \right. \\
&\quad \left. + 2m_b (\tilde{B}^{bj,ai}(p_1^2, p^2) - \tilde{A}^{bj,ai}(p_1^2, p^2)) \right], \\
\tilde{F}_6^{bj,ai}(p_1^2, p^2) &= eQ_M^{bj,ai} \left[m_b I_{MMB}^{bj,ai}(p_1^2, p^2) \right. \\
&\quad \left. - 2m_b (\tilde{B}^{bj,ai}(p_1^2, p^2) + \tilde{A}^{bj,ai}(p_1^2, p^2)) \right], \\
\tilde{F}_7^{bj,ai}(p_1^2, p^2) &= eQ_M^{bj,ai} \left[\tilde{A}^{bj,ai}(p_1^2, p^2) - \tilde{B}^{bj,ai}(p_1^2, p^2) \right. \\
&\quad \left. - 2(\tilde{C}_2^{bj,ai}(p_1^2, p^2) + \tilde{C}_3^{bj,ai}(p_1^2, p^2) - 2\tilde{C}_4^{bj,ai}(p_1^2, p^2)) \right], \\
\tilde{F}_8^{bj,ai}(p_1^2, p^2) &= eQ_M^{bj,ai} \left[\tilde{A}^{bj,ai}(p_1^2, p^2) + \tilde{B}^{bj,ai}(p_1^2, p^2) \right. \\
&\quad \left. - 2(\tilde{C}_2^{bj,ai}(p_1^2, p^2) - \tilde{C}_3^{bj,ai}(p_1^2, p^2)) \right], \\
\tilde{F}_9^{bj,ai}(p_1^2, p^2) &= eQ_M^{bj,ai} \left[\tilde{A}^{bj,ai}(p_1^2, p^2) - \tilde{B}^{bj,ai}(p_1^2, p^2) \right. \\
&\quad \left. - 2(\tilde{C}_2^{bj,ai}(p_1^2, p^2) - \tilde{C}_3^{bj,ai}(p_1^2, p^2)) \right], \\
\tilde{F}_{10}^{bj,ai}(p_1^2, p^2) &= eQ_M^{bj,ai} \left[\tilde{A}^{bj,ai}(p_1^2, p^2) + \tilde{B}^{bj,ai}(p_1^2, p^2) \right. \\
&\quad \left. - 2(\tilde{C}_2^{bj,ai}(p_1^2, p^2) + \tilde{C}_3^{bj,ai}(p_1^2, p^2) + 2\tilde{C}_4^{bj,ai}(p_1^2, p^2)) \right].
\end{aligned}$$

B.2 Integrals for the extended amplitude

In this section, all integrals that are necessary for the evaluation of the extended amplitude of chapter 4 will be evaluated. Due to the specific nature

of the coupling V_b^μ , appearing in that chapter, the loop integrals must include additional off-diagonal elements to allow for transitions between the Λ and Σ^0 channels.

First of all, the meson tadpole integral with off-diagonal elements is given by

$$\mathcal{I}_M^{bj,ai} = \int \frac{d^d l}{(2\pi)^d} \frac{i\delta^{ji}}{l^2 - M_j^2} = \delta^{ji} \left(2M_j^2 \bar{\lambda} + \frac{1}{8\pi^2} M_j^2 \log \left(\frac{M_j}{\mu_{bj}} \right) \right). \quad (\text{B.9})$$

Note, that for the calculation of the extended amplitude only three different renormalization constants are used (see section 4.1), i.e. there is one renormalization constant $\mu_{N\pi}$ for the pion-nucleon channels, one renormalization constant $\mu_{p\eta}$ for the proton- η channel and one renormalization constant μ_K for the channels including a kaon.

Furthermore, the δ^{ji} in eq. (B.9) together with the particular composition of the final state particles in the channels of the photoproduction process (see eq. (2.9)) render \mathcal{I}_M to be basically a diagonal matrix, but with two additional off-diagonal components. The δ^{ji} forces the initial and final mesons to be the same, but the only channels sharing the same meson are the ΛK^+ and the $\Sigma^0 K^+$ channels, hence the only off-diagonal components of \mathcal{I}_M are the two components mixing those two channels.

The next integral is the two-point function with one meson and one baryon:

$$\begin{aligned} \mathcal{I}_{MB,b}^{bj,ai}(p^2) &= \int \frac{d^d l}{(2\pi)^d} \frac{i\delta^{ji}}{[(p-l)^2 - m_b^2][l^2 - M_j^2]} \\ &= \frac{\delta^{ji}}{16\pi^2} \left[-1 + \log \left(\frac{m_b^2}{\mu_{bj}^2} \right) + \frac{M_j^2 - m_b^2 + p^2}{2p^2} \log \left(\frac{M_j^2}{m_b^2} \right) \right. \\ &\quad \left. - \frac{4|\mathbf{q}|^{bj,ai}}{\sqrt{p^2}} \operatorname{artanh} \left(\frac{2|\mathbf{q}|^{bj,ai} \sqrt{p^2}}{(m_b + M_j)^2 - p^2} \right) \right]. \end{aligned} \quad (\text{B.10})$$

This integral appears in two distinct forms, of which the first one is given above, whereas the second one, which will be called $\mathcal{I}_{MB,a}$, is the transpose in channel space of $\mathcal{I}_{MB,b}$, i.e. initial and final states of the off-diagonal elements are interchanged. The transpose is equivalent to replacing the final baryon state mass m_b by the initial state mass m_a :

$$\mathcal{I}_{MB,a}^{bj,ai}(p^2) = \left[(\mathcal{I}_{MB,b}(p^2))^T \right]^{bj,ai} = \mathcal{I}_{MB,b}^{bj,ai}(p^2) \Big|_{m_b \rightarrow m_a}.$$

The three-point function with one meson and two baryons can be defined in close analogy to I_{MBB} of eq. (B.3):

$$\mathcal{I}_{MBB}^{bj,ai}(p_1^2, p_2^2) = \int \frac{d^d l}{(2\pi)^d} \frac{i\delta^{ji}}{[(p-l)^2 - m_b^2][(p_1-l)^2 - m_a^2][l^2 - M_j^2]}, \quad (\text{B.11})$$

but, of course, including the off-diagonal elements. Using the Cutkosky rules again yields

$$\text{Disc}(\mathcal{I}_{MBB}^{bj,ai}(p_1^2, p^2)) = -\frac{i\delta^{ji}}{16\pi|\mathbf{k}|\sqrt{p^2}} \log\left(\frac{\mathcal{H}^{bj,ai} + 2|\mathbf{k}||\mathbf{q}|^{bj,ai}}{\mathcal{H}^{bj,ai} - 2|\mathbf{k}||\mathbf{q}|^{bj,ai}}\right).$$

The corresponding dispersion relation for the numeric computation reads

$$\mathcal{I}_{MBB}^{bj,ai}(p_1^2, p^2) = -\frac{1}{2\pi i} \int_{(m_b+M_j)^2}^{\infty} ds' \frac{\text{Disc}(\mathcal{I}_{MBB}^{bj,ai}(p_1^2, s'))}{p^2 - s'}.$$

As in the previous section, the integrals with vector and tensor structure in the numerator have to be evaluated as well. The two-point function with a vector structure can be rewritten as

$$\int \frac{d^d l}{(2\pi)^d} \frac{i\delta^{ji} l^\mu}{[(p-l)^2 - m_b^2][l^2 - M_j^2]} = p^\mu [\mathcal{I}_{MB,b}^{(1)}(p^2)]^{bj,ai}.$$

Solving for $[\mathcal{I}_{MB,b}^{(1)}(p^2)]^{bj,ai}$ leads to

$$[\mathcal{I}_{MB,b}^{(1)}(p^2)]^{bj,ai} = \frac{1}{2p^2} \left[(p^2 + M_j^2 - m_b^2) \mathcal{I}_{MB}^{bj,ai}(p^2) + \mathcal{I}_B^{bj,ai} - \mathcal{I}_M^{bj,ai} \right]. \quad (\text{B.12})$$

Due to the particular renormalization scheme described in section 4.1, the baryon tadpole integral \mathcal{I}_B as well as the baryon-baryon two-point function \mathcal{I}_{BB} are set to zero. But for completeness, they will be included in the decompositions anyway. The corresponding integral with an initial state baryon mass can be obtained by replacing $m_b \rightarrow m_a$ and can therefore be solved in complete analogy, which leads to

$$[\mathcal{I}_{MB,a}^{(1)}(p^2)]^{bj,ai} = [\mathcal{I}_{MB,b}^{(1)}(p^2)]^{bj,ai} \Big|_{m_b \rightarrow m_a}.$$

The three-point function with two baryons, one meson and a vector structure in the numerator reads

$$\int \frac{d^d l}{(2\pi)^d} \frac{i\delta^{ji} l^\mu}{[(p-l)^2 - m_b^2][(p_1-l)^2 - m_a^2][l^2 - M_j^2]} = \mathcal{A}^{bj,ai}(p_1^2, p^2) (p_1 + p)^\mu + \mathcal{B}^{bj,ai}(p_1^2, p^2) (p_1 - p)^\mu$$

Solving for \mathcal{A} and \mathcal{B} , analogously to the previous section, yields

$$\begin{aligned}\mathcal{A}^{bj,ai}(p_1^2, p^2) &= \frac{1}{2D} \left[\left(4[\tilde{M}^2]^{bj,ai} - \frac{\Delta p^2}{k^2} (\Delta p^2 + m_a^2 - m_b^2) \right) \mathcal{I}_{MBB}^{bj,ai}(p_1^2, p^2) \right. \\ &\quad \left. + 2\mathcal{I}_{BB}^{bj,ai}(k^2) - \left(1 - \frac{\Delta p^2}{k^2} \right) \mathcal{I}_{MB,a}^{bj,ai}(p_1^2) - \left(1 + \frac{\Delta p^2}{k^2} \right) \mathcal{I}_{MB,b}^{bj,ai}(p^2) \right] \\ \mathcal{B}^{bj,ai}(p_1^2, p^2) &= \frac{\Delta p^2}{2k^2 D} \left[\left(4[\tilde{M}^2]^{bj,ai} + \frac{(4\bar{p} - k^2)(-\Delta p^2 + m_b^2 - m_a^2)}{\Delta p^2} \right) \right. \\ &\quad \times \mathcal{I}_{MBB}^{bj,aj}(p_1^2, p^2) + 2\mathcal{I}_{BB}^{bj,ai}(k^2) - \left(1 - \frac{4\bar{p}^2 - k^2}{\Delta p^2} \right) \mathcal{I}_{MB,a}^{bj,ai}(p_1^2) \\ &\quad \left. - \left(1 + \frac{4\bar{p}^2 - k^2}{\Delta p^2} \right) \mathcal{I}_{MB,b}^{bj,ai}(p^2) \right],\end{aligned}$$

where

$$[\tilde{M}^2]^{bj,ai} = \frac{1}{2} \delta^{ji} (\bar{p}^2 + M_j^2 - \frac{1}{2}(m_a^2 + m_b^2)).$$

Again, $\mathcal{I}_{BB}(k^2) = 0$ is valid – the integral \mathcal{I}_{BB} appears only for completeness.

The three point function with a tensor structure in the numerator is given by

$$\begin{aligned}\int \frac{d^d l}{(2\pi)^d} \frac{i\delta^{ji} l^\mu l^\nu}{[(p-l)^2 - m_b^2][(p_1-l)^2 - m_a^2][l^2 - M_j^2]} &= \mathcal{C}_1^{bj,ai}(p_1^2, p^2) g^{\mu\nu} \\ &\quad + \mathcal{C}_2^{bj,ai}(p_1^2, p^2) (p_1 + p)^\mu (p_1 + p)^\nu \\ &\quad + \mathcal{C}_3^{bj,ai}(p_1^2, p^2) (p_1 - p)^\mu (p_1 - p)^\nu \\ &\quad + \mathcal{C}_4^{bj,ai}(p_1^2, p^2) ((p_1 + p)^\mu (p_1 - p)^\nu + (p_1 - p)^\mu (p_1 + p)^\nu).\end{aligned}\tag{B.13}$$

Contracting the equation on both sides with each Dirac structure appearing on the r.h.s. and completing squares in order to cancel the denominators leads to four independent equations, which have the solution

$$\begin{aligned}\mathcal{C}_1^{bj,ai}(p_1^2, p^2) &= \frac{1}{2(d-2)k^2 D} \left\{ 2k^2 M_j^2 D \mathcal{I}_{MBB}^{bj,ai} - 2k^2 \Delta p^2 [\mathcal{I}_{BB}^{(1)}(k^2)]^{bj,ai} \right. \\ &\quad - \left[k^4 - 2k^2 (p^2 + \bar{p}^2) + 2\Delta p^4 \right] \mathcal{I}_{BB}^{bj,ai}(k^2) \\ &\quad + 2p^2 \Delta p^2 [\mathcal{I}_{MB,b}^{(1)}(p^2)]^{bj,ai} - 2p_1^2 \Delta p^2 [\mathcal{I}_{MB,a}^{(1)}(p_1^2)]^{bj,ai} \\ &\quad + \left[(k^2 - 4\bar{p}^2) \left(4k^2 [\tilde{M}^2]^{bj,ai} + \Delta p^2 \left([\Delta m^2]^{bj,ai} - \Delta p^2 \right) \right) \right] \\ &\quad \times \mathcal{A}^{bj,ai}(p_1^2, p^2) \\ &\quad \left. + \left[2k^2 (p_1^2 m_a^2 - p^2 m_b^2 + \Delta p^2 M_j^2) + k^4 ([\Delta m^2]^{bj,ai} - \Delta p^2) \right] \right\}\end{aligned}$$

$$\begin{aligned}
& -2k^2\bar{p}^2([\Delta m^2]^{bj,ai} - 3\Delta p^2) + 2\Delta p^4([\Delta m^2]^{bj,ai} - \Delta p^2)] \\
& \quad \times \mathcal{B}^{bj,ai}(p_1^2, p^2) \Big\}, \\
\mathcal{C}_2^{bj,ai}(p_1^2, p^2) &= \frac{1}{k^2 D} \left\{ \left[k^2 M_j^2 + \frac{1}{4} [\Delta m^2]^{bj,ai} (\Delta p^2 - [\Delta m^2]^{bj,ai}) \right] \mathcal{I}_{MBB}^{bj,ai}(p_1^2, p^2) \right. \\
& \quad + k^2 \mathcal{I}_{BB}^{bj,ai}(k^2) + \frac{\Delta p^2}{2} \left[k^2 \mathcal{B}^{bj,ai}(p_1^2, p^2) - \Delta p^2 \mathcal{A}^{bj,ai}(p_1^2, p^2) \right] \\
& \quad - \frac{k^2}{4} \left[[\mathcal{I}_{MB,a}^{(1)}(p_1^2)]^{bj,ai} + [\mathcal{I}_{MB,b}^{(1)}(p^2)]^{bj,ai} \right] \\
& \quad + \frac{\Delta p^2}{4} \left[[\mathcal{I}_{MB,a}^{(1)}(p_1^2)]^{bj,ai} - [\mathcal{I}_{MB,b}^{(1)}(p^2)]^{bj,ai} \right] \\
& \quad \left. + \frac{\Delta m^2}{4} \left[\mathcal{I}_{MB,b}^{bj,ai}(p^2) - \mathcal{I}_{MB,a}^{bj,ai}(p_1^2) \right] - (d-1)k^2 \mathcal{C}_1^{bj,ai}(p_1^2, p^2) \right\}, \\
\mathcal{C}_3^{bj,ai}(p_1^2, p^2) &= \frac{1}{k^2 D} \left\{ (4\bar{p}^2 - k^2) \left[M_j^2 \mathcal{I}_{MBB}^{bj,aj}(p_1^2, p^2) + \frac{1}{2} \mathcal{I}_{BB}^{bj,ai}(k^2) \right] \right. \\
& \quad - 2[\tilde{M}^2]^{bj,ai} \left[(4\bar{p}^2 - k^2) \mathcal{A}^{bj,ai}(p_1^2, p^2) - \Delta p^2 \mathcal{B}^{bj,ai}(p_1^2, p^2) \right] \\
& \quad + \frac{1}{4} (4\bar{p}^2 - \Delta p^2 - k^2) [\mathcal{I}_{MB,a}^{(1)}(p_1^2)]^{bj,ai} \\
& \quad + \frac{1}{4} (4\bar{p} + \Delta p^2 - k^2) [\mathcal{I}_{MB,b}^{(1)}(p^2)]^{bj,ai} \\
& \quad \left. - (d-1)(4\bar{p}^2 - k^2) \mathcal{C}_1^{bj,ai}(p_1^2, p^2) \right\}, \\
\mathcal{C}_4^{bj,ai}(p_1^2, p^2) &= \frac{1}{k^2 D} \left\{ (\Delta p^2 M_j^2 + [\Delta m^2]^{bj,ai} [\tilde{M}^2]^{bj,ai}) \mathcal{I}_{MBB}^{bj,ai}(p_1^2, p^2) \right. \\
& \quad + \left(\Delta p^2 + \frac{[\Delta m^2]^{bj,ai}}{2} \right) \mathcal{I}_{BB}^{bj,ai}(k^2) \\
& \quad - \frac{\Delta p^2}{2} \left[(4\bar{p}^2 - k^2) \mathcal{A}^{bj,ai}(p_1^2, p^2) - \Delta p^2 \mathcal{B}^{bj,ai}(p_1^2, p^2) \right] \\
& \quad + \frac{1}{4} (4\bar{p}^2 - \Delta p^2 - k^2) [\mathcal{I}_{MB,a}^{(1)}(p_1^2)]^{bj,ai} \\
& \quad - \frac{1}{4} (4\bar{p}^2 + \Delta p^2 - k^2) [\mathcal{I}_{MB,b}^{(1)}(p^2)]^{bj,ai} \\
& \quad - \frac{[\Delta m^2]^{bj,ai}}{4} \left[\mathcal{I}_{MB,b}^{bj,ai}(p^2) + \mathcal{I}_{MB,a}^{bj,ai}(p_1^2) \right] \\
& \quad \left. - (d-1) \Delta p^2 \mathcal{C}_1^{bj,ai}(p_1^2, p^2) \right\}, \tag{B.14}
\end{aligned}$$

where

$$[\Delta m^2]^{bj,ai} = \delta^{ji}(m_b^2 - m_a^2).$$

Again, the coefficient \mathcal{C}_1 picks up an additional constant in the limit of $d \rightarrow 4$. Two cases of are already shown in eq. (B.8) that apply equally to \mathcal{C}_1 ,

however, a third case occurs in the course of the calculation of the extended amplitude:

$$d\mathcal{C}_1^{bj,ai} \rightarrow 4\mathcal{C}_1^{bj,ai}(d=4) - \delta^{ji} \frac{1}{32\pi^2}.$$

To conclude this appendix, one last integral will be decomposed which will be used during the evaluation of the extended amplitude:

$$\begin{aligned} & \int \frac{d^d l}{(2\pi)^d} \frac{1}{\not{p} - \not{l} - m_b} i\delta^{ji} [\not{k}, \gamma^\mu] g_b^{bj,ai} \frac{1}{(\not{p}_1 - \not{l} - m_a)(l^2 - M_j^2)} \\ &= \gamma^\mu F_{b,1}^{bj,ai}(p_1^2, p^2) + \not{p}\gamma^\mu F_{b,2}^{bj,ai}(p_1^2, p^2) + \gamma^\mu \not{p}_1 F_{b,3}^{bj,ai}(p_1^2, p^2) \\ &+ \not{p}\gamma^\mu \not{p}_1 F_{b,4}^{bj,ai}(p_1^2, p^2) + p^\mu F_{b,5}^{bj,ai}(p_1^2, p^2) + p_1^\mu F_{b,6}^{bj,ai}(p_1^2, p^2) \\ &+ p^\mu \not{p} F_{b,7}^{bj,ai}(p_1^2, p^2) + p^\mu \not{p}_1 F_{b,8}^{bj,ai}(p_1^2, p^2) + p_1^\mu \not{p} F_{b,9}^{bj,ai}(p_1^2, p^2) \\ &+ p_1^\mu \not{p}_1 F_{b,10}^{bj,ai}(p_1^2, p^2) + p^\mu \not{p}\not{p}_1 F_{b,11}^{bj,ai}(p_1^2, p^2) + p_1^\mu \not{p}\not{p}_1 F_{b,12}^{bj,ai}(p_1^2, p^2), \end{aligned}$$

where the coefficients read

$$\begin{aligned} F_{b,1}^{bj,ai}(p_1^2, p^2) &= 2g_b^{bj,ai} \left\{ m_a \left[(k^2 - 2p^2) \mathcal{A}^{bj,ai}(p_1^2, p^2) + k^2 \mathcal{B}^{bj,ai}(p_1^2, p^2) \right. \right. \\ &\quad \left. \left. + p^2 \mathcal{I}_{M_{BB}}^{bj,ai}(p_1^2, p^2) \right] + m_b \left[(k^2 - 2p_1^2) \mathcal{A}^{bj,ai}(p_1^2, p^2) \right. \right. \\ &\quad \left. \left. - k^2 \mathcal{B}^{bj,ai}(p_1^2, p^2) + p_1^2 \mathcal{I}_{M_{BB}}^{bj,ai}(p_1^2, p^2) \right] \right\}, \end{aligned}$$

$$\begin{aligned} F_{b,2}^{bj,ai}(p_1^2, p^2) &= 2g_b^{bj,ai} \left\{ m_a m_b \mathcal{I}_{M_{BB}}^{bj,ai}(p_1^2, p^2) \right. \\ &\quad \left. + p_1^2 \left[4\mathcal{C}_2^{bj,ai}(p_1^2, p^2) - 4\mathcal{A}^{bj,ai}(p_1^2, p^2) + \mathcal{I}_{M_{BB}}^{bj,ai}(p_1^2, p^2) \right] \right. \\ &\quad \left. - k^2 \left[\mathcal{B}^{bj,ai}(p_1^2, p^2) - \mathcal{A}^{bj,ai}(p_1^2, p^2) + \mathcal{C}_2^{bj,ai}(p_1^2, p^2) \right] \right. \\ &\quad \left. + \mathcal{C}_3^{bj,ai}(p_1^2, p^2) - 2\mathcal{C}_4^{bj,ai}(p_1^2, p^2) \right] + \frac{1}{32\pi^2} \left. \right\}, \end{aligned}$$

$$\begin{aligned} F_{b,3}^{bj,ai}(p_1^2, p^2) &= 2g_b^{bj,ai} \left\{ m_a m_b \mathcal{I}_{M_{BB}}^{bj,ai}(p_1^2, p^2) \right. \\ &\quad \left. + k^2 \left[\mathcal{A}^{bj,ai}(p_1^2, p^2) + \mathcal{B}^{bj,ai}(p_1^2, p^2) - \mathcal{C}_2^{bj,ai}(p_1^2, p^2) \right. \right. \\ &\quad \left. \left. - \mathcal{C}_3^{bj,ai}(p_1^2, p^2) - 2\mathcal{C}_4^{bj,ai}(p_1^2, p^2) \right] \right. \\ &\quad \left. + p^2 \left[-4\mathcal{A}^{bj,ai}(p_1^2, p^2) + 4\mathcal{C}_2^{bj,ai}(p_1^2, p^2) + \mathcal{I}_{M_{BB}}^{bj,ai}(p_1^2, p^2) \right] \right. \\ &\quad \left. + \frac{1}{32\pi^2} \right\}, \end{aligned}$$

$$F_{b,4}^{bj,ai}(p_1^2, p^2) = 2g_b^{bj,ai} (m_a + m_b) \left[\mathcal{I}_{M_{BB}}^{bj,ai}(p_1^2, p^2) - 2\mathcal{A}^{bj,ai}(p_1^2, p^2) \right],$$

$$\begin{aligned}
F_{b,5}^{bj,ai}(p_1^2, p^2) &= -2g_b^{bj,ai} \left\{ m_a m_b \mathcal{I}_{M\overline{B}B}^{bj,ai}(p_1^2, p^2) \right. \\
&\quad + \Delta p^2 \left[\mathcal{A}^{bj,ai}(p_1^2, p^2) + 2\overline{p}^2 (\mathcal{B}^{bj,ai}(p_1^2, p^2) - 2\mathcal{C}_4^{bj,ai}(p_1^2, p^2)) \right. \\
&\quad \left. \left. - (k^2 - 2\Delta p^2) \mathcal{C}_2^{bj,ai}(p_1^2, p^2) + k^2 \mathcal{C}_3^{bj,ai}(p_1^2, p^2) \right] + \frac{1}{32\pi^2} \right\}, \\
F_{b,6}^{bj,ai}(p_1^2, p^2) &= -2g_b^{bj,ai} \left\{ m_a m_b \mathcal{I}_{M\overline{B}B}^{bj,ai}(p_1^2, p^2) \right. \\
&\quad + \left[2\overline{p}^2 (\mathcal{B}^{bj,ai}(p_1^2, p^2) - 2\mathcal{C}_4^{bj,ai}(p_1^2, p^2)) - \Delta p^2 \mathcal{A}^{bj,ai}(p_1^2, p^2) \right. \\
&\quad \left. + (k^2 - 2\Delta p^2) \mathcal{C}_2^{bj,ai}(p_1^2, p^2) - k^2 \mathcal{C}_3^{bj,ai}(p_1^2, p^2) \right] + \frac{1}{32\pi^2} \right\}, \\
F_{b,7}^{bj,ai}(p_1^2, p^2) &= 2g_b^{bj,ai} \left\{ m_a \left[\mathcal{A}^{bj,ai}(p_1^2, p^2) - \mathcal{B}^{bj,ai}(p_1^2, p^2) - \mathcal{I}_{M\overline{B}B}^{bj,ai}(p_1^2, p^2) \right] \right. \\
&\quad \left. + m_b \left[\mathcal{B}^{bj,ai}(p_1^2, p^2) - \mathcal{A}^{bj,ai}(p_1^2, p^2) \right] \right\}, \\
F_{b,8}^{bj,ai}(p_1^2, p^2) &= 2g_b^{bj,ai} \left\{ m_a \left[\mathcal{A}^{bj,ai}(p_1^2, p^2) + \mathcal{B}^{bj,ai}(p_1^2, p^2) \right] \right. \\
&\quad \left. + m_b \left[3\mathcal{A}^{bj,ai}(p_1^2, p^2) - \mathcal{B}^{bj,ai}(p_1^2, p^2) - \mathcal{I}_{M\overline{B}B}^{bj,ai}(p_1^2, p^2) \right] \right\}, \\
F_{b,9}^{bj,ai}(p_1^2, p^2) &= 2g_b^{bj,ai} \left\{ m_a \left[3\mathcal{A}^{bj,ai}(p_1^2, p^2) + \mathcal{B}^{bj,ai}(p_1^2, p^2) - \mathcal{I}_{M\overline{B}B}^{bj,ai}(p_1^2, p^2) \right] \right. \\
&\quad \left. + m_b \left[\mathcal{A}^{bj,ai}(p_1^2, p^2) - \mathcal{B}^{bj,ai}(p_1^2, p^2) \right] \right\}, \\
F_{b,10}^{bj,ai}(p_1^2, p^2) &= 2g_b^{bj,ai} \left\{ m_b \left[\mathcal{A}^{bj,ai}(p_1^2, p^2) + \mathcal{B}^{bj,ai}(p_1^2, p^2) - \mathcal{I}_{M\overline{B}B}^{bj,ai}(p_1^2, p^2) \right] \right. \\
&\quad \left. - m_a \left[\mathcal{A}^{bj,ai}(p_1^2, p^2) + \mathcal{B}^{bj,ai}(p_1^2, p^2) \right] \right\}, \\
F_{b,11}^{bj,ai}(p_1^2, p^2) &= 2g_b^{bj,ai} \left\{ 4\mathcal{A}^{bj,ai}(p_1^2, p^2) - 2\mathcal{B}^{bj,ai}(p_1^2, p^2) - 4\mathcal{C}_2^{bj,ai}(p_1^2, p^2) \right. \\
&\quad \left. + 4\mathcal{C}_4^{bj,ai}(p_1^2, p^2) - \mathcal{I}_{M\overline{B}B}^{bj,ai}(p_1^2, p^2) \right\}, \\
F_{b,12}^{bj,ai}(p_1^2, p^2) &= 2g_b^{bj,ai} \left\{ 4\mathcal{A}^{bj,ai}(p_1^2, p^2) + 2\mathcal{B}^{bj,ai}(p_1^2, p^2) \right. \\
&\quad \left. - 4 \left[\mathcal{C}_2^{bj,ai}(p_1^2, p^2) + \mathcal{C}_4^{bj,ai}(p_1^2, p^2) \right] - \mathcal{I}_{M\overline{B}B}^{bj,ai}(p_1^2, p^2) \right\}.
\end{aligned}$$

Appendix C

Gauge invariance of \mathcal{M}^μ

In this appendix, the gauge invariance of the leading order photoproduction amplitude \mathcal{M}^μ of chapter 3 shall be proven. The proof will proceed in analogy to [31]. To this end, the Ward-Takahashi identity $k_\mu \mathcal{M}^\mu = 0$ shall be used, where k is the momentum of the external photon. Note, that the proof needs the external particles to be set on the mass shell. First, consider

$$\frac{1}{\not{p} - m_p} \not{k} = \frac{1}{\not{p} - m_p} (\not{p} - \not{p}_1) = 1,$$

where in the first step it was used that the total momentum is $p = p_1 + k$ and in the second step the proton momentum p_1 was set on-shell. With this identity, the amplitude S_s^μ of eq. (3.4) can be reduced upon contraction with k_μ to

$$k_\mu S_s^\mu = -e\Gamma(\not{q}, \not{p}).$$

Similarly, with $k = p - p_1 = -(p_1 - q - p_2)$ the identity

$$\not{k} \frac{1}{\not{p}_1 - \not{q} - m} = -1$$

holds, where p_2 was set on-shell. Thus the amplitude S_u^μ of eq. (3.5) yields

$$k_\mu S_u^\mu = eQ_B \Gamma(\not{q}, \not{p}_1).$$

And likewise

$$k_\mu (2q - k)^\mu \frac{1}{(q - k)^2 - M^2} = -((q - k)^2 - M^2) \frac{1}{(q - k)^2 - M^2} = -1,$$

can be used for the amplitude S_t^μ of eq. (3.7) to obtain

$$k_\mu S_t^\mu = eQ_M \Gamma(\not{q} - \not{k}, \not{p}_1).$$

Such simplifications can be used also to contract the other amplitudes S_B^μ of eq. (3.6), S_M^μ of eq. (3.8), S_{KR}^μ of eq. (3.9), S_{WT1}^μ of eq. (3.10) and S_{WT2}^μ of eq. (3.11) to obtain

$$\begin{aligned}
k_\mu S_B^\mu &= \int \frac{d^d l}{(2\pi)^d} T(\not{q}, \not{l}; p) iS(\not{p} - \not{l}) \Delta(l) eQ_B \Gamma(\not{l}, \not{p}_1) \\
&\quad - \int \frac{d^d l}{(2\pi)^d} T(\not{q}, \not{l}; p) eQ_B iS(\not{p}_1 - \not{l}) \Delta(l) \Gamma(\not{l}, \not{p}_1), \\
k_\mu S_M^\mu &= \int \frac{d^d l}{(2\pi)^d} T(\not{q}, \not{l}; p) iS(\not{p} - \not{l}) \Delta(l) eQ_M \Gamma(\not{l} - \not{k}, \not{p}_1) \\
&\quad - \int \frac{d^d l}{(2\pi)^d} T(\not{q}, \not{l} + \not{k}; p) eQ_M iS(\not{p}_1 - \not{l}) \Delta(l) \Gamma(\not{l}, \not{p}_1), \\
k_\mu S_{KR}^\mu &= eQ_M \hat{g} \not{k} \gamma_5 + \int \frac{d^d l}{(2\pi)^d} T(\not{q}, \not{l}; p) iS(\not{p} - \not{l}) \Delta(l) eQ_M \hat{g} \not{k} \gamma_5, \\
k_\mu S_{WT1}^\mu &= e\hat{k} \{Q_M, g\} \int \frac{d^d l}{(2\pi)^d} iS(\not{p}_1 - \not{l}) \Delta(l) \Gamma(\not{l}, \not{p}_1), \\
k_\mu S_{WT2}^\mu &= \int \frac{d^d \tilde{l}}{(2\pi)^d} T(\not{q}, \tilde{\not{l}}; p) iS(\not{p} - \tilde{\not{l}}) \Delta(\tilde{l}) e\hat{k} \{Q_M, g\} \\
&\quad \times \int \frac{d^d l}{(2\pi)^d} iS(\not{p}_1 - \not{l}) \Delta(l) \Gamma(\not{l}, \not{p}_1).
\end{aligned}$$

The cancellation of these graphs occurs on two different levels. The first being the cancellation of the tree graphs: The tree part of $k_\mu(S_s^\mu + S_u^\mu + S_t^\mu + S_{KR}^\mu)$ can be evaluated as

$$\begin{aligned}
&-e\hat{g}\gamma_5 + eQ_B \hat{g} \not{q} \gamma_5 + eQ_M \hat{g} (\not{q} - \not{k}) \gamma_5 + eQ_M \hat{g} \not{k} \gamma_5 \\
&= -e\hat{g}\gamma_5 + eQ_B \hat{g} \not{q} \gamma_5 + eQ_M \hat{g} \not{q} \gamma_5 \\
&= 0,
\end{aligned}$$

where in the last step $Q_B + Q_M = 1$ was used. The other cancellations happen for the loop contributions. To see this, consider the integral equations

$$T(\not{q}, \not{l}; p) = g(\not{q} + \not{l}) + \int \frac{d^d \tilde{l}}{(2\pi)^d} T(\not{q}, \tilde{\not{l}}; p) iS(\not{p} - \tilde{\not{l}}) \Delta(\tilde{l}) g(\not{l} + \tilde{\not{l}}), \quad (\text{C.1})$$

$$\Gamma(\not{l}, \not{p}_1) = \hat{g} \not{l} \gamma_5 + \int \frac{d^d \tilde{l}}{(2\pi)^d} g(\not{l} + \tilde{\not{l}}) iS(\not{p}_1 - \tilde{\not{l}}) \Delta(\tilde{l}) \Gamma(\tilde{\not{l}}, \not{p}_1), \quad (\text{C.2})$$

which are equivalent to eq. (2.4) and eq. (3.1), respectively. The equivalence can be easily seen by explicitly iterating the integral equations. Using eq. (C.1) in the second term of $k_\mu S_B^\mu$ and $k_\mu S_M^\mu$ and using eq. (C.2) in the first term of $k_\mu S_B^\mu$ and $k_\mu S_M^\mu$ leads to a rather lengthy but trivial cancellation of all loop contributions. This, together with the cancellation of the tree graphs, leads to $k_\mu \mathcal{M}^\mu = 0$ and therefore the amplitude \mathcal{M}^μ is indeed gauge invariant.

Appendix D

Decompositions of the amplitudes

This appendix provides the decompositions into independent Lorentz structures of the various amplitudes entering the photoproduction amplitudes. Section D.1 is dedicated to the amplitudes necessary for the leading order calculation of chapter 3, whereas section D.2 contains the additional amplitudes for the extension of chapter 4. All integrals used in this chapter are provided in appendix B.

D.1 Decompositions for the leading order calculation

The amplitude S_s^μ of eq. (3.4) can be decomposed as follows:

$$S_s^\mu = (\not{q}\not{p}S_s^{\not{q}\not{p}\gamma} + \not{q}S_s^{\not{q}\gamma} + \not{p}S_s^{\not{p}\gamma} + S_s^\gamma)\gamma^\mu\gamma_5$$

with

$$\begin{aligned} S_s^{\not{q}\not{p}\gamma} &= \frac{e}{m_p^2 - s}(\Gamma_2(p) - m_p\Gamma_1(p)), \\ S_s^{\not{q}\gamma} &= \frac{e}{m_p^2 - s}(s\Gamma_1(p) - m_p\Gamma_2(p)), \\ S_s^{\not{p}\gamma} &= \frac{e}{m_p^2 - s}(\Gamma_4(p) - m_p\Gamma_3(p)), \\ S_s^\gamma &= \frac{e}{m_p^2 - s}(s\Gamma_3(p) - m_p\Gamma_4(p)), \end{aligned}$$

where m_p is the proton mass of eq. (2.15), the Γ_i are the coefficients of the decomposition of Γ of eq. (3.2) and $s = p^2 = (p_1 + k)^2$ is the squared center-of-mass energy. Moreover, channel indices will be omitted for brevity.

Before proceeding, some functions will be introduced for a more compact notation:

$$\begin{aligned} Y_1 &= m_p^2 \Gamma_1(p_1) - m_p (\Gamma_2(p_1) + \Gamma_3(p_1)) + \Gamma_4(p_1) \\ Y_2 &= \Gamma_2(p_1) - m_p \Gamma_1(p_1) \\ Y_3 &= -(m_p + m) \Gamma_2(p_1) + (m_p^2 + m_p m) \Gamma_1(p_1) - m_p \Gamma_3(p_1) + \Gamma_4(p_1). \end{aligned}$$

Note, that the proton mass m_p is a number, while m is a matrix with the baryon masses on its diagonal as given by eq. (2.5). Therefore, any numbers like m_p are understood to be multiplied by the identity matrix in channel space. Furthermore, the Mandelstam variables t and u that are needed for the following amplitudes are defined as

$$\begin{aligned} t &= M^2 + k^2 - 2E_k E_q + 2|\mathbf{k}||\mathbf{q}| \cos \theta, \\ u &= k^2 + m_p^2 + m^2 + M^2 - s - t, \end{aligned}$$

where $|\mathbf{k}|$ and $|\mathbf{q}|$ are the moduli of the center-of-mass three-momenta of the photon and the meson, respectively, and θ is the scattering angle in the center-of-mass system. The center-of-mass energies are given by

$$E_k = \sqrt{|\mathbf{k}|^2 + k^2}, \quad E_q = \sqrt{|\mathbf{q}|^2 + M^2}.$$

Note, that the Mandelstam variables t and u are matrices in channel space. Now, the amplitude S_u^μ of eq. (3.5) can be decomposed as

$$S_u^\mu = (q^\mu S_u^q + \not{q} \gamma^\mu S_u^{q\gamma} + \gamma^\mu S_u^\gamma) \gamma_5$$

with

$$\begin{aligned} S_u^q &= -2S_u^{q\gamma} = \frac{2eQ_B}{u - m^2} Y_3, \\ S_u^\gamma &= \frac{eQ_B}{m^2 - u} \left(\Gamma_1(p_1) m_p (u - m_p^2) - \Gamma_2(p_1) (u - m_p^2) + (m_p^2 - m_p m) \Gamma_3(p_1) \right. \\ &\quad \left. + (m - m_p) \Gamma_4(p_1) \right). \end{aligned}$$

Here, matrices appearing in the denominator denote matrix inversion. The amplitude S_t^μ of eq. (3.7) reads

$$\begin{aligned} S_t^\mu &= (p^\mu S_t^p + p_1^\mu S_t^{p_1} + q^\mu S_t^q + \not{q} q^\mu S_t^{qq} + \not{p} q^\mu S_t^{pq} + \not{p} p^\mu S_t^{pp} + \not{p} p_1^\mu S_t^{pp_1} \\ &\quad + \not{p} p_1^\mu S_t^{pp_1}) \gamma_5 \end{aligned}$$

with

$$\begin{aligned} S_t^p &= \frac{eQ_M}{t - M^2} Y_1, & S_t^{p_1} &= -S_t^p, & S_t^q &= -2S_t^p, \\ S_t^{qq} &= -\frac{2eQ_M}{t - M^2} Y_2, & S_t^{pq} &= -S_t^{qq}, & S_t^{pp} &= \frac{eQ_M}{t - M^2} Y_2, \end{aligned}$$

$$S_t^{\not{p}p} = -S_t^{\not{q}p}, \quad S_t^{\not{q}p_1} = -S_t^{\not{q}p}, \quad S_t^{\not{p}p_1} = S_t^{\not{q}p}.$$

The next graph is S_B^μ of eq. (3.6), whose decomposition reads

$$S_B^\mu = \left(\gamma^\mu S_B^\gamma + p^\mu S_B^p + p_1^\mu S_B^{p_1} + \not{q}\gamma^\mu S_B^{\not{q}\gamma} + \not{p}\gamma^\mu S_B^{\not{p}\gamma} + \not{q}\not{p}\gamma^\mu S_B^{\not{q}\not{p}\gamma} + \not{q}p^\mu S_B^{\not{q}p} \right. \\ \left. + \not{p}p^\mu S_B^{\not{p}p} + \not{q}\not{p}p^\mu S_B^{\not{q}\not{p}p} + \not{q}p_1^\mu S_B^{\not{q}p_1} + \not{p}p_1^\mu S_B^{\not{p}p_1} + \not{q}\not{p}p_1^\mu S_B^{\not{q}\not{p}p_1} \right) \gamma_5$$

with

$$S_B^\gamma = -s \left(T_3 m G_1(p) e_{QB} Y_2 - T_3 G_0(p) e_{QB} Y_2 - T_5 G_1(p) e_{QB} Y_2 \right. \\ \left. - T_7 G_1(p) e_{QB} Y_2 - T_3 m F_2 Y_3 + T_3 F_1 Y_3 + T_5 F_2 Y_3 + T_7 F_2 Y_3 \right) \\ + m_p \left(-T_5 e_{QB} G_1(p_1) + s(-T_3 m F_4 + T_3 F_3 + T_5 F_4 + T_7 F_4) \right. \\ \left. - T_5 m F_3 + T_8 F_3 \right) Y_3 - T_5 m G_0(p) e_{QB} Y_2 + T_5 e_{QB} G_0(p_1) Y_3 \\ + T_8 G_0(p) e_{QB} Y_2 - T_5 e_{QB} I_M Y_2 + T_5 m F_1 Y_3 - T_8 F_1 Y_3, \\ S_B^p = m_p (-T_5 m F_8 Y_3 + s T_3 F_8 Y_3 + T_8 F_8 Y_3) + T_5 m F_5 Y_3 - T_8 F_5 Y_3 \\ - s(-T_3 m F_7 Y_3 + T_3 F_5 Y_3 + T_5 F_7 Y_3 + T_7 F_7 Y_3), \\ S_B^{p_1} = m_p (-T_5 m F_{10} Y_3 + s T_3 F_{10} Y_3 + T_8 F_{10} Y_3) + T_5 m F_6 Y_3 - T_8 F_6 Y_3 \\ - s(-T_3 m F_9 + T_3 F_6 + T_5 F_9 + T_7 F_9) Y_3, \\ S_B^{\not{q}\gamma} = -s \left(T_1 m G_1(p) e_{QB} Y_2 - T_1 G_0(p) e_{QB} Y_2 - T_2 G_1(p) e_{QB} Y_2 \right. \\ \left. - T_4 G_1(p) e_{QB} Y_2 - T_1 m F_2 Y_3 + T_1 F_1 Y_3 + T_2 F_2 Y_3 + T_4 F_2 Y_3 \right) \\ + m_p \left(-T_2 e_{QB} G_1(p_1) + s(-T_1 m F_4 + T_1 F_3 + T_2 F_4 + T_4 F_4) \right. \\ \left. - T_2 m F_3 + T_6 F_3 \right) Y_3 - T_2 m G_0(p) e_{QB} Y_2 + T_2 e_{QB} G_0(p_1) Y_3 \\ + T_6 G_0(p) e_{QB} Y_2 - T_2 e_{QB} I_M Y_2 + T_2 m F_1 Y_3 - T_6 F_1 Y_3, \\ S_B^{\not{p}\gamma} = m_p \left(-T_3 e_{QB} G_1(p_1) - T_3 m F_3 - T_5 m F_4 + s T_3 F_4 + T_5 F_3 + T_7 F_3 \right. \\ \left. + T_8 F_4 \right) Y_3 + s(T_3 G_1(p) e_{QB} Y_2 - T_3 F_2 Y_3) - T_3 m G_0(p) e_{QB} Y_2 \\ - T_5 m G_1(p) e_{QB} Y_2 + T_3 e_{QB} G_0(p_1) Y_3 + T_5 G_0(p) e_{QB} Y_2 \\ + T_7 G_0(p) e_{QB} Y_2 + T_8 G_1(p) e_{QB} Y_2 - T_3 e_{QB} I_M Y_2 + T_3 m F_1 Y_3 \\ + T_5 m F_2 Y_3 - T_5 F_1 Y_3 - T_7 F_1 Y_3 - T_8 F_2 Y_3, \\ S_B^{\not{q}\not{p}\gamma} = m_p \left(-T_1 e_{QB} G_1(p_1) - T_1 m F_3 - T_2 m F_4 + s T_1 F_4 + T_2 F_3 + T_4 F_3 \right. \\ \left. + T_6 F_4 \right) Y_3 - s(T_1 F_2 Y_3 - T_1 G_1(p) e_{QB} Y_2) - T_1 m G_0(p) e_{QB} Y_2 \\ - T_2 m G_1(p) e_{QB} Y_2 + T_1 e_{QB} G_0(p_1) Y_3 + T_2 G_0(p) e_{QB} Y_2 \\ + T_4 G_0(p) e_{QB} Y_2 + T_6 G_1(p) e_{QB} Y_2 - T_1 e_{QB} I_M Y_2 + T_1 m F_1 Y_3 \\ + T_2 m F_2 Y_3 - T_2 F_1 Y_3 - T_4 F_1 Y_3 - T_6 F_2 Y_3,$$

$$\begin{aligned}
S_B^{\not{q}p} &= m_p(-T_2mF_8 + sT_1F_8 + T_6F_8)Y_3 + T_2mF_5Y_3 - T_6F_5Y_3 \\
&\quad - s(-T_1mF_7 + T_1F_5 + T_2F_7 + T_4F_7)Y_3, \\
S_B^{\not{p}p} &= m_p(-T_3mF_8 + T_5F_8 + T_7F_8)Y_3 \\
&\quad - (-T_3mF_5 - T_5mF_7 + sT_3F_7 + T_5F_5 + T_7F_5 + T_8F_7)Y_3, \\
S_B^{\not{q}\not{p}p} &= m_p(-T_1mF_8 + T_2F_8 + T_4F_8)Y_3 \\
&\quad - (-T_1mF_5 - T_2mF_7 + sT_1F_7 + T_2F_5 + T_4F_5 + T_6F_7)Y_3, \\
S_B^{\not{q}p_1} &= m_p(-T_2mF_{10} + sT_1F_{10} + T_6F_{10})Y_3 + T_2mF_6Y_3 - T_6F_6Y_3 \\
&\quad - s(-T_1mF_9 + T_1F_6 + T_2F_9 + T_4F_9)Y_3, \\
S_B^{\not{p}p_1} &= m_p(-T_3mF_{10} + T_5F_{10} + T_7F_{10})Y_3 \\
&\quad - (-T_3mF_6 - T_5mF_9 + sT_3F_9 + T_5F_6 + T_7F_6 + T_8F_9)Y_3, \\
S_B^{\not{q}\not{p}p_1} &= m_p(-T_1mF_{10} + T_2F_{10} + T_4F_{10})Y_3 \\
&\quad - (-T_1mF_6 - T_2mF_9 + sT_1F_9 + T_2F_6 + T_4F_6 + T_6F_9)Y_3.
\end{aligned}$$

The demposition of S_M^μ of eq. (3.8) is given by

$$\begin{aligned}
S_M^\mu &= \left(\gamma^\mu S_M^\gamma + p^\mu S_M^p + p_1^\mu S_M^{p_1} + \not{q}\gamma^\mu S_M^{\not{q}\gamma} + \not{p}\gamma^\mu S_M^{\not{p}\gamma} + \not{q}\not{p}\gamma^\mu S_M^{\not{q}\not{p}\gamma} + \not{q}p^\mu S_M^{\not{q}p} \right. \\
&\quad \left. + \not{p}p^\mu S_M^{\not{p}p} + \not{q}\not{p}p^\mu S_M^{\not{q}\not{p}p} + \not{q}p_1^\mu S_M^{\not{q}p_1} + \not{p}p_1^\mu S_M^{\not{p}p_1} + \not{q}\not{p}p_1^\mu S_M^{\not{q}\not{p}p_1} \right) \gamma_5
\end{aligned}$$

with

$$\begin{aligned}
S_M^\gamma &= -T_5eQ_M d_1 Y_2 + T_5m\tilde{F}_1 Y_3 - sT_3\tilde{F}_1 Y_3 - T_8\tilde{F}_1 Y_3, \\
S_M^p &= m_p(-T_5eQ_M d_2 Y_2 - T_5m\tilde{F}_8 Y_3 + sT_3\tilde{F}_8 Y_3 + T_8\tilde{F}_8 Y_3) \\
&\quad - s(T_3eQ_M d_2 Y_2 - T_3m\tilde{F}_7 Y_3 + T_3\tilde{F}_5 Y_3 + T_5\tilde{F}_7 Y_3 + T_7\tilde{F}_7 Y_3) \\
&\quad + T_5m\tilde{F}_5 Y_3 - T_8\tilde{F}_5 Y_3, \\
S_M^{p_1} &= m_p(T_5eQ_M d_2 Y_2 - T_5m\tilde{F}_{10} Y_3 + sT_3\tilde{F}_{10} Y_3 + T_8\tilde{F}_{10} Y_3) \\
&\quad + sT_3eQ_M d_2 Y_2 - s(-T_3m\tilde{F}_9 + T_3\tilde{F}_6 + T_5\tilde{F}_9 + T_7\tilde{F}_9)Y_3 + T_5m\tilde{F}_6 Y_3 \\
&\quad - T_8\tilde{F}_6 Y_3, \\
S_M^{\not{q}\gamma} &= -T_2eQ_M d_1 Y_2 + T_2m\tilde{F}_1 Y_3 - sT_1\tilde{F}_1 Y_3 - T_6\tilde{F}_1 Y_3, \\
S_M^{\not{p}\gamma} &= -T_3eQ_M d_1 Y_2 + T_3m\tilde{F}_1 Y_3 - T_5\tilde{F}_1 Y_3 - T_7\tilde{F}_1 Y_3, \\
S_M^{\not{q}\not{p}\gamma} &= -T_1eQ_M d_1 Y_2 + T_1m\tilde{F}_1 Y_3 - T_2\tilde{F}_1 Y_3 - T_4\tilde{F}_1 Y_3, \\
S_M^{\not{q}p} &= m_p(-T_2eQ_M d_2 Y_2 - T_2m\tilde{F}_8 Y_3 + sT_1\tilde{F}_8 Y_3 + T_6\tilde{F}_8 Y_3) - sT_1eQ_M d_2 Y_2 \\
&\quad - s(-T_1m\tilde{F}_7 + T_1\tilde{F}_5 + T_2\tilde{F}_7 + T_4\tilde{F}_7)Y_3 + T_2m\tilde{F}_5 Y_3 - T_6\tilde{F}_5 Y_3, \\
S_M^{\not{p}p} &= m_p(-T_3eQ_M d_2 Y_2 - T_3m\tilde{F}_8 Y_3 + T_5\tilde{F}_8 Y_3 + T_7\tilde{F}_8 Y_3) - T_5eQ_M d_2 Y_2 \\
&\quad - (-T_3m\tilde{F}_5 - T_5m\tilde{F}_7 + T_5\tilde{F}_5 + T_7\tilde{F}_5 + T_8\tilde{F}_7)Y_3 - sT_3\tilde{F}_7 Y_3, \\
S_M^{\not{q}\not{p}p} &= m_p(-T_1eQ_M d_2 Y_2 - T_1m\tilde{F}_8 Y_3 + T_2\tilde{F}_8 Y_3 + T_4\tilde{F}_8 Y_3) - T_2eQ_M d_2 Y_2
\end{aligned}$$

D.1. DECOMPOSITIONS FOR THE LEADING ORDER CALCULATION 93

$$\begin{aligned}
& -(-T_1 m \tilde{F}_5 - T_2 m \tilde{F}_7 + T_2 \tilde{F}_5 + T_4 \tilde{F}_5 + T_6 \tilde{F}_7) Y_3 - s T_1 \tilde{F}_7 Y_3, \\
S_M^{q p_1} &= m_p (T_2 e Q_M d_2 Y_2 - T_2 m \tilde{F}_{10} Y_3 + s T_1 \tilde{F}_{10} Y_3 + T_6 \tilde{F}_{10} Y_3) + s T_1 e Q_M d_2 Y_2 \\
& - s(-T_1 m \tilde{F}_9 + T_1 \tilde{F}_6 + T_2 \tilde{F}_9 + T_4 \tilde{F}_9) Y_3 + T_2 m \tilde{F}_6 Y_3 - T_6 \tilde{F}_6 Y_3, \\
S_M^{\not{p} p_1} &= m_p (T_3 e Q_M d_2 Y_2 - T_3 m \tilde{F}_{10} Y_3 + T_5 \tilde{F}_{10} Y_3 + T_7 \tilde{F}_{10} Y_3) + T_5 e Q_M d_2 Y_2 \\
& - (-T_3 m \tilde{F}_6 - T_5 m \tilde{F}_9 + T_5 \tilde{F}_6 + T_7 \tilde{F}_6 + T_8 \tilde{F}_9) Y_3 - s T_3 \tilde{F}_9 Y_3, \\
S_M^{q \not{p} p_1} &= m_p (T_1 e Q_M d_2 Y_2 - T_1 m \tilde{F}_{10} Y_3 + T_2 \tilde{F}_{10} Y_3 + T_4 \tilde{F}_{10} Y_3) + T_2 e Q_M d_2 Y_2 \\
& - (-T_1 m \tilde{F}_6 - T_2 m \tilde{F}_9 + T_2 \tilde{F}_6 + T_4 \tilde{F}_6 + T_6 \tilde{F}_9) Y_3 - s T_1 \tilde{F}_9 Y_3,
\end{aligned}$$

where the abbreviations $T_i = T_i(p)$ and

$$\begin{aligned}
d_1 &= -2 \left(\frac{1}{3} \left((M^2 - \frac{1}{4} k^2) I_{MM}(k^2) + I_M \right) + \frac{1}{48 \pi^2} \left(\frac{1}{6} k^2 - M^2 \right) \right), \\
d_2 &= \frac{1}{2} I_{MM}(k^2) - \frac{2}{k^2} \left(\frac{1}{3} \left((k^2 - M^2) I_{MM}(k^2) + I_M \right) - \frac{1}{48 \pi^2} \left(\frac{1}{6} k^2 - M^2 \right) \right)
\end{aligned}$$

where used. The next graph is S_{KR}^μ of eq. (3.9):

$$S_{KR}^\mu = (S_{KR}^\gamma + \not{q} S_{KR}^{q\gamma} + \not{p} S_{KR}^{\not{p}\gamma} + \not{q} \not{p} S_{KR}^{q \not{p}\gamma}) \gamma^\mu \gamma_5$$

with

$$\begin{aligned}
S_{KR}^\gamma &= e Q_M \hat{g} + \left(s(-T_3 m + T_5 + T_7) G_1(p) + (-T_5 m + s T_3 + T_8) G_0(p) \right. \\
& \left. - T_5 I_M \right) e Q_M \hat{g}, \\
S_{KR}^{q\gamma} &= \left(s(-T_1 m + T_2 + T_4) G_1(p) + (-T_2 m + s T_1 + T_6) G_0(p) \right. \\
& \left. - T_2 I_M \right) e Q_M \hat{g}, \\
S_{KR}^{\not{p}\gamma} &= \left((-T_5 m + s T_3 + T_8) G_1(p) + (-T_3 m + T_5 + T_7) G_0(p) \right. \\
& \left. - T_3 I_M \right) e Q_M \hat{g}, \\
S_{KR}^{q \not{p}\gamma} &= \left((-T_2 m + s T_1 + T_6) G_1(p) + (-T_1 m + T_2 + T_4) G_0(p) \right. \\
& \left. - T_1 I_M \right) e Q_M \hat{g}
\end{aligned}$$

The graph S_{WT1}^μ of eq. (3.10) is given by

$$S_{WT1}^\mu = \gamma^\mu \gamma_5 S_{WT1}^\gamma$$

with

$$S_{WT1}^\gamma = e(Q_M g + g Q_M) \left((G_0(p_1) - m_p G_1(p_1)) Y_3 - I_M Y_2 \right).$$

And lastly, the decomposition of the graph S_{WT2}^μ of eq. (3.11) reads

$$S_{WT2}^\mu = (S_{WT2}^\gamma + \not{q}S_{WT2}^{\not{q}\gamma} + \not{p}S_{WT2}^{\not{p}\gamma} + \not{q}\not{p}S_{WT2}^{\not{q}\not{p}\gamma})\gamma^\mu\gamma_5$$

with

$$\begin{aligned} S_{WT2}^\gamma &= (s(-T_3m + T_5 + T_7)G_1(p) + (-T_5m + sT_3 + T_8)G_0(p) \\ &\quad - T_5I_M)S_{WT1}^\gamma, \\ S_{WT2}^{\not{q}\gamma} &= (s(-T_1m + T_2 + T_4)G_1(p) + (-T_2m + sT_1 + T_6)G_0(p) \\ &\quad - T_2I_M)S_{WT1}^\gamma, \\ S_{WT2}^{\not{p}\gamma} &= ((-T_5m + sT_3 + T_8)G_1(p) + (-T_3m + T_5 + T_7)G_0(p) \\ &\quad - T_3I_M)S_{WT1}^\gamma, \\ S_{WT2}^{\not{q}\not{p}\gamma} &= ((-T_2m + sT_1 + T_6)G_1(p) + (-T_1m + T_2 + T_4)G_0(p) \\ &\quad - T_1I_M)S_{WT1}^\gamma. \end{aligned}$$

The total amplitude can be obtained by adding all amplitudes. Then, the decomposition of the total amplitude is given by

$$\begin{aligned} \mathcal{M}^\mu &= \gamma^\mu\gamma_5\mathcal{M}_1 + \not{q}^\mu\gamma_5\mathcal{M}_2 + \not{p}^\mu\gamma_5\mathcal{M}_3 + \not{p}_1^\mu\gamma_5\mathcal{M}_4 + \not{q}\gamma^\mu\gamma_5\mathcal{M}_5 + \not{p}\gamma^\mu\gamma_5\mathcal{M}_6 \\ &\quad + \not{q}\not{p}\gamma^\mu\gamma_5\mathcal{M}_7 + \not{q}\not{q}^\mu\gamma_5\mathcal{M}_8 + \not{p}\not{q}^\mu\gamma_5\mathcal{M}_9 + \not{q}\not{p}^\mu\gamma_5\mathcal{M}_{10} + \not{p}\not{p}^\mu\gamma_5\mathcal{M}_{11} \\ &\quad + \not{q}\not{p}\not{p}^\mu\gamma_5\mathcal{M}_{12} + \not{q}\not{p}_1^\mu\gamma_5\mathcal{M}_{13} + \not{p}\not{p}_1^\mu\gamma_5\mathcal{M}_{14} + \not{q}\not{p}\not{p}_1^\mu\gamma_5\mathcal{M}_{15}. \end{aligned}$$

D.2 Decomposition of the extended amplitude

In this section, the additional amplitudes entering the extended amplitude of chapter 4 will be decomposed. The first amplitude that will be decomposed is $S_{b,s}$ of eq. (4.3):

$$\begin{aligned} S_{b,s}^\mu &= \left(\gamma^\mu S_{b,s}^\gamma + \not{p}^\mu S_{b,s}^p + \not{p}_1^\mu S_{b,s}^{p_1} + \not{q}\gamma^\mu S_{b,s}^{\not{q}\gamma} + \not{p}\gamma^\mu S_{b,s}^{\not{p}\gamma} + \not{q}\not{p}\gamma^\mu S_{b,s}^{\not{q}\not{p}\gamma} + \not{q}\not{p}^\mu S_{b,s}^{\not{q}p} \right. \\ &\quad \left. + \not{p}\not{p}^\mu S_{b,s}^{\not{p}p} + \not{q}\not{p}\not{p}^\mu S_{b,s}^{\not{q}\not{p}p} + \not{q}\not{p}_1^\mu S_{b,s}^{\not{q}p_1} + \not{p}\not{p}_1^\mu S_{b,s}^{\not{p}p_1} + \not{q}\not{p}\not{p}_1^\mu S_{b,s}^{\not{q}\not{p}p_1} \right) \gamma_5 \end{aligned}$$

with

$$\begin{aligned} S_{b,s}^\gamma &= \frac{1}{s - m_p^2} (2g_b^{p,p} m_p^2 \Gamma_4(p) - 4sg_b^{p,p} m_p \Gamma_3(p) + 2sg_b^{p,p} \Gamma_4(p)), \\ S_{b,s}^p &= \frac{1}{m_p^2 - s} (2sg_b^{p,p} \Gamma_3(p) - 2g_b^{p,p} m_p \Gamma_4(p)), \\ S_{b,s}^{p_1} &= S_{b,s}^p, \\ S_{b,s}^{\not{q}\gamma} &= \frac{1}{s - m_p^2} (2g_b^{p,p} m_p^2 \Gamma_2(p) - 4sg_b^{p,p} m_p \Gamma_1(p) + 2sg_b^{p,p} \Gamma_2(p)), \\ S_{b,s}^{\not{p}\gamma} &= \frac{1}{s - m_p^2} (2g_b^{p,p} m_p^2 \Gamma_3(p) - 4g_b^{p,p} m_p \Gamma_4(p) + 2sg_b^{p,p} \Gamma_3(p)), \end{aligned}$$

$$\begin{aligned}
S_{b,s}^{\not{q}\not{p}\gamma} &= \frac{1}{s - m_p^2} (2g_b^{p,p} m_p^2 \Gamma_1(p) - 4g_b^{p,p} m_p \Gamma_2(p) + 2s g_b^{p,p} \Gamma_1(p)), \\
S_{b,s}^{\not{q}p} &= \frac{1}{s - m_p^2} (2g_b^{p,p} m_p \Gamma_2(p) - 2s g_b^{p,p} \Gamma_1(p)), \\
S_{b,s}^{\not{p}p} &= \frac{1}{s - m_p^2} (2g_b^{p,p} m_p \Gamma_3(p) - 2g_b^{p,p} \Gamma_4(p)), \\
S_{b,s}^{\not{q}\not{p}p} &= \frac{1}{s - m_p^2} (2g_b^{p,p} m_p \Gamma_1(p) - 2g_b^{p,p} \Gamma_2(p)), \\
S_{b,s}^{\not{q}p_1} &= S_{b,s}^{\not{q}p}, \\
S_{b,s}^{\not{p}p_1} &= S_{b,s}^{\not{p}p}, \\
S_{b,s}^{\not{q}\not{p}p_1} &= S_{b,s}^{\not{q}\not{p}p},
\end{aligned}$$

where the coupling $g_b^{p,p}$ is the component of g_b that corresponds to a $\gamma p \rightarrow p$ vertex, i.e. the photon couples to the proton. The decomposition of $S_{b,u}^\mu$ of eq. (4.4) is given by

$$\begin{aligned}
S_{b,u}^\mu &= \left(\gamma^\mu S_{b,u}^\gamma + p^\mu S_{b,u}^p + p_1^\mu S_{b,u}^{p_1} + \not{q}\gamma^\mu S_{b,u}^{\not{q}\gamma} + \not{p}\gamma^\mu S_{b,u}^{\not{p}\gamma} + \not{q}\not{p}\gamma^\mu S_{b,u}^{\not{q}\not{p}\gamma} + \not{q}p^\mu S_{b,u}^{\not{q}p} \right. \\
&\quad \left. + \not{q}p_1^\mu S_{b,u}^{\not{q}p_1} + q^\mu S_{b,u}^q + \not{p}q^\mu S_{b,u}^{\not{p}q} \right) \gamma_5
\end{aligned}$$

with

$$\begin{aligned}
S_{b,u}^\gamma &= 2g_b \frac{1}{u - m^2} \left(-k^2 m_p^2 \Gamma_1(p_1) + k^2 m_p \Gamma_2(p_1) + k^2 m_p \Gamma_3(p_1) - m k^2 m_p \Gamma_1(p_1) \right. \\
&\quad \left. + m k^2 \Gamma_2(p_1) - k^2 \Gamma_4(p_1) - M^2 m_p^2 \Gamma_1(p_1) + M^2 m_p \Gamma_2(p_1) + M^2 m_p \Gamma_3(p_1) \right. \\
&\quad \left. - m M^2 m_p \Gamma_1(p_1) + m M^2 \Gamma_2(p_1) - m_p^4 \Gamma_1(p_1) + m_p^3 \Gamma_2(p_1) + m_p^3 \Gamma_3(p_1) \right. \\
&\quad \left. - m_p^2 \Gamma_4(p_1) - m_p^2 m \Gamma_3(p_1) + m_p m \Gamma_4(p_1) - M^2 \Gamma_4(p_1) \right) \\
&\quad + 2t g_b \frac{1}{u - m^2} \left(m_p^2 \Gamma_1(p_1) - m_p \Gamma_2(p_1) - m_p \Gamma_3(p_1) + m_p m \Gamma_1(p_1) \right. \\
&\quad \left. - m \Gamma_2(p_1) + \Gamma_4(p_1) \right) + 2u g_b \frac{g_b}{u - m^2} (m_p^2 \Gamma_1(p_1) - m_p \Gamma_2(p_1)), \\
S_{b,u}^p &= -2 \left(g_b \frac{1}{u - m^2} (m_p - m) \Gamma_4(p_1) + g_b \frac{1}{u - m^2} (m_p m - m_p^2) \Gamma_3(p_1) \right. \\
&\quad \left. + (u - m_p^2) g_b \frac{1}{u - m^2} \Gamma_2(p_1) + (m_p^3 - m_p u) g_b \frac{1}{u - m^2} \Gamma_1(p_1) \right), \\
S_{b,u}^{p_1} &= S_{b,u}^p, \\
S_{b,u}^{\not{q}\not{p}\gamma} &= 2g_b \frac{1}{u - m^2} Y_3, \\
S_{b,u}^{\not{q}\gamma} &= -m_p S_{b,u}^{\not{q}\not{p}\gamma}, \\
S_{b,u}^{\not{p}\gamma} &= -S_{b,u}^p,
\end{aligned}$$

$$\begin{aligned}
S_{b,u}^{\not{q}p} &= -S_{b,u}^{\not{q}\not{p}\gamma}, \\
S_{b,u}^{\not{q}p_1} &= S_{b,u}^{\not{q}p}, \\
S_{b,u}^q &= -2m_p S_{b,u}^{\not{q}p}, \\
S_{b,u}^{\not{p}q} &= -2S_{b,u}^{\not{q}p}.
\end{aligned}$$

The amplitude $S_{b,B}^\mu$ of eq. (4.5) can be decomposed as

$$\begin{aligned}
S_{b,B}^\mu &= \left(\gamma^\mu S_{b,B}^\gamma + p^\mu S_{b,B}^p + p_1^\mu S_{b,B}^{p_1} + \not{q}\gamma^\mu S_{b,B}^{\not{q}\gamma} + \not{p}\gamma^\mu S_{b,B}^{\not{p}\gamma} + \not{q}\not{p}\gamma^\mu S_{b,B}^{\not{q}\not{p}\gamma} + \not{q}p^\mu S_{b,B}^{\not{q}p} \right. \\
&\quad \left. + \not{p}p^\mu S_{b,B}^{\not{p}p} + \not{q}\not{p}p^\mu S_{b,B}^{\not{q}\not{p}p} + \not{q}p_1^\mu S_{b,B}^{\not{q}p_1} + \not{p}p_1^\mu S_{b,B}^{\not{p}p_1} + \not{q}\not{p}p_1^\mu S_{b,B}^{\not{q}\not{p}p_1} \right) \gamma_5
\end{aligned}$$

with

$$\begin{aligned}
S_{b,B}^\gamma &= T_3(-sF_{b,1})\Gamma_4(p_1) + T_3(sm_p F_{b,1})\Gamma_2(p_1) + T_3(sm_p F_{b,1})\Gamma_3(p_1) \\
&\quad + T_3(-sm_p^2 F_{b,1})\Gamma_1(p_1) + T_3(sm_p F_{b,3})\Gamma_4(p_1) + T_3(-sm_p^2 F_{b,3})\Gamma_2(p_1) \\
&\quad + T_3(-sm_p^2 F_{b,3})\Gamma_3(p_1) + T_3(sm_p^3 F_{b,3})\Gamma_1(p_1) + T_5(-sF_{b,2})\Gamma_4(p_1) \\
&\quad + T_5(sm_p F_{b,2})\Gamma_2(p_1) + T_5(sm_p F_{b,2})\Gamma_3(p_1) + T_5(-sm_p^2 F_{b,2})\Gamma_1(p_1) \\
&\quad + T_5(sm_p F_{b,4})\Gamma_4(p_1) + T_5(-sm_p^2 F_{b,4})\Gamma_2(p_1) + T_5(-sm_p^2 F_{b,4})\Gamma_3(p_1) \\
&\quad + T_5(sm_p^3 F_{b,4})\Gamma_1(p_1) + T_7(-sF_{b,2})\Gamma_4(p_1) + T_7(sm_p F_{b,2})\Gamma_2(p_1) \\
&\quad + T_7(sm_p F_{b,2})\Gamma_3(p_1) + T_7(-sm_p^2 F_{b,2})\Gamma_1(p_1) + T_7(sm_p F_{b,4})\Gamma_4(p_1) \\
&\quad + T_7(-sm_p^2 F_{b,4})\Gamma_2(p_1) + T_7(-sm_p^2 F_{b,4})\Gamma_3(p_1) + T_7(sm_p^3 F_{b,4})\Gamma_1(p_1) \\
&\quad + T_8(-F_{b,1})\Gamma_4(p_1) + T_8(m_p F_{b,1})\Gamma_2(p_1) + T_8(m_p F_{b,1})\Gamma_3(p_1) \\
&\quad + T_8(-m_p^2 F_{b,1})\Gamma_1(p_1) + T_8(m_p F_{b,3})\Gamma_4(p_1) + T_8(-m_p^2 F_{b,3})\Gamma_2(p_1) \\
&\quad + T_8(-m_p^2 F_{b,3})\Gamma_3(p_1) + T_8(m_p^3 F_{b,3})\Gamma_1(p_1) + T_3 m(sF_{b,2})\Gamma_4(p_1) \\
&\quad + T_3 m(-sm_p F_{b,2})\Gamma_2(p_1) + T_3 m(-sm_p F_{b,2})\Gamma_3(p_1) + T_3 m(sm_p^2 F_{b,2})\Gamma_1(p_1) \\
&\quad + T_3 m(-sm_p F_{b,4})\Gamma_4(p_1) + T_3 m(sm_p^2 F_{b,4})\Gamma_2(p_1) + T_3 m(sm_p^2 F_{b,4})\Gamma_3(p_1) \\
&\quad + T_3 m(-sm_p^3 F_{b,4})\Gamma_1(p_1) + T_3(-2sI_M)g_b\Gamma_2(p_1) + T_3 g_b(2sG_0(p_1))\Gamma_4(p_1) \\
&\quad + T_3 g_b(-2sm_p G_0(p_1))\Gamma_2(p_1) + T_3 g_b(-2sm_p G_0(p_1))\Gamma_3(p_1) \\
&\quad + T_3 g_b(2sm_p^2 G_0(p_1))\Gamma_1(p_1) + T_3 g_b(-2sm_p G_1(p_1))\Gamma_4(p_1) \\
&\quad + T_3 g_b(2sm_p^2 G_1(p_1))\Gamma_2(p_1) + T_3 g_b(2sm_p^2 G_1(p_1))\Gamma_3(p_1) \\
&\quad + T_3 g_b(-2sm_p^3 G_1(p_1))\Gamma_1(p_1) + T_3(2sI_M m_p)g_b\Gamma_1(p_1) + T_3(sF_{b,1})m\Gamma_2(p_1) \\
&\quad + T_3(-sm_p F_{b,1})m\Gamma_1(p_1) + T_3(-sm_p F_{b,3})m\Gamma_2(p_1) + T_3(sm_p^2 F_{b,3})m\Gamma_1(p_1) \\
&\quad + T_3(-2sm_p G_0(p))g_b\Gamma_2(p_1) + T_3(2sm_p^2 G_0(p))g_b\Gamma_1(p_1) \\
&\quad + T_3(2s^2 G_1(p))g_b\Gamma_2(p_1) + T_3(-2s^2 m_p G_1(p))g_b\Gamma_1(p_1) + T_5 m F_{b,1}\Gamma_4(p_1) \\
&\quad + T_5 m(-m_p F_{b,1})\Gamma_2(p_1) + T_5 m(-m_p F_{b,1})\Gamma_3(p_1) + T_5 m(m_p^2 F_{b,1})\Gamma_1(p_1) \\
&\quad + T_5 m(-m_p F_{b,3})\Gamma_4(p_1) + T_5 m(m_p^2 F_{b,3})\Gamma_2(p_1) + T_5 m(m_p^2 F_{b,3})\Gamma_3(p_1)
\end{aligned}$$

$$\begin{aligned}
& + T_5 m(-m_p^3 F_{b,3}) \Gamma_1(p_1) + T_5 g_b(-2m_p G_0(p_1)) \Gamma_4(p_1) + T_5 g_b(2m_p^2 G_0(p_1)) \Gamma_2(p_1) \\
& + T_5 g_b(2m_p^2 G_0(p_1)) \Gamma_3(p_1) + T_5 g_b(-2m_p^3 G_0(p_1)) \Gamma_1(p_1) \\
& + T_5 g_b(2m_p^2 G_1(p_1)) \Gamma_4(p_1) + T_5 g_b(-2m_p^3 G_1(p_1)) \Gamma_2(p_1) \\
& + T_5 g_b(-2m_p^3 G_1(p_1)) \Gamma_3(p_1) + T_5 g_b(2m_p^4 G_1(p_1)) \Gamma_1(p_1) \\
& + T_5(2I_M m_p) g_b \Gamma_2(p_1) + T_5(-2I_M m_p^2) g_b \Gamma_1(p_1) + T_5(sF_{b,2}) m \Gamma_2(p_1) \\
& + T_5(-sm_p F_{b,2}) m \Gamma_1(p_1) + T_5(-sm_p F_{b,4}) m \Gamma_2(p_1) + T_5(sm_p^2 F_{b,4}) m \Gamma_1(p_1) \\
& + T_5(2sG_0(p)) g_b \Gamma_2(p_1) + T_5(-2sm_p G_0(p)) g_b \Gamma_1(p_1) + T_5(-2sm_p G_1(p)) g_b \Gamma_2(p_1) \\
& + T_5(2sm_p^2 G_1(p)) g_b \Gamma_1(p_1) + T_7(sF_{b,2}) m \Gamma_2(p_1) + T_7(-sm_p F_{b,2}) m \Gamma_1(p_1) \\
& + T_7(-sm_p F_{b,4}) m \Gamma_2(p_1) + T_7(sm_p^2 F_{b,4}) m \Gamma_1(p_1) + T_7(2sG_0(p)) g_b \Gamma_2(p_1) \\
& + T_7(-2sm_p G_0(p)) g_b \Gamma_1(p_1) + T_7(-2sm_p G_1(p)) g_b \Gamma_2(p_1) + T_7(2sm_p^2 G_1(p)) g_b \Gamma_1(p_1) \\
& + T_8 F_{b,1} m \Gamma_2(p_1) + T_8(-m_p F_{b,1}) m \Gamma_1(p_1) + T_8(-m_p F_{b,3}) m \Gamma_2(p_1) \\
& + T_8(m_p^2 F_{b,3}) m \Gamma_1(p_1) + T_8(-2m_p G_0(p)) g_b \Gamma_2(p_1) + T_8(2m_p^2 G_0(p)) g_b \Gamma_1(p_1) \\
& + T_8(2sG_1(p)) g_b \Gamma_2(p_1) + T_8(-2sm_p G_1(p)) g_b \Gamma_1(p_1) + T_3 m(-sF_{b,2}) m \Gamma_2(p_1) \\
& + T_3 m(sm_p F_{b,2}) m \Gamma_1(p_1) + T_3 m(sm_p F_{b,4}) m \Gamma_2(p_1) + T_3 m(-sm_p^2 F_{b,4}) m \Gamma_1(p_1) \\
& + T_3 m(-2sG_0(p)) g_b \Gamma_2(p_1) + T_3 m(2sm_p G_0(p)) g_b \Gamma_1(p_1) + T_3 m(2sm_p G_1(p)) g_b \Gamma_2(p_1) \\
& + T_3 m(-2sm_p^2 G_1(p)) g_b \Gamma_1(p_1) + T_3 g_b(-2sG_0(p_1)) m \Gamma_2(p_1) + T_3 g_b(2sm_p G_0(p_1)) m \Gamma_1(p_1) \\
& + T_3 g_b(2sm_p G_1(p_1)) m \Gamma_2(p_1) + T_3 g_b(-2sm_p^2 G_1(p_1)) m \Gamma_1(p_1) + T_5 m(-F_{b,1}) m \Gamma_2(p_1) \\
& + T_5 m(m_p F_{b,1}) m \Gamma_1(p_1) + T_5 m(m_p F_{b,3}) m \Gamma_2(p_1) + T_5 m(-m_p^2 F_{b,3}) m \Gamma_1(p_1) \\
& + T_5 m(2m_p G_0(p)) g_b \Gamma_2(p_1) + T_5 m(-2m_p^2 G_0(p)) g_b \Gamma_1(p_1) + T_5 m(-2sG_1(p)) g_b \Gamma_2(p_1) \\
& + T_5 m(2sm_p G_1(p)) g_b \Gamma_1(p_1) + T_5 g_b(2m_p G_0(p_1)) m \Gamma_2(p_1) \\
& + T_5 g_b(-2m_p^2 G_0(p_1)) m \Gamma_1(p_1) + T_5 g_b(-2m_p^2 G_1(p_1)) m \Gamma_2(p_1) \\
& + T_5 g_b(2m_p^3 G_1(p_1)) m \Gamma_1(p_1), \\
S_{b,B}^p = & T_3(-sF_{b,5}) \Gamma_4(p_1) + T_3(sm_p F_{b,5}) \Gamma_2(p_1) + T_3(sm_p F_{b,5}) \Gamma_3(p_1) \\
& + T_3(-sm_p^2 F_{b,5}) \Gamma_1(p_1) + T_3(sm_p F_{b,8}) \Gamma_4(p_1) + T_3(-sm_p^2 F_{b,8}) \Gamma_2(p_1) \\
& + T_3(-sm_p^2 F_{b,8}) \Gamma_3(p_1) + T_3(sm_p^3 F_{b,8}) \Gamma_1(p_1) + T_5(-sF_{b,7}) \Gamma_4(p_1) \\
& + T_5(sm_p F_{b,7}) \Gamma_2(p_1) + T_5(sm_p F_{b,7}) \Gamma_3(p_1) + T_5(-sm_p^2 F_{b,7}) \Gamma_1(p_1) \\
& + T_5(sm_p F_{b,11}) \Gamma_4(p_1) + T_5(-sm_p^2 F_{b,11}) \Gamma_2(p_1) + T_5(-sm_p^2 F_{b,11}) \Gamma_3(p_1) \\
& + T_5(sm_p^3 F_{b,11}) \Gamma_1(p_1) + T_7(-sF_{b,7}) \Gamma_4(p_1) + T_7(sm_p F_{b,7}) \Gamma_2(p_1) \\
& + T_7(sm_p F_{b,7}) \Gamma_3(p_1) + T_7(-sm_p^2 F_{b,7}) \Gamma_1(p_1) + T_7(sm_p F_{b,11}) \Gamma_4(p_1) \\
& + T_7(-sm_p^2 F_{b,11}) \Gamma_2(p_1) + T_7(-sm_p^2 F_{b,11}) \Gamma_3(p_1) + T_7(sm_p^3 F_{b,11}) \Gamma_1(p_1) \\
& + T_8(-F_{b,5}) \Gamma_4(p_1) + T_8(m_p F_{b,5}) \Gamma_2(p_1) + T_8(m_p F_{b,5}) \Gamma_3(p_1) \\
& + T_8(-m_p^2 F_{b,5}) \Gamma_1(p_1) + T_8(m_p F_{b,8}) \Gamma_4(p_1) + T_8(-m_p^2 F_{b,8}) \Gamma_2(p_1) \\
& + T_8(-m_p^2 F_{b,8}) \Gamma_3(p_1) + T_8(m_p^3 F_{b,8}) \Gamma_1(p_1) + T_3 m(sF_{b,7}) \Gamma_4(p_1)
\end{aligned}$$

$$\begin{aligned}
& + T_3 m(-sm_p F_{b,7}) \Gamma_2(p_1) + T_3 m(-sm_p F_{b,7}) \Gamma_3(p_1) + T_3 m(sm_p^2 F_{b,7}) \Gamma_1(p_1) \\
& + T_3 m(-sm_p F_{b,11}) \Gamma_4(p_1) + T_3 m(sm_p^2 F_{b,11}) \Gamma_2(p_1) \\
& + T_3 m(sm_p^2 F_{b,11}) \Gamma_3(p_1) + T_3 m(-sm_p^3 F_{b,11}) \Gamma_1(p_1) + T_3 (sF_{b,5}) m \Gamma_2(p_1) \\
& + T_3 (-sm_p F_{b,5}) m \Gamma_1(p_1) + T_3 (-sm_p F_{b,8}) m \Gamma_2(p_1) + T_3 (sm_p^2 F_{b,8}) m \Gamma_1(p_1) \\
& + T_3 (-2sG_0(p)) g_b \Gamma_2(p_1) + T_3 (2sm_p G_0(p)) g_b \Gamma_1(p_1) + T_5 m F_{b,5} \Gamma_4(p_1) \\
& + T_5 m(-m_p F_{b,5}) \Gamma_2(p_1) + T_5 m(-m_p F_{b,5}) \Gamma_3(p_1) + T_5 m(m_p^2 F_{b,5}) \Gamma_1(p_1) \\
& + T_5 m(-m_p F_{b,8}) \Gamma_4(p_1) + T_5 m(m_p^2 F_{b,8}) \Gamma_2(p_1) + T_5 m(m_p^2 F_{b,8}) \Gamma_3(p_1) \\
& + T_5 m(-m_p^3 F_{b,8}) \Gamma_1(p_1) + T_5 (2I_M) g_b \Gamma_2(p_1) + T_5 g_b (-2G_0(p_1)) \Gamma_4(p_1) \\
& + T_5 g_b (2m_p G_0(p_1)) \Gamma_2(p_1) + T_5 g_b (2m_p G_0(p_1)) \Gamma_3(p_1) \\
& + T_5 g_b (-2m_p^2 G_0(p_1)) \Gamma_1(p_1) + T_5 g_b (2m_p G_1(p_1)) \Gamma_4(p_1) \\
& + T_5 g_b (-2m_p^2 G_1(p_1)) \Gamma_2(p_1) + T_5 g_b (-2m_p^2 G_1(p_1)) \Gamma_3(p_1) \\
& + T_5 g_b (2m_p^3 G_1(p_1)) \Gamma_1(p_1) + T_5 (-2I_M m_p) g_b \Gamma_1(p_1) + T_5 (sF_{b,7}) m \Gamma_2(p_1) \\
& + T_5 (-sm_p F_{b,7}) m \Gamma_1(p_1) + T_5 (-sm_p F_{b,11}) m \Gamma_2(p_1) \\
& + T_5 (sm_p^2 F_{b,11}) m \Gamma_1(p_1) + T_5 (-2sG_1(p)) g_b \Gamma_2(p_1) \\
& + T_5 (2sm_p G_1(p)) g_b \Gamma_1(p_1) + T_7 (sF_{b,7}) m \Gamma_2(p_1) + T_7 (-sm_p F_{b,7}) m \Gamma_1(p_1) \\
& + T_7 (-sm_p F_{b,11}) m \Gamma_2(p_1) + T_7 (sm_p^2 F_{b,11}) m \Gamma_1(p_1) \\
& + T_7 (-2sG_1(p)) g_b \Gamma_2(p_1) + T_7 (2sm_p G_1(p)) g_b \Gamma_1(p_1) + T_8 F_{b,5} m \Gamma_2(p_1) \\
& + T_8 (-m_p F_{b,5}) m \Gamma_1(p_1) + T_8 (-m_p F_{b,8}) m \Gamma_2(p_1) + T_8 (m_p^2 F_{b,8}) m \Gamma_1(p_1) \\
& + T_8 (-2G_0(p)) g_b \Gamma_2(p_1) + T_8 (2m_p G_0(p)) g_b \Gamma_1(p_1) + T_3 m(-sF_{b,7}) m \Gamma_2(p_1) \\
& + T_3 m(sm_p F_{b,7}) m \Gamma_1(p_1) + T_3 m(sm_p F_{b,11}) m \Gamma_2(p_1) \\
& + T_3 m(-sm_p^2 F_{b,11}) m \Gamma_1(p_1) + T_3 m(2sG_1(p)) g_b \Gamma_2(p_1) \\
& + T_3 m(-2sm_p G_1(p)) g_b \Gamma_1(p_1) + T_5 m(-F_{b,5}) m \Gamma_2(p_1) \\
& + T_5 m(m_p F_{b,5}) m \Gamma_1(p_1) + T_5 m(m_p F_{b,8}) m \Gamma_2(p_1) \\
& + T_5 m(-m_p^2 F_{b,8}) m \Gamma_1(p_1) + T_5 m(2G_0(p)) g_b \Gamma_2(p_1) \\
& + T_5 m(-2m_p G_0(p)) g_b \Gamma_1(p_1) + T_5 g_b (2G_0(p_1)) m \Gamma_2(p_1) \\
& + T_5 g_b (-2m_p G_0(p_1)) m \Gamma_1(p_1) + T_5 g_b (-2m_p G_1(p_1)) m \Gamma_2(p_1) \\
& + T_5 g_b (2m_p^2 G_1(p_1)) m \Gamma_1(p_1), \\
S_{b,B}^{p_1} & = T_3 (-sF_{b,6}) \Gamma_4(p_1) + T_3 (sm_p F_{b,6}) \Gamma_2(p_1) + T_3 (sm_p F_{b,6}) \Gamma_3(p_1) \\
& + T_3 (-sm_p^2 F_{b,6}) \Gamma_1(p_1) + T_3 (sm_p F_{b,10}) \Gamma_4(p_1) \\
& + T_3 (-sm_p^2 F_{b,10}) \Gamma_2(p_1) + T_3 (-sm_p^2 F_{b,10}) \Gamma_3(p_1) \\
& + T_3 (sm_p^3 F_{b,10}) \Gamma_1(p_1) + T_5 (-sF_{b,9}) \Gamma_4(p_1) + T_5 (sm_p F_{b,9}) \Gamma_2(p_1) \\
& + T_5 (sm_p F_{b,9}) \Gamma_3(p_1) + T_5 (-sm_p^2 F_{b,9}) \Gamma_1(p_1) \\
& + T_5 (sm_p F_{b,12}) \Gamma_4(p_1) + T_5 (-sm_p^2 F_{b,12}) \Gamma_2(p_1)
\end{aligned}$$

$$\begin{aligned}
& + T_5(-sm_p^2 F_{b,12})\Gamma_3(p_1) + T_5(sm_p^3 F_{b,12})\Gamma_1(p_1) \\
& + T_7(-sF_{b,9})\Gamma_4(p_1) + T_7(sm_p F_{b,9})\Gamma_2(p_1) + T_7(sm_p F_{b,9})\Gamma_3(p_1) \\
& + T_7(-sm_p^2 F_{b,9})\Gamma_1(p_1) + T_7(sm_p F_{b,12})\Gamma_4(p_1) \\
& + T_7(-sm_p^2 F_{b,12})\Gamma_2(p_1) + T_7(-sm_p^2 F_{b,12})\Gamma_3(p_1) \\
& + T_7(sm_p^3 F_{b,12})\Gamma_1(p_1) + T_8(-F_{b,6})\Gamma_4(p_1) \\
& + T_8(m_p F_{b,6})\Gamma_2(p_1) + T_8(m_p F_{b,6})\Gamma_3(p_1) \\
& + T_8(-m_p^2 F_{b,6})\Gamma_1(p_1) + T_8(m_p F_{b,10})\Gamma_4(p_1) \\
& + T_8(-m_p^2 F_{b,10})\Gamma_2(p_1) + T_8(-m_p^2 F_{b,10})\Gamma_3(p_1) \\
& + T_8(m_p^3 F_{b,10})\Gamma_1(p_1) + T_3 m(sF_{b,9})\Gamma_4(p_1) \\
& + T_3 m(-sm_p F_{b,9})\Gamma_2(p_1) + T_3 m(-sm_p F_{b,9})\Gamma_3(p_1) \\
& + T_3 m(sm_p^2 F_{b,9})\Gamma_1(p_1) + T_3 m(-sm_p F_{b,12})\Gamma_4(p_1) \\
& + T_3 m(sm_p^2 F_{b,12})\Gamma_2(p_1) + T_3 m(sm_p^2 F_{b,12})\Gamma_3(p_1) \\
& + T_3 m(-sm_p^3 F_{b,12})\Gamma_1(p_1) + T_3(sF_{b,6})m\Gamma_2(p_1) \\
& + T_3(-sm_p F_{b,6})m\Gamma_1(p_1) + T_3(-sm_p F_{b,10})m\Gamma_2(p_1) \\
& + T_3(sm_p^2 F_{b,10})m\Gamma_1(p_1) + T_3(-2sG_0(p))g_b\Gamma_2(p_1) \\
& + T_3(2sm_p G_0(p))g_b\Gamma_1(p_1) + T_5 m F_{b,6}\Gamma_4(p_1) \\
& + T_5 m(-m_p F_{b,6})\Gamma_2(p_1) + T_5 m(-m_p F_{b,6})\Gamma_3(p_1) \\
& + T_5 m(m_p^2 F_{b,6})\Gamma_1(p_1) + T_5 m(-m_p F_{b,10})\Gamma_4(p_1) \\
& + T_5 m(m_p^2 F_{b,10})\Gamma_2(p_1) + T_5 m(m_p^2 F_{b,10})\Gamma_3(p_1) \\
& + T_5 m(-m_p^3 F_{b,10})\Gamma_1(p_1) + T_5(2I_M)g_b\Gamma_2(p_1) \\
& + T_5 g_b(-2G_0(p_1))\Gamma_4(p_1) + T_5 g_b(2m_p G_0(p_1))\Gamma_2(p_1) \\
& + T_5 g_b(2m_p G_0(p_1))\Gamma_3(p_1) + T_5 g_b(-2m_p^2 G_0(p_1))\Gamma_1(p_1) \\
& + T_5 g_b(2m_p G_1(p_1))\Gamma_4(p_1) + T_5 g_b(-2m_p^2 G_1(p_1))\Gamma_2(p_1) \\
& + T_5 g_b(-2m_p^2 G_1(p_1))\Gamma_3(p_1) + T_5 g_b(2m_p^3 G_1(p_1))\Gamma_1(p_1) \\
& + T_5(-2I_M m_p)g_b\Gamma_1(p_1) + T_5(sF_{b,9})m\Gamma_2(p_1) \\
& + T_5(-sm_p F_{b,9})m\Gamma_1(p_1) + T_5(-sm_p F_{b,12})m\Gamma_2(p_1) \\
& + T_5(sm_p^2 F_{b,12})m\Gamma_1(p_1) + T_5(-2sG_1(p))g_b\Gamma_2(p_1) \\
& + T_5(2sm_p G_1(p))g_b\Gamma_1(p_1) + T_7(sF_{b,9})m\Gamma_2(p_1) \\
& + T_7(-sm_p F_{b,9})m\Gamma_1(p_1) + T_7(-sm_p F_{b,12})m\Gamma_2(p_1) \\
& + T_7(sm_p^2 F_{b,12})m\Gamma_1(p_1) + T_7(-2sG_1(p))g_b\Gamma_2(p_1) \\
& + T_7(2sm_p G_1(p))g_b\Gamma_1(p_1) + T_8 F_{b,6}m\Gamma_2(p_1) \\
& + T_8(-m_p F_{b,6})m\Gamma_1(p_1) + T_8(-m_p F_{b,10})m\Gamma_2(p_1) \\
& + T_8(m_p^2 F_{b,10})m\Gamma_1(p_1) + T_8(-2G_0(p))g_b\Gamma_2(p_1) \\
& + T_8(2m_p G_0(p))g_b\Gamma_1(p_1) + T_3 m(-sF_{b,9})m\Gamma_2(p_1)
\end{aligned}$$

$$\begin{aligned}
& + T_3 m(sm_p F_{b,9}) m\Gamma_1(p_1) + T_3 m(sm_p F_{b,12}) m\Gamma_2(p_1) \\
& + T_3 m(-sm_p^2 F_{b,12}) m\Gamma_1(p_1) + T_3 m(2sG_1(p)) g_b \Gamma_2(p_1) \\
& + T_3 m(-2sm_p G_1(p)) g_b \Gamma_1(p_1) + T_5 m(-F_{b,6}) m\Gamma_2(p_1) \\
& + T_5 m(m_p F_{b,6}) m\Gamma_1(p_1) + T_5 m(m_p F_{b,10}) m\Gamma_2(p_1) \\
& + T_5 m(-m_p^2 F_{b,10}) m\Gamma_1(p_1) + T_5 m(2G_0(p)) g_b \Gamma_2(p_1) \\
& + T_5 m(-2m_p G_0(p)) g_b \Gamma_1(p_1) + T_5 g_b(2G_0(p_1)) m\Gamma_2(p_1) \\
& + T_5 g_b(-2m_p G_0(p_1)) m\Gamma_1(p_1) + T_5 g_b(-2m_p G_1(p_1)) m\Gamma_2(p_1) \\
& + T_5 g_b(2m_p^2 G_1(p_1)) m\Gamma_1(p_1), \\
S_{b,B}^{d\gamma} = & T_1(-sF_{b,1}) \Gamma_4(p_1) + T_1(sm_p F_{b,1}) \Gamma_2(p_1) \\
& + T_1(sm_p F_{b,1}) \Gamma_3(p_1) + T_1(-sm_p^2 F_{b,1}) \Gamma_1(p_1) \\
& + T_1(sm_p F_{b,3}) \Gamma_4(p_1) + T_1(-sm_p^2 F_{b,3}) \Gamma_2(p_1) \\
& + T_1(-sm_p^2 F_{b,3}) \Gamma_3(p_1) + T_1(sm_p^3 F_{b,3}) \Gamma_1(p_1) \\
& + T_2(-sF_{b,2}) \Gamma_4(p_1) + T_2(sm_p F_{b,2}) \Gamma_2(p_1) \\
& + T_2(sm_p F_{b,2}) \Gamma_3(p_1) + T_2(-sm_p^2 F_{b,2}) \Gamma_1(p_1) \\
& + T_2(sm_p F_{b,4}) \Gamma_4(p_1) + T_2(-sm_p^2 F_{b,4}) \Gamma_2(p_1) \\
& + T_2(-sm_p^2 F_{b,4}) \Gamma_3(p_1) + T_2(sm_p^3 F_{b,4}) \Gamma_1(p_1) \\
& + T_4(-sF_{b,2}) \Gamma_4(p_1) + T_4(sm_p F_{b,2}) \Gamma_2(p_1) \\
& + T_4(sm_p F_{b,2}) \Gamma_3(p_1) + T_4(-sm_p^2 F_{b,2}) \Gamma_1(p_1) \\
& + T_4(sm_p F_{b,4}) \Gamma_4(p_1) + T_4(-sm_p^2 F_{b,4}) \Gamma_2(p_1) \\
& + T_4(-sm_p^2 F_{b,4}) \Gamma_3(p_1) + T_4(sm_p^3 F_{b,4}) \Gamma_1(p_1) \\
& + T_6(-F_{b,1}) \Gamma_4(p_1) + T_6(m_p F_{b,1}) \Gamma_2(p_1) + T_6(m_p F_{b,1}) \Gamma_3(p_1) \\
& + T_6(-m_p^2 F_{b,1}) \Gamma_1(p_1) + T_6(m_p F_{b,3}) \Gamma_4(p_1) \\
& + T_6(-m_p^2 F_{b,3}) \Gamma_2(p_1) + T_6(-m_p^2 F_{b,3}) \Gamma_3(p_1) \\
& + T_6(m_p^3 F_{b,3}) \Gamma_1(p_1) + T_1 m(sF_{b,2}) \Gamma_4(p_1) \\
& + T_1 m(-sm_p F_{b,2}) \Gamma_2(p_1) + T_1 m(-sm_p F_{b,2}) \Gamma_3(p_1) \\
& + T_1 m(sm_p^2 F_{b,2}) \Gamma_1(p_1) + T_1 m(-sm_p F_{b,4}) \Gamma_4(p_1) \\
& + T_1 m(sm_p^2 F_{b,4}) \Gamma_2(p_1) + T_1 m(sm_p^2 F_{b,4}) \Gamma_3(p_1) \\
& + T_1 m(-sm_p^3 F_{b,4}) \Gamma_1(p_1) + T_1(-2sI_M) g_b \Gamma_2(p_1) \\
& + T_1 g_b(2sG_0(p_1)) \Gamma_4(p_1) + T_1 g_b(-2sm_p G_0(p_1)) \Gamma_2(p_1) \\
& + T_1 g_b(-2sm_p G_0(p_1)) \Gamma_3(p_1) + T_1 g_b(2sm_p^2 G_0(p_1)) \Gamma_1(p_1) \\
& + T_1 g_b(-2sm_p G_1(p_1)) \Gamma_4(p_1) + T_1 g_b(2sm_p^2 G_1(p_1)) \Gamma_2(p_1) \\
& + T_1 g_b(2sm_p^2 G_1(p_1)) \Gamma_3(p_1) + T_1 g_b(-2sm_p^3 G_1(p_1)) \Gamma_1(p_1) \\
& + T_1(2sI_M m_p) g_b \Gamma_1(p_1) + T_1(sF_{b,1}) m\Gamma_2(p_1)
\end{aligned}$$

$$\begin{aligned}
& + T_1(-sm_p F_{b,1})m\Gamma_1(p_1) + T_1(-sm_p F_{b,3})m\Gamma_2(p_1) \\
& + T_1(sm_p^2 F_{b,3})m\Gamma_1(p_1) + T_1(-2sm_p G_0(p))g_b\Gamma_2(p_1) \\
& + T_1(2sm_p^2 G_0(p))g_b\Gamma_1(p_1) + T_1(2s^2 G_1(p))g_b\Gamma_2(p_1) \\
& + T_1(-2s^2 m_p G_1(p))g_b\Gamma_1(p_1) + T_2 m F_{b,1}\Gamma_4(p_1) \\
& + T_2 m(-m_p F_{b,1})\Gamma_2(p_1) + T_2 m(-m_p F_{b,1})\Gamma_3(p_1) \\
& + T_2 m(m_p^2 F_{b,1})\Gamma_1(p_1) + T_2 m(-m_p F_{b,3})\Gamma_4(p_1) \\
& + T_2 m(m_p^2 F_{b,3})\Gamma_2(p_1) + T_2 m(m_p^2 F_{b,3})\Gamma_3(p_1) \\
& + T_2 m(-m_p^3 F_{b,3})\Gamma_1(p_1) + T_2 g_b(-2m_p G_0(p_1))\Gamma_4(p_1) \\
& + T_2 g_b(2m_p^2 G_0(p_1))\Gamma_2(p_1) + T_2 g_b(2m_p^2 G_0(p_1))\Gamma_3(p_1) \\
& + T_2 g_b(-2m_p^3 G_0(p_1))\Gamma_1(p_1) + T_2 g_b(2m_p^2 G_1(p_1))\Gamma_4(p_1) \\
& + T_2 g_b(-2m_p^3 G_1(p_1))\Gamma_2(p_1) + T_2 g_b(-2m_p^3 G_1(p_1))\Gamma_3(p_1) \\
& + T_2 g_b(2m_p^4 G_1(p_1))\Gamma_1(p_1) + T_2(2I_M m_p)g_b\Gamma_2(p_1) \\
& + T_2(-2I_M m_p^2)g_b\Gamma_1(p_1) + T_2(s F_{b,2})m\Gamma_2(p_1) \\
& + T_2(-sm_p F_{b,2})m\Gamma_1(p_1) + T_2(-sm_p F_{b,4})m\Gamma_2(p_1) \\
& + T_2(sm_p^2 F_{b,4})m\Gamma_1(p_1) + T_2(2s G_0(p))g_b\Gamma_2(p_1) \\
& + T_2(-2sm_p G_0(p))g_b\Gamma_1(p_1) + T_2(-2sm_p G_1(p))g_b\Gamma_2(p_1) \\
& + T_2(2sm_p^2 G_1(p))g_b\Gamma_1(p_1) + T_4(s F_{b,2})m\Gamma_2(p_1) \\
& + T_4(-sm_p F_{b,2})m\Gamma_1(p_1) + T_4(-sm_p F_{b,4})m\Gamma_2(p_1) \\
& + T_4(sm_p^2 F_{b,4})m\Gamma_1(p_1) + T_4(2s G_0(p))g_b\Gamma_2(p_1) \\
& + T_4(-2sm_p G_0(p))g_b\Gamma_1(p_1) + T_4(-2sm_p G_1(p))g_b\Gamma_2(p_1) \\
& + T_4(2sm_p^2 G_1(p))g_b\Gamma_1(p_1) + T_6 F_{b,1}m\Gamma_2(p_1) \\
& + T_6(-m_p F_{b,1})m\Gamma_1(p_1) + T_6(-m_p F_{b,3})m\Gamma_2(p_1) \\
& + T_6(m_p^2 F_{b,3})m\Gamma_1(p_1) + T_6(-2m_p G_0(p))g_b\Gamma_2(p_1) \\
& + T_6(2m_p^2 G_0(p))g_b\Gamma_1(p_1) + T_6(2s G_1(p))g_b\Gamma_2(p_1) \\
& + T_6(-2sm_p G_1(p))g_b\Gamma_1(p_1) + T_1 m(-s F_{b,2})m\Gamma_2(p_1) \\
& + T_1 m(sm_p F_{b,2})m\Gamma_1(p_1) + T_1 m(sm_p F_{b,4})m\Gamma_2(p_1) \\
& + T_1 m(-sm_p^2 F_{b,4})m\Gamma_1(p_1) + T_1 m(-2s G_0(p))g_b\Gamma_2(p_1) \\
& + T_1 m(2sm_p G_0(p))g_b\Gamma_1(p_1) + T_1 m(2sm_p G_1(p))g_b\Gamma_2(p_1) \\
& + T_1 m(-2sm_p^2 G_1(p))g_b\Gamma_1(p_1) + T_1 g_b(-2s G_0(p_1))m\Gamma_2(p_1) \\
& + T_1 g_b(2sm_p G_0(p_1))m\Gamma_1(p_1) + T_1 g_b(2sm_p G_1(p_1))m\Gamma_2(p_1) \\
& + T_1 g_b(-2sm_p^2 G_1(p_1))m\Gamma_1(p_1) + T_2 m(-F_{b,1})m\Gamma_2(p_1) \\
& + T_2 m(m_p F_{b,1})m\Gamma_1(p_1) + T_2 m(m_p F_{b,3})m\Gamma_2(p_1) \\
& + T_2 m(-m_p^2 F_{b,3})m\Gamma_1(p_1) + T_2 m(2m_p G_0(p))g_b\Gamma_2(p_1)
\end{aligned}$$

$$\begin{aligned}
& + T_2 m(-2m_p^2 G_0(p)) g_b \Gamma_1(p_1) + T_2 m(-2s G_1(p)) g_b \Gamma_2(p_1) \\
& + T_2 m(2sm_p G_1(p)) g_b \Gamma_1(p_1) + T_2 g_b(2m_p G_0(p_1)) m \Gamma_2(p_1) \\
& + T_2 g_b(-2m_p^2 G_0(p_1)) m \Gamma_1(p_1) + T_2 g_b(-2m_p^2 G_1(p_1)) m \Gamma_2(p_1) \\
& + T_2 g_b(2m_p^3 G_1(p_1)) m \Gamma_1(p_1), \\
S_{b,B}^{\phi\gamma} = & T_3(-s F_{b,2}) \Gamma_4(p_1) + T_3(sm_p F_{b,2}) \Gamma_2(p_1) + \\
& T_3(sm_p F_{b,2}) \Gamma_3(p_1) + T_3(-sm_p^2 F_{b,2}) \Gamma_1(p_1) + \\
& T_3(sm_p F_{b,4}) \Gamma_4(p_1) + T_3(-sm_p^2 F_{b,4}) \Gamma_2(p_1) + \\
& T_3(-sm_p^2 F_{b,4}) \Gamma_3(p_1) + T_3(sm_p^3 F_{b,4}) \Gamma_1(p_1) + \\
& T_5(-F_{b,1}) \Gamma_4(p_1) + T_5(m_p F_{b,1}) \Gamma_2(p_1) + T_5(m_p F_{b,1}) \Gamma_3(p_1) \\
& + T_5(-m_p^2 F_{b,1}) \Gamma_1(p_1) + T_5(m_p F_{b,3}) \Gamma_4(p_1) \\
& + T_5(-m_p^2 F_{b,3}) \Gamma_2(p_1) + T_5(-m_p^2 F_{b,3}) \Gamma_3(p_1) \\
& + T_5(m_p^3 F_{b,3}) \Gamma_1(p_1) + T_7(-F_{b,1}) \Gamma_4(p_1) \\
& + T_7(m_p F_{b,1}) \Gamma_2(p_1) + T_7(m_p F_{b,1}) \Gamma_3(p_1) \\
& + T_7(-m_p^2 F_{b,1}) \Gamma_1(p_1) + T_7(m_p F_{b,3}) \Gamma_4(p_1) \\
& + T_7(-m_p^2 F_{b,3}) \Gamma_2(p_1) + T_7(-m_p^2 F_{b,3}) \Gamma_3(p_1) \\
& + T_7(m_p^3 F_{b,3}) \Gamma_1(p_1) + T_8(-F_{b,2}) \Gamma_4(p_1) \\
& + T_8(m_p F_{b,2}) \Gamma_2(p_1) + T_8(m_p F_{b,2}) \Gamma_3(p_1) \\
& + T_8(-m_p^2 F_{b,2}) \Gamma_1(p_1) + T_8(m_p F_{b,4}) \Gamma_4(p_1) \\
& + T_8(-m_p^2 F_{b,4}) \Gamma_2(p_1) + T_8(-m_p^2 F_{b,4}) \Gamma_3(p_1) \\
& + T_8(m_p^3 F_{b,4}) \Gamma_1(p_1) + T_3 m F_{b,1} \Gamma_4(p_1) \\
& + T_3 m(-m_p F_{b,1}) \Gamma_2(p_1) + T_3 m(-m_p F_{b,1}) \Gamma_3(p_1) \\
& + T_3 m(m_p^2 F_{b,1}) \Gamma_1(p_1) + T_3 m(-m_p F_{b,3}) \Gamma_4(p_1) \\
& + T_3 m(m_p^2 F_{b,3}) \Gamma_2(p_1) + T_3 m(m_p^2 F_{b,3}) \Gamma_3(p_1) \\
& + T_3 m(-m_p^3 F_{b,3}) \Gamma_1(p_1) + T_3 g_b(-2m_p G_0(p_1)) \Gamma_4(p_1) \\
& + T_3 g_b(2m_p^2 G_0(p_1)) \Gamma_2(p_1) + T_3 g_b(2m_p^2 G_0(p_1)) \Gamma_3(p_1) \\
& + T_3 g_b(-2m_p^3 G_0(p_1)) \Gamma_1(p_1) + T_3 g_b(2m_p^2 G_1(p_1)) \Gamma_4(p_1) \\
& + T_3 g_b(-2m_p^3 G_1(p_1)) \Gamma_2(p_1) + T_3 g_b(-2m_p^3 G_1(p_1)) \Gamma_3(p_1) \\
& + T_3 g_b(2m_p^4 G_1(p_1)) \Gamma_1(p_1) + T_3(2I_M m_p) g_b \Gamma_2(p_1) \\
& + T_3(-2I_M m_p^2) g_b \Gamma_1(p_1) + T_3(s F_{b,2}) m \Gamma_2(p_1) \\
& + T_3(-sm_p F_{b,2}) m \Gamma_1(p_1) + T_3(-sm_p F_{b,4}) m \Gamma_2(p_1) \\
& + T_3(sm_p^2 F_{b,4}) m \Gamma_1(p_1) + T_3(2s G_0(p)) g_b \Gamma_2(p_1) \\
& + T_3(-2sm_p G_0(p)) g_b \Gamma_1(p_1) + T_3(-2sm_p G_1(p)) g_b \Gamma_2(p_1) \\
& + T_3(2sm_p^2 G_1(p)) g_b \Gamma_1(p_1) + T_5 m F_{b,2} \Gamma_4(p_1)
\end{aligned}$$

$$\begin{aligned}
& + T_5 m(-m_p F_{b,2}) \Gamma_2(p_1) + T_5 m(-m_p F_{b,2}) \Gamma_3(p_1) \\
& + T_5 m(m_p^2 F_{b,2}) \Gamma_1(p_1) + T_5 m(-m_p F_{b,4}) \Gamma_4(p_1) \\
& + T_5 m(m_p^2 F_{b,4}) \Gamma_2(p_1) + T_5 m(m_p^2 F_{b,4}) \Gamma_3(p_1) \\
& + T_5 m(-m_p^3 F_{b,4}) \Gamma_1(p_1) + T_5 (-2I_M) g_b \Gamma_2(p_1) \\
& + T_5 g_b (2G_0(p_1)) \Gamma_4(p_1) + T_5 g_b (-2m_p G_0(p_1)) \Gamma_2(p_1) \\
& + T_5 g_b (-2m_p G_0(p_1)) \Gamma_3(p_1) + T_5 g_b (2m_p^2 G_0(p_1)) \Gamma_1(p_1) \\
& + T_5 g_b (-2m_p G_1(p_1)) \Gamma_4(p_1) + T_5 g_b (2m_p^2 G_1(p_1)) \Gamma_2(p_1) \\
& + T_5 g_b (2m_p^2 G_1(p_1)) \Gamma_3(p_1) + T_5 g_b (-2m_p^3 G_1(p_1)) \Gamma_1(p_1) \\
& + T_5 (2I_M m_p) g_b \Gamma_1(p_1) + T_5 F_{b,1} m \Gamma_2(p_1) \\
& + T_5 (-m_p F_{b,1}) m \Gamma_1(p_1) + T_5 (-m_p F_{b,3}) m \Gamma_2(p_1) \\
& + T_5 (m_p^2 F_{b,3}) m \Gamma_1(p_1) + T_5 (-2m_p G_0(p)) g_b \Gamma_2(p_1) \\
& + T_5 (2m_p^2 G_0(p)) g_b \Gamma_1(p_1) + T_5 (2s G_1(p)) g_b \Gamma_2(p_1) \\
& + T_5 (-2sm_p G_1(p)) g_b \Gamma_1(p_1) + T_7 F_{b,1} m \Gamma_2(p_1) \\
& + T_7 (-m_p F_{b,1}) m \Gamma_1(p_1) + T_7 (-m_p F_{b,3}) m \Gamma_2(p_1) \\
& + T_7 (m_p^2 F_{b,3}) m \Gamma_1(p_1) + T_7 (-2m_p G_0(p)) g_b \Gamma_2(p_1) \\
& + T_7 (2m_p^2 G_0(p)) g_b \Gamma_1(p_1) + T_7 (2s G_1(p)) g_b \Gamma_2(p_1) \\
& + T_7 (-2sm_p G_1(p)) g_b \Gamma_1(p_1) + T_8 F_{b,2} m \Gamma_2(p_1) \\
& + T_8 (-m_p F_{b,2}) m \Gamma_1(p_1) + T_8 (-m_p F_{b,4}) m \Gamma_2(p_1) \\
& + T_8 (m_p^2 F_{b,4}) m \Gamma_1(p_1) + T_8 (2G_0(p)) g_b \Gamma_2(p_1) \\
& + T_8 (-2m_p G_0(p)) g_b \Gamma_1(p_1) + T_8 (-2m_p G_1(p)) g_b \Gamma_2(p_1) \\
& + T_8 (2m_p^2 G_1(p)) g_b \Gamma_1(p_1) + T_3 m(-F_{b,1}) m \Gamma_2(p_1) \\
& + T_3 m(m_p F_{b,1}) m \Gamma_1(p_1) + T_3 m(m_p F_{b,3}) m \Gamma_2(p_1) \\
& + T_3 m(-m_p^2 F_{b,3}) m \Gamma_1(p_1) + T_3 m(2m_p G_0(p)) g_b \Gamma_2(p_1) \\
& + T_3 m(-2m_p^2 G_0(p)) g_b \Gamma_1(p_1) + T_3 m(-2s G_1(p)) g_b \Gamma_2(p_1) \\
& + T_3 m(2sm_p G_1(p)) g_b \Gamma_1(p_1) + T_3 g_b (2m_p G_0(p_1)) m \Gamma_2(p_1) \\
& + T_3 g_b (-2m_p^2 G_0(p_1)) m \Gamma_1(p_1) + T_3 g_b (-2m_p^2 G_1(p_1)) m \Gamma_2(p_1) \\
& + T_3 g_b (2m_p^3 G_1(p_1)) m \Gamma_1(p_1) + T_5 m(-F_{b,2}) m \Gamma_2(p_1) \\
& + T_5 m(m_p F_{b,2}) m \Gamma_1(p_1) + T_5 m(m_p F_{b,4}) m \Gamma_2(p_1) \\
& + T_5 m(-m_p^2 F_{b,4}) m \Gamma_1(p_1) + T_5 m(-2G_0(p)) g_b \Gamma_2(p_1) \\
& + T_5 m(2m_p G_0(p)) g_b \Gamma_1(p_1) + T_5 m(2m_p G_1(p)) g_b \Gamma_2(p_1) \\
& + T_5 m(-2m_p^2 G_1(p)) g_b \Gamma_1(p_1) + T_5 g_b (-2G_0(p_1)) m \Gamma_2(p_1) \\
& + T_5 g_b (2m_p G_0(p_1)) m \Gamma_1(p_1) + T_5 g_b (2m_p G_1(p_1)) m \Gamma_2(p_1) \\
& + T_5 g_b (-2m_p^2 G_1(p_1)) m \Gamma_1(p_1),
\end{aligned}$$

$$\begin{aligned}
S_{b,B}^{\#p\gamma} = & T_1(-sF_{b,2})\Gamma_4(p_1) + T_1(sm_p F_{b,2})\Gamma_2(p_1) \\
& + T_1(sm_p F_{b,2})\Gamma_3(p_1) + T_1(-sm_p^2 F_{b,2})\Gamma_1(p_1) \\
& + T_1(sm_p F_{b,4})\Gamma_4(p_1) + T_1(-sm_p^2 F_{b,4})\Gamma_2(p_1) \\
& + T_1(-sm_p^2 F_{b,4})\Gamma_3(p_1) + T_1(sm_p^3 F_{b,4})\Gamma_1(p_1) \\
& + T_2(-F_{b,1})\Gamma_4(p_1) + T_2(m_p F_{b,1})\Gamma_2(p_1) \\
& + T_2(m_p F_{b,1})\Gamma_3(p_1) + T_2(-m_p^2 F_{b,1})\Gamma_1(p_1) \\
& + T_2(m_p F_{b,3})\Gamma_4(p_1) + T_2(-m_p^2 F_{b,3})\Gamma_2(p_1) \\
& + T_2(-m_p^2 F_{b,3})\Gamma_3(p_1) + T_2(m_p^3 F_{b,3})\Gamma_1(p_1) \\
& + T_4(-F_{b,1})\Gamma_4(p_1) + T_4(m_p F_{b,1})\Gamma_2(p_1) \\
& + T_4(m_p F_{b,1})\Gamma_3(p_1) + T_4(-m_p^2 F_{b,1})\Gamma_1(p_1) \\
& + T_4(m_p F_{b,3})\Gamma_4(p_1) + T_4(-m_p^2 F_{b,3})\Gamma_2(p_1) \\
& + T_4(-m_p^2 F_{b,3})\Gamma_3(p_1) + T_4(m_p^3 F_{b,3})\Gamma_1(p_1) \\
& + T_6(-F_{b,2})\Gamma_4(p_1) + T_6(m_p F_{b,2})\Gamma_2(p_1) \\
& + T_6(m_p F_{b,2})\Gamma_3(p_1) + T_6(-m_p^2 F_{b,2})\Gamma_1(p_1) \\
& + T_6(m_p F_{b,4})\Gamma_4(p_1) + T_6(-m_p^2 F_{b,4})\Gamma_2(p_1) \\
& + T_6(-m_p^2 F_{b,4})\Gamma_3(p_1) + T_6(m_p^3 F_{b,4})\Gamma_1(p_1) \\
& + T_1 m F_{b,1} \Gamma_4(p_1) + T_1 m (-m_p F_{b,1}) \Gamma_2(p_1) \\
& + T_1 m (-m_p F_{b,1}) \Gamma_3(p_1) + T_1 m (m_p^2 F_{b,1}) \Gamma_1(p_1) \\
& + T_1 m (-m_p F_{b,3}) \Gamma_4(p_1) + T_1 m (m_p^2 F_{b,3}) \Gamma_2(p_1) \\
& + T_1 m (m_p^2 F_{b,3}) \Gamma_3(p_1) + T_1 m (-m_p^3 F_{b,3}) \Gamma_1(p_1) \\
& + T_1 g_b (-2m_p G_0(p_1)) \Gamma_4(p_1) + T_1 g_b (2m_p^2 G_0(p_1)) \Gamma_2(p_1) \\
& + T_1 g_b (2m_p^2 G_0(p_1)) \Gamma_3(p_1) + T_1 g_b (-2m_p^3 G_0(p_1)) \Gamma_1(p_1) \\
& + T_1 g_b (2m_p^2 G_1(p_1)) \Gamma_4(p_1) + T_1 g_b (-2m_p^3 G_1(p_1)) \Gamma_2(p_1) \\
& + T_1 g_b (-2m_p^3 G_1(p_1)) \Gamma_3(p_1) + T_1 g_b (2m_p^4 G_1(p_1)) \Gamma_1(p_1) \\
& + T_1 (2I_M m_p) g_b \Gamma_2(p_1) + T_1 (-2I_M m_p^2) g_b \Gamma_1(p_1) \\
& + T_1 (sF_{b,2}) m \Gamma_2(p_1) + T_1 (-sm_p F_{b,2}) m \Gamma_1(p_1) \\
& + T_1 (-sm_p F_{b,4}) m \Gamma_2(p_1) + T_1 (sm_p^2 F_{b,4}) m \Gamma_1(p_1) \\
& + T_1 (2sG_0(p)) g_b \Gamma_2(p_1) + T_1 (-2sm_p G_0(p)) g_b \Gamma_1(p_1) \\
& + T_1 (-2sm_p G_1(p)) g_b \Gamma_2(p_1) + T_1 (2sm_p^2 G_1(p)) g_b \Gamma_1(p_1) \\
& + T_2 m F_{b,2} \Gamma_4(p_1) + T_2 m (-m_p F_{b,2}) \Gamma_2(p_1) \\
& + T_2 m (-m_p F_{b,2}) \Gamma_3(p_1) + T_2 m (m_p^2 F_{b,2}) \Gamma_1(p_1) \\
& + T_2 m (-m_p F_{b,4}) \Gamma_4(p_1) + T_2 m (m_p^2 F_{b,4}) \Gamma_2(p_1) \\
& + T_2 m (m_p^2 F_{b,4}) \Gamma_3(p_1) + T_2 m (-m_p^3 F_{b,4}) \Gamma_1(p_1)
\end{aligned}$$

$$\begin{aligned}
& + T_2(-2I_M)g_b\Gamma_2(p_1) + T_2g_b(2G_0(p_1))\Gamma_4(p_1) \\
& + T_2g_b(-2m_pG_0(p_1))\Gamma_2(p_1) + T_2g_b(-2m_pG_0(p_1))\Gamma_3(p_1) \\
& + T_2g_b(2m_p^2G_0(p_1))\Gamma_1(p_1) + T_2g_b(-2m_pG_1(p_1))\Gamma_4(p_1) \\
& + T_2g_b(2m_p^2G_1(p_1))\Gamma_2(p_1) + T_2g_b(2m_p^2G_1(p_1))\Gamma_3(p_1) \\
& + T_2g_b(-2m_p^3G_1(p_1))\Gamma_1(p_1) + T_2(2I_Mm_p)g_b\Gamma_1(p_1) \\
& + T_2F_{b,1}m\Gamma_2(p_1) + T_2(-m_pF_{b,1})m\Gamma_1(p_1) \\
& + T_2(-m_pF_{b,3})m\Gamma_2(p_1) + T_2(m_p^2F_{b,3})m\Gamma_1(p_1) \\
& + T_2(-2m_pG_0(p))g_b\Gamma_2(p_1) + T_2(2m_p^2G_0(p))g_b\Gamma_1(p_1) \\
& + T_2(2sG_1(p))g_b\Gamma_2(p_1) + T_2(-2sm_pG_1(p))g_b\Gamma_1(p_1) \\
& + T_4F_{b,1}m\Gamma_2(p_1) + T_4(-m_pF_{b,1})m\Gamma_1(p_1) \\
& + T_4(-m_pF_{b,3})m\Gamma_2(p_1) + T_4(m_p^2F_{b,3})m\Gamma_1(p_1) \\
& + T_4(-2m_pG_0(p))g_b\Gamma_2(p_1) + T_4(2m_p^2G_0(p))g_b\Gamma_1(p_1) \\
& + T_4(2sG_1(p))g_b\Gamma_2(p_1) + T_4(-2sm_pG_1(p))g_b\Gamma_1(p_1) \\
& + T_6F_{b,2}m\Gamma_2(p_1) + T_6(-m_pF_{b,2})m\Gamma_1(p_1) \\
& + T_6(-m_pF_{b,4})m\Gamma_2(p_1) + T_6(m_p^2F_{b,4})m\Gamma_1(p_1) \\
& + T_6(2G_0(p))g_b\Gamma_2(p_1) + T_6(-2m_pG_0(p))g_b\Gamma_1(p_1) \\
& + T_6(-2m_pG_1(p))g_b\Gamma_2(p_1) + T_6(2m_p^2G_1(p))g_b\Gamma_1(p_1) \\
& + T_1m(-F_{b,1})m\Gamma_2(p_1) + T_1m(m_pF_{b,1})m\Gamma_1(p_1) \\
& + T_1m(m_pF_{b,3})m\Gamma_2(p_1) + T_1m(-m_p^2F_{b,3})m\Gamma_1(p_1) \\
& + T_1m(2m_pG_0(p))g_b\Gamma_2(p_1) + T_1m(-2m_p^2G_0(p))g_b\Gamma_1(p_1) \\
& + T_1m(-2sG_1(p))g_b\Gamma_2(p_1) + T_1m(2sm_pG_1(p))g_b\Gamma_1(p_1) \\
& + T_1g_b(2m_pG_0(p_1))m\Gamma_2(p_1) + T_1g_b(-2m_p^2G_0(p_1))m\Gamma_1(p_1) \\
& + T_1g_b(-2m_p^2G_1(p_1))m\Gamma_2(p_1) + T_1g_b(2m_p^3G_1(p_1))m\Gamma_1(p_1) \\
& + T_2m(-F_{b,2})m\Gamma_2(p_1) + T_2m(m_pF_{b,2})m\Gamma_1(p_1) \\
& + T_2m(m_pF_{b,4})m\Gamma_2(p_1) + T_2m(-m_p^2F_{b,4})m\Gamma_1(p_1) \\
& + T_2m(-2G_0(p))g_b\Gamma_2(p_1) + T_2m(2m_pG_0(p))g_b\Gamma_1(p_1) \\
& + T_2m(2m_pG_1(p))g_b\Gamma_2(p_1) + T_2m(-2m_p^2G_1(p))g_b\Gamma_1(p_1) \\
& + T_2g_b(-2G_0(p_1))m\Gamma_2(p_1) + T_2g_b(2m_pG_0(p_1))m\Gamma_1(p_1) \\
& + T_2g_b(2m_pG_1(p_1))m\Gamma_2(p_1) + T_2g_b(-2m_p^2G_1(p_1))m\Gamma_1(p_1), \\
S_{b,B}^{\not{p}} = & T_1(-sF_{b,5})\Gamma_4(p_1) + T_1(sm_pF_{b,5})\Gamma_2(p_1) \\
& + T_1(sm_pF_{b,5})\Gamma_3(p_1) + T_1(-sm_p^2F_{b,5})\Gamma_1(p_1) \\
& + T_1(sm_pF_{b,8})\Gamma_4(p_1) + T_1(-sm_p^2F_{b,8})\Gamma_2(p_1) \\
& + T_1(-sm_p^2F_{b,8})\Gamma_3(p_1) + T_1(sm_p^3F_{b,8})\Gamma_1(p_1)
\end{aligned}$$

$$\begin{aligned}
& + T_2(-sF_{b,7})\Gamma_4(p_1) + T_2(sm_p F_{b,7})\Gamma_2(p_1) \\
& + T_2(sm_p F_{b,7})\Gamma_3(p_1) + T_2(-sm_p^2 F_{b,7})\Gamma_1(p_1) \\
& + T_2(sm_p F_{b,11})\Gamma_4(p_1) + T_2(-sm_p^2 F_{b,11})\Gamma_2(p_1) \\
& + T_2(-sm_p^2 F_{b,11})\Gamma_3(p_1) + T_2(sm_p^3 F_{b,11})\Gamma_1(p_1) \\
& + T_4(-sF_{b,7})\Gamma_4(p_1) + T_4(sm_p F_{b,7})\Gamma_2(p_1) \\
& + T_4(sm_p F_{b,7})\Gamma_3(p_1) + T_4(-sm_p^2 F_{b,7})\Gamma_1(p_1) \\
& + T_4(sm_p F_{b,11})\Gamma_4(p_1) + T_4(-sm_p^2 F_{b,11})\Gamma_2(p_1) \\
& + T_4(-sm_p^2 F_{b,11})\Gamma_3(p_1) + T_4(sm_p^3 F_{b,11})\Gamma_1(p_1) \\
& + T_6(-F_{b,5})\Gamma_4(p_1) + T_6(m_p F_{b,5})\Gamma_2(p_1) \\
& + T_6(m_p F_{b,5})\Gamma_3(p_1) + T_6(-m_p^2 F_{b,5})\Gamma_1(p_1) \\
& + T_6(m_p F_{b,8})\Gamma_4(p_1) + T_6(-m_p^2 F_{b,8})\Gamma_2(p_1) \\
& + T_6(-m_p^2 F_{b,8})\Gamma_3(p_1) + T_6(m_p^3 F_{b,8})\Gamma_1(p_1) \\
& + T_1 m(sF_{b,7})\Gamma_4(p_1) + T_1 m(-sm_p F_{b,7})\Gamma_2(p_1) \\
& + T_1 m(-sm_p F_{b,7})\Gamma_3(p_1) + T_1 m(sm_p^2 F_{b,7})\Gamma_1(p_1) \\
& + T_1 m(-sm_p F_{b,11})\Gamma_4(p_1) + T_1 m(sm_p^2 F_{b,11})\Gamma_2(p_1) \\
& + T_1 m(sm_p^2 F_{b,11})\Gamma_3(p_1) + T_1 m(-sm_p^3 F_{b,11})\Gamma_1(p_1) \\
& + T_1(sF_{b,5})m\Gamma_2(p_1) + T_1(-sm_p F_{b,5})m\Gamma_1(p_1) \\
& + T_1(-sm_p F_{b,8})m\Gamma_2(p_1) + T_1(sm_p^2 F_{b,8})m\Gamma_1(p_1) \\
& + T_1(-2sG_0(p))g_b\Gamma_2(p_1) + T_1(2sm_p G_0(p))g_b\Gamma_1(p_1) \\
& + T_2 m F_{b,5}\Gamma_4(p_1) + T_2 m(-m_p F_{b,5})\Gamma_2(p_1) \\
& + T_2 m(-m_p F_{b,5})\Gamma_3(p_1) + T_2 m(m_p^2 F_{b,5})\Gamma_1(p_1) \\
& + T_2 m(-m_p F_{b,8})\Gamma_4(p_1) + T_2 m(m_p^2 F_{b,8})\Gamma_2(p_1) \\
& + T_2 m(m_p^2 F_{b,8})\Gamma_3(p_1) + T_2 m(-m_p^3 F_{b,8})\Gamma_1(p_1) \\
& + T_2(2I_M)g_b\Gamma_2(p_1) + T_2 g_b(-2G_0(p_1))\Gamma_4(p_1) \\
& + T_2 g_b(2m_p G_0(p_1))\Gamma_2(p_1) + T_2 g_b(2m_p G_0(p_1))\Gamma_3(p_1) \\
& + T_2 g_b(-2m_p^2 G_0(p_1))\Gamma_1(p_1) + T_2 g_b(2m_p G_1(p_1))\Gamma_4(p_1) \\
& + T_2 g_b(-2m_p^2 G_1(p_1))\Gamma_2(p_1) + T_2 g_b(-2m_p^2 G_1(p_1))\Gamma_3(p_1) \\
& + T_2 g_b(2m_p^3 G_1(p_1))\Gamma_1(p_1) + T_2(-2I_M m_p)g_b\Gamma_1(p_1) \\
& + T_2(sF_{b,7})m\Gamma_2(p_1) + T_2(-sm_p F_{b,7})m\Gamma_1(p_1) \\
& + T_2(-sm_p F_{b,11})m\Gamma_2(p_1) + T_2(sm_p^2 F_{b,11})m\Gamma_1(p_1) \\
& + T_2(-2sG_1(p))g_b\Gamma_2(p_1) + T_2(2sm_p G_1(p))g_b\Gamma_1(p_1) \\
& + T_4(sF_{b,7})m\Gamma_2(p_1) + T_4(-sm_p F_{b,7})m\Gamma_1(p_1) \\
& + T_4(-sm_p F_{b,11})m\Gamma_2(p_1) + T_4(sm_p^2 F_{b,11})m\Gamma_1(p_1)
\end{aligned}$$

$$\begin{aligned}
& + T_4(-2sG_1(p))g_b\Gamma_2(p_1) + T_4(2sm_pG_1(p))g_b\Gamma_1(p_1) \\
& + T_6F_{b,5}m\Gamma_2(p_1) + T_6(-m_pF_{b,5})m\Gamma_1(p_1) \\
& + T_6(-m_pF_{b,8})m\Gamma_2(p_1) + T_6(m_p^2F_{b,8})m\Gamma_1(p_1) \\
& + T_6(-2G_0(p))g_b\Gamma_2(p_1) + T_6(2m_pG_0(p))g_b\Gamma_1(p_1) \\
& + T_1m(-sF_{b,7})m\Gamma_2(p_1) + T_1m(sm_pF_{b,7})m\Gamma_1(p_1) \\
& + T_1m(sm_pF_{b,11})m\Gamma_2(p_1) + T_1m(-sm_p^2F_{b,11})m\Gamma_1(p_1) \\
& + T_1m(2sG_1(p))g_b\Gamma_2(p_1) + T_1m(-2sm_pG_1(p))g_b\Gamma_1(p_1) \\
& + T_2m(-F_{b,5})m\Gamma_2(p_1) + T_2m(m_pF_{b,5})m\Gamma_1(p_1) \\
& + T_2m(m_pF_{b,8})m\Gamma_2(p_1) + T_2m(-m_p^2F_{b,8})m\Gamma_1(p_1) \\
& + T_2m(2G_0(p))g_b\Gamma_2(p_1) + T_2m(-2m_pG_0(p))g_b\Gamma_1(p_1) \\
& + T_2g_b(2G_0(p_1))m\Gamma_2(p_1) + T_2g_b(-2m_pG_0(p_1))m\Gamma_1(p_1) \\
& + T_2g_b(-2m_pG_1(p_1))m\Gamma_2(p_1) + T_2g_b(2m_p^2G_1(p_1))m\Gamma_1(p_1), \\
S_{b,B}^{\not{p}p} = & T_3(-sF_{b,7})\Gamma_4(p_1) + T_3(sm_pF_{b,7})\Gamma_2(p_1) \\
& + T_3(sm_pF_{b,7})\Gamma_3(p_1) + T_3(-sm_p^2F_{b,7})\Gamma_1(p_1) \\
& + T_3(sm_pF_{b,11})\Gamma_4(p_1) + T_3(-sm_p^2F_{b,11})\Gamma_2(p_1) \\
& + T_3(-sm_p^2F_{b,11})\Gamma_3(p_1) + T_3(sm_p^3F_{b,11})\Gamma_1(p_1) \\
& + T_5(-F_{b,5})\Gamma_4(p_1) + T_5(m_pF_{b,5})\Gamma_2(p_1) \\
& + T_5(m_pF_{b,5})\Gamma_3(p_1) + T_5(-m_p^2F_{b,5})\Gamma_1(p_1) \\
& + T_5(m_pF_{b,8})\Gamma_4(p_1) + T_5(-m_p^2F_{b,8})\Gamma_2(p_1) \\
& + T_5(-m_p^2F_{b,8})\Gamma_3(p_1) + T_5(m_p^3F_{b,8})\Gamma_1(p_1) \\
& + T_7(-F_{b,5})\Gamma_4(p_1) + T_7(m_pF_{b,5})\Gamma_2(p_1) \\
& + T_7(m_pF_{b,5})\Gamma_3(p_1) + T_7(-m_p^2F_{b,5})\Gamma_1(p_1) \\
& + T_7(m_pF_{b,8})\Gamma_4(p_1) + T_7(-m_p^2F_{b,8})\Gamma_2(p_1) \\
& + T_7(-m_p^2F_{b,8})\Gamma_3(p_1) + T_7(m_p^3F_{b,8})\Gamma_1(p_1) \\
& + T_8(-F_{b,7})\Gamma_4(p_1) + T_8(m_pF_{b,7})\Gamma_2(p_1) \\
& + T_8(m_pF_{b,7})\Gamma_3(p_1) + T_8(-m_p^2F_{b,7})\Gamma_1(p_1) \\
& + T_8(m_pF_{b,11})\Gamma_4(p_1) + T_8(-m_p^2F_{b,11})\Gamma_2(p_1) \\
& + T_8(-m_p^2F_{b,11})\Gamma_3(p_1) + T_8(m_p^3F_{b,11})\Gamma_1(p_1) \\
& + T_3mF_{b,5}\Gamma_4(p_1) + T_3m(-m_pF_{b,5})\Gamma_2(p_1) \\
& + T_3m(-m_pF_{b,5})\Gamma_3(p_1) + T_3m(m_p^2F_{b,5})\Gamma_1(p_1) \\
& + T_3m(-m_pF_{b,8})\Gamma_4(p_1) + T_3m(m_p^2F_{b,8})\Gamma_2(p_1) \\
& + T_3m(m_p^2F_{b,8})\Gamma_3(p_1) + T_3m(-m_p^3F_{b,8})\Gamma_1(p_1) \\
& + T_3(2I_M)g_b\Gamma_2(p_1) + T_3g_b(-2G_0(p_1))\Gamma_4(p_1)
\end{aligned}$$

$$\begin{aligned}
& + T_3 g_b(2m_p G_0(p_1)) \Gamma_2(p_1) + T_3 g_b(2m_p G_0(p_1)) \Gamma_3(p_1) \\
& + T_3 g_b(-2m_p^2 G_0(p_1)) \Gamma_1(p_1) + T_3 g_b(2m_p G_1(p_1)) \Gamma_4(p_1) \\
& + T_3 g_b(-2m_p^2 G_1(p_1)) \Gamma_2(p_1) + T_3 g_b(-2m_p^2 G_1(p_1)) \Gamma_3(p_1) \\
& + T_3 g_b(2m_p^3 G_1(p_1)) \Gamma_1(p_1) + T_3(-2I_M m_p) g_b \Gamma_1(p_1) \\
& + T_3(s F_{b,7}) m \Gamma_2(p_1) + T_3(-s m_p F_{b,7}) m \Gamma_1(p_1) \\
& + T_3(-s m_p F_{b,11}) m \Gamma_2(p_1) + T_3(s m_p^2 F_{b,11}) m \Gamma_1(p_1) \\
& + T_3(-2s G_1(p)) g_b \Gamma_2(p_1) + T_3(2s m_p G_1(p)) g_b \Gamma_1(p_1) \\
& + T_5 m F_{b,7} \Gamma_4(p_1) + T_5 m(-m_p F_{b,7}) \Gamma_2(p_1) \\
& + T_5 m(-m_p F_{b,7}) \Gamma_3(p_1) + T_5 m(m_p^2 F_{b,7}) \Gamma_1(p_1) \\
& + T_5 m(-m_p F_{b,11}) \Gamma_4(p_1) + T_5 m(m_p^2 F_{b,11}) \Gamma_2(p_1) \\
& + T_5 m(m_p^2 F_{b,11}) \Gamma_3(p_1) + T_5 m(-m_p^3 F_{b,11}) \Gamma_1(p_1) \\
& + T_5 F_{b,5} m \Gamma_2(p_1) + T_5(-m_p F_{b,5}) m \Gamma_1(p_1) \\
& + T_5(-m_p F_{b,8}) m \Gamma_2(p_1) + T_5(m_p^2 F_{b,8}) m \Gamma_1(p_1) \\
& + T_5(-2G_0(p)) g_b \Gamma_2(p_1) + T_5(2m_p G_0(p)) g_b \Gamma_1(p_1) \\
& + T_7 F_{b,5} m \Gamma_2(p_1) + T_7(-m_p F_{b,5}) m \Gamma_1(p_1) \\
& + T_7(-m_p F_{b,8}) m \Gamma_2(p_1) + T_7(m_p^2 F_{b,8}) m \Gamma_1(p_1) \\
& + T_7(-2G_0(p)) g_b \Gamma_2(p_1) + T_7(2m_p G_0(p)) g_b \Gamma_1(p_1) \\
& + T_8 F_{b,7} m \Gamma_2(p_1) + T_8(-m_p F_{b,7}) m \Gamma_1(p_1) \\
& + T_8(-m_p F_{b,11}) m \Gamma_2(p_1) + T_8(m_p^2 F_{b,11}) m \Gamma_1(p_1) \\
& + T_8(-2G_1(p)) g_b \Gamma_2(p_1) + T_8(2m_p G_1(p)) g_b \Gamma_1(p_1) \\
& + T_3 m(-F_{b,5}) m \Gamma_2(p_1) + T_3 m(m_p F_{b,5}) m \Gamma_1(p_1) \\
& + T_3 m(m_p F_{b,8}) m \Gamma_2(p_1) + T_3 m(-m_p^2 F_{b,8}) m \Gamma_1(p_1) \\
& + T_3 m(2G_0(p)) g_b \Gamma_2(p_1) + T_3 m(-2m_p G_0(p)) g_b \Gamma_1(p_1) \\
& + T_3 g_b(2G_0(p_1)) m \Gamma_2(p_1) + T_3 g_b(-2m_p G_0(p_1)) m \Gamma_1(p_1) \\
& + T_3 g_b(-2m_p G_1(p_1)) m \Gamma_2(p_1) + T_3 g_b(2m_p^2 G_1(p_1)) m \Gamma_1(p_1) \\
& + T_5 m(-F_{b,7}) m \Gamma_2(p_1) + T_5 m(m_p F_{b,7}) m \Gamma_1(p_1) \\
& + T_5 m(m_p F_{b,11}) m \Gamma_2(p_1) + T_5 m(-m_p^2 F_{b,11}) m \Gamma_1(p_1) \\
& + T_5 m(2G_1(p)) g_b \Gamma_2(p_1) + T_5 m(-2m_p G_1(p)) g_b \Gamma_1(p_1), \\
S_{b,B}^{ppp} = & T_1(-s F_{b,7}) \Gamma_4(p_1) + T_1(s m_p F_{b,7}) \Gamma_2(p_1) \\
& + T_1(s m_p F_{b,7}) \Gamma_3(p_1) + T_1(-s m_p^2 F_{b,7}) \Gamma_1(p_1) \\
& + T_1(s m_p F_{b,11}) \Gamma_4(p_1) + T_1(-s m_p^2 F_{b,11}) \Gamma_2(p_1) \\
& + T_1(-s m_p^2 F_{b,11}) \Gamma_3(p_1) + T_1(s m_p^3 F_{b,11}) \Gamma_1(p_1) \\
& + T_2(-F_{b,5}) \Gamma_4(p_1) + T_2(m_p F_{b,5}) \Gamma_2(p_1) \\
& + T_2(m_p F_{b,5}) \Gamma_3(p_1) + T_2(-m_p^2 F_{b,5}) \Gamma_1(p_1)
\end{aligned}$$

$$\begin{aligned}
& + T_2(m_p F_{b,8})\Gamma_4(p_1) + T_2(-m_p^2 F_{b,8})\Gamma_2(p_1) \\
& + T_2(-m_p^2 F_{b,8})\Gamma_3(p_1) + T_2(m_p^3 F_{b,8})\Gamma_1(p_1) \\
& + T_4(-F_{b,5})\Gamma_4(p_1) + T_4(m_p F_{b,5})\Gamma_2(p_1) \\
& + T_4(m_p F_{b,5})\Gamma_3(p_1) + T_4(-m_p^2 F_{b,5})\Gamma_1(p_1) \\
& + T_4(m_p F_{b,8})\Gamma_4(p_1) + T_4(-m_p^2 F_{b,8})\Gamma_2(p_1) \\
& + T_4(-m_p^2 F_{b,8})\Gamma_3(p_1) + T_4(m_p^3 F_{b,8})\Gamma_1(p_1) \\
& + T_6(-F_{b,7})\Gamma_4(p_1) + T_6(m_p F_{b,7})\Gamma_2(p_1) \\
& + T_6(m_p F_{b,7})\Gamma_3(p_1) + T_6(-m_p^2 F_{b,7})\Gamma_1(p_1) \\
& + T_6(m_p F_{b,11})\Gamma_4(p_1) + T_6(-m_p^2 F_{b,11})\Gamma_2(p_1) \\
& + T_6(-m_p^2 F_{b,11})\Gamma_3(p_1) + T_6(m_p^3 F_{b,11})\Gamma_1(p_1) \\
& + T_1 m F_{b,5} \Gamma_4(p_1) + T_1 m (-m_p F_{b,5}) \Gamma_2(p_1) \\
& + T_1 m (-m_p F_{b,5}) \Gamma_3(p_1) + T_1 m (m_p^2 F_{b,5}) \Gamma_1(p_1) \\
& + T_1 m (-m_p F_{b,8}) \Gamma_4(p_1) + T_1 m (m_p^2 F_{b,8}) \Gamma_2(p_1) \\
& + T_1 m (m_p^2 F_{b,8}) \Gamma_3(p_1) + T_1 m (-m_p^3 F_{b,8}) \Gamma_1(p_1) \\
& + T_1 (2I_M) g_b \Gamma_2(p_1) + T_1 g_b (-2G_0(p_1)) \Gamma_4(p_1) \\
& + T_1 g_b (2m_p G_0(p_1)) \Gamma_2(p_1) + T_1 g_b (2m_p G_0(p_1)) \Gamma_3(p_1) \\
& + T_1 g_b (-2m_p^2 G_0(p_1)) \Gamma_1(p_1) + T_1 g_b (2m_p G_1(p_1)) \Gamma_4(p_1) \\
& + T_1 g_b (-2m_p^2 G_1(p_1)) \Gamma_2(p_1) + T_1 g_b (-2m_p^2 G_1(p_1)) \Gamma_3(p_1) \\
& + T_1 g_b (2m_p^3 G_1(p_1)) \Gamma_1(p_1) + T_1 (-2I_M m_p) g_b \Gamma_1(p_1) \\
& + T_1 (s F_{b,7}) m \Gamma_2(p_1) + T_1 (-s m_p F_{b,7}) m \Gamma_1(p_1) \\
& + T_1 (-s m_p F_{b,11}) m \Gamma_2(p_1) + T_1 (s m_p^2 F_{b,11}) m \Gamma_1(p_1) \\
& + T_1 (-2s G_1(p)) g_b \Gamma_2(p_1) + T_1 (2s m_p G_1(p)) g_b \Gamma_1(p_1) \\
& + T_2 m F_{b,7} \Gamma_4(p_1) + T_2 m (-m_p F_{b,7}) \Gamma_2(p_1) \\
& + T_2 m (-m_p F_{b,7}) \Gamma_3(p_1) + T_2 m (m_p^2 F_{b,7}) \Gamma_1(p_1) \\
& + T_2 m (-m_p F_{b,11}) \Gamma_4(p_1) + T_2 m (m_p^2 F_{b,11}) \Gamma_2(p_1) \\
& + T_2 m (m_p^2 F_{b,11}) \Gamma_3(p_1) + T_2 m (-m_p^3 F_{b,11}) \Gamma_1(p_1) \\
& + T_2 F_{b,5} m \Gamma_2(p_1) + T_2 (-m_p F_{b,5}) m \Gamma_1(p_1) \\
& + T_2 (-m_p F_{b,8}) m \Gamma_2(p_1) + T_2 (m_p^2 F_{b,8}) m \Gamma_1(p_1) \\
& + T_2 (-2G_0(p)) g_b \Gamma_2(p_1) + T_2 (2m_p G_0(p)) g_b \Gamma_1(p_1) \\
& + T_4 F_{b,5} m \Gamma_2(p_1) + T_4 (-m_p F_{b,5}) m \Gamma_1(p_1) \\
& + T_4 (-m_p F_{b,8}) m \Gamma_2(p_1) + T_4 (m_p^2 F_{b,8}) m \Gamma_1(p_1) \\
& + T_4 (-2G_0(p)) g_b \Gamma_2(p_1) + T_4 (2m_p G_0(p)) g_b \Gamma_1(p_1) \\
& + T_6 F_{b,7} m \Gamma_2(p_1) + T_6 (-m_p F_{b,7}) m \Gamma_1(p_1) \\
& + T_6 (-m_p F_{b,11}) m \Gamma_2(p_1) + T_6 (m_p^2 F_{b,11}) m \Gamma_1(p_1)
\end{aligned}$$

$$\begin{aligned}
& + T_6(-2G_1(p))g_b\Gamma_2(p_1) + T_6(2m_p G_1(p))g_b\Gamma_1(p_1) \\
& + T_1m(-F_{b,5})m\Gamma_2(p_1) + T_1m(m_p F_{b,5})m\Gamma_1(p_1) \\
& + T_1m(m_p F_{b,8})m\Gamma_2(p_1) + T_1m(-m_p^2 F_{b,8})m\Gamma_1(p_1) \\
& + T_1m(2G_0(p))g_b\Gamma_2(p_1) + T_1m(-2m_p G_0(p))g_b\Gamma_1(p_1) \\
& + T_1g_b(2G_0(p_1))m\Gamma_2(p_1) + T_1g_b(-2m_p G_0(p_1))m\Gamma_1(p_1) \\
& + T_1g_b(-2m_p G_1(p_1))m\Gamma_2(p_1) + T_1g_b(2m_p^2 G_1(p_1))m\Gamma_1(p_1) \\
& + T_2m(-F_{b,7})m\Gamma_2(p_1) + T_2m(m_p F_{b,7})m\Gamma_1(p_1) \\
& + T_2m(m_p F_{b,11})m\Gamma_2(p_1) + T_2m(-m_p^2 F_{b,11})m\Gamma_1(p_1) \\
& + T_2m(2G_1(p))g_b\Gamma_2(p_1) + T_2m(-2m_p G_1(p))g_b\Gamma_1(p_1), \\
S_{b,B}^{qp_1} = & T_1(-sF_{b,6})\Gamma_4(p_1) + T_1(sm_p F_{b,6})\Gamma_2(p_1) \\
& + T_1(sm_p F_{b,6})\Gamma_3(p_1) + T_1(-sm_p^2 F_{b,6})\Gamma_1(p_1) \\
& + T_1(sm_p F_{b,10})\Gamma_4(p_1) + T_1(-sm_p^2 F_{b,10})\Gamma_2(p_1) \\
& + T_1(-sm_p^2 F_{b,10})\Gamma_3(p_1) + T_1(sm_p^3 F_{b,10})\Gamma_1(p_1) \\
& + T_2(-sF_{b,9})\Gamma_4(p_1) + T_2(sm_p F_{b,9})\Gamma_2(p_1) \\
& + T_2(sm_p F_{b,9})\Gamma_3(p_1) + T_2(-sm_p^2 F_{b,9})\Gamma_1(p_1) \\
& + T_2(sm_p F_{b,12})\Gamma_4(p_1) + T_2(-sm_p^2 F_{b,12})\Gamma_2(p_1) \\
& + T_2(-sm_p^2 F_{b,12})\Gamma_3(p_1) + T_2(sm_p^3 F_{b,12})\Gamma_1(p_1) \\
& + T_4(-sF_{b,9})\Gamma_4(p_1) + T_4(sm_p F_{b,9})\Gamma_2(p_1) \\
& + T_4(sm_p F_{b,9})\Gamma_3(p_1) + T_4(-sm_p^2 F_{b,9})\Gamma_1(p_1) \\
& + T_4(sm_p F_{b,12})\Gamma_4(p_1) + T_4(-sm_p^2 F_{b,12})\Gamma_2(p_1) \\
& + T_4(-sm_p^2 F_{b,12})\Gamma_3(p_1) + T_4(sm_p^3 F_{b,12})\Gamma_1(p_1) \\
& + T_6(-F_{b,6})\Gamma_4(p_1) + T_6(m_p F_{b,6})\Gamma_2(p_1) \\
& + T_6(m_p F_{b,6})\Gamma_3(p_1) + T_6(-m_p^2 F_{b,6})\Gamma_1(p_1) \\
& + T_6(m_p F_{b,10})\Gamma_4(p_1) + T_6(-m_p^2 F_{b,10})\Gamma_2(p_1) \\
& + T_6(-m_p^2 F_{b,10})\Gamma_3(p_1) + T_6(m_p^3 F_{b,10})\Gamma_1(p_1) \\
& + T_1m(sF_{b,9})\Gamma_4(p_1) + T_1m(-sm_p F_{b,9})\Gamma_2(p_1) \\
& + T_1m(-sm_p F_{b,9})\Gamma_3(p_1) + T_1m(sm_p^2 F_{b,9})\Gamma_1(p_1) \\
& + T_1m(-sm_p F_{b,12})\Gamma_4(p_1) + T_1m(sm_p^2 F_{b,12})\Gamma_2(p_1) \\
& + T_1m(sm_p^2 F_{b,12})\Gamma_3(p_1) + T_1m(-sm_p^3 F_{b,12})\Gamma_1(p_1) \\
& + T_1(sF_{b,6})m\Gamma_2(p_1) + T_1(-sm_p F_{b,6})m\Gamma_1(p_1) \\
& + T_1(-sm_p F_{b,10})m\Gamma_2(p_1) + T_1(sm_p^2 F_{b,10})m\Gamma_1(p_1) \\
& + T_1(-2sG_0(p))g_b\Gamma_2(p_1) + T_1(2sm_p G_0(p))g_b\Gamma_1(p_1) \\
& + T_2mF_{b,6}\Gamma_4(p_1) + T_2m(-m_p F_{b,6})\Gamma_2(p_1)
\end{aligned}$$

$$\begin{aligned}
& + T_2 m(-m_p F_{b,6}) \Gamma_3(p_1) + T_2 m(m_p^2 F_{b,6}) \Gamma_1(p_1) \\
& + T_2 m(-m_p F_{b,10}) \Gamma_4(p_1) + T_2 m(m_p^2 F_{b,10}) \Gamma_2(p_1) \\
& + T_2 m(m_p^2 F_{b,10}) \Gamma_3(p_1) + T_2 m(-m_p^3 F_{b,10}) \Gamma_1(p_1) \\
& + T_2 (2I_M) g_b \Gamma_2(p_1) + T_2 g_b(-2G_0(p_1)) \Gamma_4(p_1) \\
& + T_2 g_b(2m_p G_0(p_1)) \Gamma_2(p_1) + T_2 g_b(2m_p G_0(p_1)) \Gamma_3(p_1) \\
& + T_2 g_b(-2m_p^2 G_0(p_1)) \Gamma_1(p_1) + T_2 g_b(2m_p G_1(p_1)) \Gamma_4(p_1) \\
& + T_2 g_b(-2m_p^2 G_1(p_1)) \Gamma_2(p_1) + T_2 g_b(-2m_p^2 G_1(p_1)) \Gamma_3(p_1) \\
& + T_2 g_b(2m_p^3 G_1(p_1)) \Gamma_1(p_1) + T_2(-2I_M m_p) g_b \Gamma_1(p_1) \\
& + T_2(s F_{b,9}) m \Gamma_2(p_1) + T_2(-s m_p F_{b,9}) m \Gamma_1(p_1) \\
& + T_2(-s m_p F_{b,12}) m \Gamma_2(p_1) + T_2(s m_p^2 F_{b,12}) m \Gamma_1(p_1) \\
& + T_2(-2s G_1(p)) g_b \Gamma_2(p_1) + T_2(2s m_p G_1(p)) g_b \Gamma_1(p_1) \\
& + T_4(s F_{b,9}) m \Gamma_2(p_1) + T_4(-s m_p F_{b,9}) m \Gamma_1(p_1) \\
& + T_4(-s m_p F_{b,12}) m \Gamma_2(p_1) + T_4(s m_p^2 F_{b,12}) m \Gamma_1(p_1) \\
& + T_4(-2s G_1(p)) g_b \Gamma_2(p_1) + T_4(2s m_p G_1(p)) g_b \Gamma_1(p_1) \\
& + T_6 F_{b,6} m \Gamma_2(p_1) + T_6(-m_p F_{b,6}) m \Gamma_1(p_1) \\
& + T_6(-m_p F_{b,10}) m \Gamma_2(p_1) + T_6(m_p^2 F_{b,10}) m \Gamma_1(p_1) \\
& + T_6(-2G_0(p)) g_b \Gamma_2(p_1) + T_6(2m_p G_0(p)) g_b \Gamma_1(p_1) \\
& + T_1 m(-s F_{b,9}) m \Gamma_2(p_1) + T_1 m(s m_p F_{b,9}) m \Gamma_1(p_1) \\
& + T_1 m(s m_p F_{b,12}) m \Gamma_2(p_1) + T_1 m(-s m_p^2 F_{b,12}) m \Gamma_1(p_1) \\
& + T_1 m(2s G_1(p)) g_b \Gamma_2(p_1) + T_1 m(-2s m_p G_1(p)) g_b \Gamma_1(p_1) \\
& + T_2 m(-F_{b,6}) m \Gamma_2(p_1) + T_2 m(m_p F_{b,6}) m \Gamma_1(p_1) \\
& + T_2 m(m_p F_{b,10}) m \Gamma_2(p_1) + T_2 m(-m_p^2 F_{b,10}) m \Gamma_1(p_1) \\
& + T_2 m(2G_0(p)) g_b \Gamma_2(p_1) + T_2 m(-2m_p G_0(p)) g_b \Gamma_1(p_1) \\
& + T_2 g_b(2G_0(p_1)) m \Gamma_2(p_1) + T_2 g_b(-2m_p G_0(p_1)) m \Gamma_1(p_1) \\
& + T_2 g_b(-2m_p G_1(p_1)) m \Gamma_2(p_1) + T_2 g_b(2m_p^2 G_1(p_1)) m \Gamma_1(p_1),
\end{aligned}$$

$$\begin{aligned}
S_{b,B}^{\#p_1} & = T_3(-s F_{b,9}) \Gamma_4(p_1) + T_3(s m_p F_{b,9}) \Gamma_2(p_1) \\
& + T_3(s m_p F_{b,9}) \Gamma_3(p_1) + T_3(-s m_p^2 F_{b,9}) \Gamma_1(p_1) \\
& + T_3(s m_p F_{b,12}) \Gamma_4(p_1) + T_3(-s m_p^2 F_{b,12}) \Gamma_2(p_1) \\
& + T_3(-s m_p^2 F_{b,12}) \Gamma_3(p_1) + T_3(s m_p^3 F_{b,12}) \Gamma_1(p_1) \\
& + T_5(-F_{b,6}) \Gamma_4(p_1) + T_5(m_p F_{b,6}) \Gamma_2(p_1) \\
& + T_5(m_p F_{b,6}) \Gamma_3(p_1) + T_5(-m_p^2 F_{b,6}) \Gamma_1(p_1) \\
& + T_5(m_p F_{b,10}) \Gamma_4(p_1) + T_5(-m_p^2 F_{b,10}) \Gamma_2(p_1) \\
& + T_5(-m_p^2 F_{b,10}) \Gamma_3(p_1) + T_5(m_p^3 F_{b,10}) \Gamma_1(p_1) \\
& + T_7(-F_{b,6}) \Gamma_4(p_1) + T_7(m_p F_{b,6}) \Gamma_2(p_1)
\end{aligned}$$

$$\begin{aligned}
& + T_7(m_p F_{b,6})\Gamma_3(p_1) + T_7(-m_p^2 F_{b,6})\Gamma_1(p_1) \\
& + T_7(m_p F_{b,10})\Gamma_4(p_1) + T_7(-m_p^2 F_{b,10})\Gamma_2(p_1) \\
& + T_7(-m_p^2 F_{b,10})\Gamma_3(p_1) + T_7(m_p^3 F_{b,10})\Gamma_1(p_1) \\
& + T_8(-F_{b,9})\Gamma_4(p_1) + T_8(m_p F_{b,9})\Gamma_2(p_1) \\
& + T_8(m_p F_{b,9})\Gamma_3(p_1) + T_8(-m_p^2 F_{b,9})\Gamma_1(p_1) \\
& + T_8(m_p F_{b,12})\Gamma_4(p_1) + T_8(-m_p^2 F_{b,12})\Gamma_2(p_1) \\
& + T_8(-m_p^2 F_{b,12})\Gamma_3(p_1) + T_8(m_p^3 F_{b,12})\Gamma_1(p_1) \\
& + T_3 m F_{b,6} \Gamma_4(p_1) + T_3 m (-m_p F_{b,6}) \Gamma_2(p_1) \\
& + T_3 m (-m_p F_{b,6}) \Gamma_3(p_1) + T_3 m (m_p^2 F_{b,6}) \Gamma_1(p_1) \\
& + T_3 m (-m_p F_{b,10}) \Gamma_4(p_1) + T_3 m (m_p^2 F_{b,10}) \Gamma_2(p_1) \\
& + T_3 m (m_p^2 F_{b,10}) \Gamma_3(p_1) + T_3 m (-m_p^3 F_{b,10}) \Gamma_1(p_1) \\
& + T_3 (2I_M) g_b \Gamma_2(p_1) + T_3 g_b (-2G_0(p_1)) \Gamma_4(p_1) \\
& + T_3 g_b (2m_p G_0(p_1)) \Gamma_2(p_1) + T_3 g_b (2m_p G_0(p_1)) \Gamma_3(p_1) \\
& + T_3 g_b (-2m_p^2 G_0(p_1)) \Gamma_1(p_1) + T_3 g_b (2m_p G_1(p_1)) \Gamma_4(p_1) \\
& + T_3 g_b (-2m_p^2 G_1(p_1)) \Gamma_2(p_1) + T_3 g_b (-2m_p^2 G_1(p_1)) \Gamma_3(p_1) \\
& + T_3 g_b (2m_p^3 G_1(p_1)) \Gamma_1(p_1) + T_3 (-2I_M m_p) g_b \Gamma_1(p_1) \\
& + T_3 (s F_{b,9}) m \Gamma_2(p_1) + T_3 (-s m_p F_{b,9}) m \Gamma_1(p_1) \\
& + T_3 (-s m_p F_{b,12}) m \Gamma_2(p_1) + T_3 (s m_p^2 F_{b,12}) m \Gamma_1(p_1) \\
& + T_3 (-2s G_1(p)) g_b \Gamma_2(p_1) + T_3 (2s m_p G_1(p)) g_b \Gamma_1(p_1) \\
& + T_5 m F_{b,9} \Gamma_4(p_1) + T_5 m (-m_p F_{b,9}) \Gamma_2(p_1) \\
& + T_5 m (-m_p F_{b,9}) \Gamma_3(p_1) + T_5 m (m_p^2 F_{b,9}) \Gamma_1(p_1) \\
& + T_5 m (-m_p F_{b,12}) \Gamma_4(p_1) + T_5 m (m_p^2 F_{b,12}) \Gamma_2(p_1) \\
& + T_5 m (m_p^2 F_{b,12}) \Gamma_3(p_1) + T_5 m (-m_p^3 F_{b,12}) \Gamma_1(p_1) \\
& + T_5 F_{b,6} m \Gamma_2(p_1) + T_5 (-m_p F_{b,6}) m \Gamma_1(p_1) \\
& + T_5 (-m_p F_{b,10}) m \Gamma_2(p_1) + T_5 (m_p^2 F_{b,10}) m \Gamma_1(p_1) \\
& + T_5 (-2G_0(p)) g_b \Gamma_2(p_1) + T_5 (2m_p G_0(p)) g_b \Gamma_1(p_1) \\
& + T_7 F_{b,6} m \Gamma_2(p_1) + T_7 (-m_p F_{b,6}) m \Gamma_1(p_1) \\
& + T_7 (-m_p F_{b,10}) m \Gamma_2(p_1) + T_7 (m_p^2 F_{b,10}) m \Gamma_1(p_1) \\
& + T_7 (-2G_0(p)) g_b \Gamma_2(p_1) + T_7 (2m_p G_0(p)) g_b \Gamma_1(p_1) \\
& + T_8 F_{b,9} m \Gamma_2(p_1) + T_8 (-m_p F_{b,9}) m \Gamma_1(p_1) \\
& + T_8 (-m_p F_{b,12}) m \Gamma_2(p_1) + T_8 (m_p^2 F_{b,12}) m \Gamma_1(p_1) \\
& + T_8 (-2G_1(p)) g_b \Gamma_2(p_1) + T_8 (2m_p G_1(p)) g_b \Gamma_1(p_1) \\
& + T_3 m (-F_{b,6}) m \Gamma_2(p_1) + T_3 m (m_p F_{b,6}) m \Gamma_1(p_1) \\
& + T_3 m (m_p F_{b,10}) m \Gamma_2(p_1) + T_3 m (-m_p^2 F_{b,10}) m \Gamma_1(p_1)
\end{aligned}$$

$$\begin{aligned}
& + T_3 m(2G_0(p)) g_b \Gamma_2(p_1) + T_3 m(-2m_p G_0(p)) g_b \Gamma_1(p_1) \\
& + T_3 g_b(2G_0(p_1)) m \Gamma_2(p_1) + T_3 g_b(-2m_p G_0(p_1)) m \Gamma_1(p_1) \\
& + T_3 g_b(-2m_p G_1(p_1)) m \Gamma_2(p_1) + T_3 g_b(2m_p^2 G_1(p_1)) m \Gamma_1(p_1) \\
& + T_5 m(-F_{b,9}) m \Gamma_2(p_1) + T_5 m(m_p F_{b,9}) m \Gamma_1(p_1) \\
& + T_5 m(m_p F_{b,12}) m \Gamma_2(p_1) + T_5 m(-m_p^2 F_{b,12}) m \Gamma_1(p_1) \\
& + T_5 m(2G_1(p)) g_b \Gamma_2(p_1) + T_5 m(-2m_p G_1(p)) g_b \Gamma_1(p_1),
\end{aligned}$$

$$\begin{aligned}
S_{b,B}^{4pp_1} = & T_1(-sF_{b,9}) \Gamma_4(p_1) + T_1(sm_p F_{b,9}) \Gamma_2(p_1) \\
& + T_1(sm_p F_{b,9}) \Gamma_3(p_1) + T_1(-sm_p^2 F_{b,9}) \Gamma_1(p_1) \\
& + T_1(sm_p F_{b,12}) \Gamma_4(p_1) + T_1(-sm_p^2 F_{b,12}) \Gamma_2(p_1) \\
& + T_1(-sm_p^2 F_{b,12}) \Gamma_3(p_1) + T_1(sm_p^3 F_{b,12}) \Gamma_1(p_1) \\
& + T_2(-F_{b,6}) \Gamma_4(p_1) + T_2(m_p F_{b,6}) \Gamma_2(p_1) \\
& + T_2(m_p F_{b,6}) \Gamma_3(p_1) + T_2(-m_p^2 F_{b,6}) \Gamma_1(p_1) \\
& + T_2(m_p F_{b,10}) \Gamma_4(p_1) + T_2(-m_p^2 F_{b,10}) \Gamma_2(p_1) \\
& + T_2(-m_p^2 F_{b,10}) \Gamma_3(p_1) + T_2(m_p^3 F_{b,10}) \Gamma_1(p_1) \\
& + T_4(-F_{b,6}) \Gamma_4(p_1) + T_4(m_p F_{b,6}) \Gamma_2(p_1) \\
& + T_4(m_p F_{b,6}) \Gamma_3(p_1) + T_4(-m_p^2 F_{b,6}) \Gamma_1(p_1) \\
& + T_4(m_p F_{b,10}) \Gamma_4(p_1) + T_4(-m_p^2 F_{b,10}) \Gamma_2(p_1) \\
& + T_4(-m_p^2 F_{b,10}) \Gamma_3(p_1) + T_4(m_p^3 F_{b,10}) \Gamma_1(p_1) \\
& + T_6(-F_{b,9}) \Gamma_4(p_1) + T_6(m_p F_{b,9}) \Gamma_2(p_1) \\
& + T_6(m_p F_{b,9}) \Gamma_3(p_1) + T_6(-m_p^2 F_{b,9}) \Gamma_1(p_1) \\
& + T_6(m_p F_{b,12}) \Gamma_4(p_1) + T_6(-m_p^2 F_{b,12}) \Gamma_2(p_1) \\
& + T_6(-m_p^2 F_{b,12}) \Gamma_3(p_1) + T_6(m_p^3 F_{b,12}) \Gamma_1(p_1) \\
& + T_1 m F_{b,6} \Gamma_4(p_1) + T_1 m(-m_p F_{b,6}) \Gamma_2(p_1) \\
& + T_1 m(-m_p F_{b,6}) \Gamma_3(p_1) + T_1 m(m_p^2 F_{b,6}) \Gamma_1(p_1) \\
& + T_1 m(-m_p F_{b,10}) \Gamma_4(p_1) + T_1 m(m_p^2 F_{b,10}) \Gamma_2(p_1) \\
& + T_1 m(m_p^2 F_{b,10}) \Gamma_3(p_1) + T_1 m(-m_p^3 F_{b,10}) \Gamma_1(p_1) \\
& + T_1(2I_M) g_b \Gamma_2(p_1) + T_1 g_b(-2G_0(p_1)) \Gamma_4(p_1) \\
& + T_1 g_b(2m_p G_0(p_1)) \Gamma_2(p_1) + T_1 g_b(2m_p G_0(p_1)) \Gamma_3(p_1) \\
& + T_1 g_b(-2m_p^2 G_0(p_1)) \Gamma_1(p_1) + T_1 g_b(2m_p G_1(p_1)) \Gamma_4(p_1) \\
& + T_1 g_b(-2m_p^2 G_1(p_1)) \Gamma_2(p_1) + T_1 g_b(-2m_p^2 G_1(p_1)) \Gamma_3(p_1) \\
& + T_1 g_b(2m_p^3 G_1(p_1)) \Gamma_1(p_1) + T_1(-2I_M m_p) g_b \Gamma_1(p_1) \\
& + T_1(sF_{b,9}) m \Gamma_2(p_1) + T_1(-sm_p F_{b,9}) m \Gamma_1(p_1) \\
& + T_1(-sm_p F_{b,12}) m \Gamma_2(p_1) + T_1(sm_p^2 F_{b,12}) m \Gamma_1(p_1)
\end{aligned}$$

$$\begin{aligned}
& + T_1(-2sG_1(p))g_b\Gamma_2(p_1) + T_1(2sm_pG_1(p))g_b\Gamma_1(p_1) \\
& + T_2mF_{b,9}\Gamma_4(p_1) + T_2m(-m_pF_{b,9})\Gamma_2(p_1) \\
& + T_2m(-m_pF_{b,9})\Gamma_3(p_1) + T_2m(m_p^2F_{b,9})\Gamma_1(p_1) \\
& + T_2m(-m_pF_{b,12})\Gamma_4(p_1) + T_2m(m_p^2F_{b,12})\Gamma_2(p_1) \\
& + T_2m(m_p^2F_{b,12})\Gamma_3(p_1) + T_2m(-m_p^3F_{b,12})\Gamma_1(p_1) \\
& + T_2F_{b,6}m\Gamma_2(p_1) + T_2(-m_pF_{b,6})m\Gamma_1(p_1) \\
& + T_2(-m_pF_{b,10})m\Gamma_2(p_1) + T_2(m_p^2F_{b,10})m\Gamma_1(p_1) \\
& + T_2(-2G_0(p))g_b\Gamma_2(p_1) + T_2(2m_pG_0(p))g_b\Gamma_1(p_1) \\
& + T_4F_{b,6}m\Gamma_2(p_1) + T_4(-m_pF_{b,6})m\Gamma_1(p_1) \\
& + T_4(-m_pF_{b,10})m\Gamma_2(p_1) + T_4(m_p^2F_{b,10})m\Gamma_1(p_1) \\
& + T_4(-2G_0(p))g_b\Gamma_2(p_1) + T_4(2m_pG_0(p))g_b\Gamma_1(p_1) \\
& + T_6F_{b,9}m\Gamma_2(p_1) + T_6(-m_pF_{b,9})m\Gamma_1(p_1) \\
& + T_6(-m_pF_{b,12})m\Gamma_2(p_1) + T_6(m_p^2F_{b,12})m\Gamma_1(p_1) \\
& + T_6(-2G_1(p))g_b\Gamma_2(p_1) + T_6(2m_pG_1(p))g_b\Gamma_1(p_1) \\
& + T_1m(-F_{b,6})m\Gamma_2(p_1) + T_1m(m_pF_{b,6})m\Gamma_1(p_1) \\
& + T_1m(m_pF_{b,10})m\Gamma_2(p_1) + T_1m(-m_p^2F_{b,10})m\Gamma_1(p_1) \\
& + T_1m(2G_0(p))g_b\Gamma_2(p_1) + T_1m(-2m_pG_0(p))g_b\Gamma_1(p_1) \\
& + T_1g_b(2G_0(p_1))m\Gamma_2(p_1) + T_1g_b(-2m_pG_0(p_1))m\Gamma_1(p_1) \\
& + T_1g_b(-2m_pG_1(p_1))m\Gamma_2(p_1) + T_1g_b(2m_p^2G_1(p_1))m\Gamma_1(p_1) \\
& + T_2m(-F_{b,9})m\Gamma_2(p_1) + T_2m(m_pF_{b,9})m\Gamma_1(p_1) \\
& + T_2m(m_pF_{b,12})m\Gamma_2(p_1) + T_2m(-m_p^2F_{b,12})m\Gamma_1(p_1) \\
& + T_2m(2G_1(p))g_b\Gamma_2(p_1) + T_2m(-2m_pG_1(p))g_b\Gamma_1(p_1),
\end{aligned}$$

The graph $S_{b,WT1}^\mu$ of eq. (4.6) decomposes as

$$S_{b,WT1}^\mu = (\not{p}\gamma^\mu S_{b,WT1}^{\not{p}\gamma} + \gamma^\mu S_{b,WT1}^\gamma + p^\mu S_{b,WT1}^p + p_1\mu S_{b,WT1}^{p_1})\gamma_5$$

with

$$\begin{aligned}
S_{b,WT1}^{\not{p}\gamma} &= 2\hat{g}_b\left((G_0(p_1) - m_pG_1(p_1))Y_3 - I_M Y_2\right), \\
S_{b,WT1}^\gamma &= -m_p S_{b,WT1}^{\not{p}\gamma}, \\
S_{b,WT1}^p &= -S_{b,WT1}^{\not{p}\gamma}, \\
S_{b,WT1}^{p_1} &= -S_{b,WT1}^{\not{p}\gamma}.
\end{aligned}$$

Finally, the decomposition of $S_{b,WT2}^\mu$ of eq. (4.7) is given by

$$\begin{aligned} S_{b,WT2}^\mu = & (\not{p}\gamma^\mu S_{b,WT2}^{\not{p}\gamma} + \gamma^\mu S_{b,WT2}^\gamma + \not{q}\gamma^\mu S_{b,WT2}^{\not{q}\gamma} + \not{q}\not{p}\gamma^\mu S_{b,WT2}^{\not{q}\not{p}\gamma} + \not{q}\not{p}p_1^\mu S_{b,WT2}^{\not{q}\not{p}p_1} \\ & + \not{p}p_1^\mu S_{b,WT2}^{\not{p}p_1} + \not{q}p_1^\mu S_{b,WT2}^{\not{q}p_1} + p_1^\mu S_{b,WT2}^{p_1} + \not{q}\not{p}p^\mu S_{b,WT2}^{\not{q}\not{p}p} + \not{p}p^\mu S_{b,WT2}^{\not{p}p} \\ & + \not{q}p^\mu S_{b,WT2}^{\not{q}p} + p^\mu S_{b,WT2}^p) \gamma_5 \end{aligned}$$

with

$$\begin{aligned} S_{b,WT2}^{\not{p}\gamma} &= Z_1 S_{b,WT1}^{\not{p}\gamma} + Z_3 S_{b,WT1}^\gamma, \\ S_{b,WT2}^\gamma &= Z_1 S_{b,WT1}^\gamma + s Z_3 S_{b,WT1}^{\not{p}\gamma}, \\ S_{b,WT2}^{\not{q}\gamma} &= Z_2 S_{b,WT1}^\gamma + s Z_4 S_{b,WT1}^{\not{p}\gamma}, \\ S_{b,WT2}^{\not{q}\not{p}\gamma} &= Z_2 S_{b,WT1}^{\not{p}\gamma} + Z_4 S_{b,WT1}^\gamma, \\ S_{b,WT2}^{\not{q}\not{p}p_1} &= Z_4 S_{b,WT1}^{p_1}, \\ S_{b,WT2}^{\not{p}p_1} &= Z_3 S_{b,WT1}^{p_1}, \\ S_{b,WT2}^{\not{q}p_1} &= Z_2 S_{b,WT1}^{p_1}, \\ S_{b,WT2}^{p_1} &= Z_1 S_{b,WT1}^{p_1}, \\ S_{b,WT2}^{\not{q}\not{p}p} &= Z_4 S_{b,WT1}^p, \\ S_{b,WT2}^{\not{p}p} &= Z_3 S_{b,WT1}^p, \\ S_{b,WT2}^{\not{q}p} &= Z_2 S_{b,WT1}^p, \\ S_{b,WT2}^p &= Z_1 S_{b,WT1}^p, \end{aligned}$$

where the abbreviations

$$\begin{aligned} Z_1 &= s(-T_3 m + T_5 + T_7)G_1(p) + (-T_5 m + sT_3 + T_8)G_0(p) - T_5 I_M, \\ Z_2 &= s(-T_1 m + T_2 + T_4)G_1(p) + (-T_2 m + sT_1 + T_6)G_0(p) - T_2 I_M, \\ Z_3 &= (-T_5 m + sT_3 + T_8)G_1(p) + (-T_3 m + T_5 + T_7)G_0(p) - T_3 I_M, \\ Z_4 &= (-T_2 m + sT_1 + T_6)G_1(p) + (-T_1 m + T_2 + T_4)G_0(p) - T_1 I_M, \end{aligned}$$

were used. The total amplitude has the same Dirac structures as in the leading order approach and can be obtained by adding all contributions of the various amplitudes:

$$\begin{aligned} \mathcal{M}^\mu = & \gamma^\mu \gamma_5 \mathcal{M}_1 + \not{q}^\mu \gamma_5 \mathcal{M}_2 + p^\mu \gamma_5 \mathcal{M}_3 + p_1^\mu \gamma_5 \mathcal{M}_4 + \not{q}\gamma^\mu \gamma_5 \mathcal{M}_5 + \not{p}\gamma^\mu \gamma_5 \mathcal{M}_6 \\ & + \not{q}\not{p}\gamma^\mu \gamma_5 \mathcal{M}_7 + \not{q}q^\mu \gamma_5 \mathcal{M}_8 + \not{p}q^\mu \gamma_5 \mathcal{M}_9 + \not{q}p^\mu \gamma_5 \mathcal{M}_{10} + \not{p}p^\mu \gamma_5 \mathcal{M}_{11} \\ & + \not{q}\not{p}p^\mu \gamma_5 \mathcal{M}_{12} + \not{q}p_1^\mu \gamma_5 \mathcal{M}_{13} + \not{p}p_1^\mu \gamma_5 \mathcal{M}_{14} + \not{q}\not{p}p_1^\mu \gamma_5 \mathcal{M}_{15}. \end{aligned} \tag{D.1}$$

Note, that the amplitudes of the leading order approach, that were decomposed in the previous section, have to be included as well.

Appendix E

Calculation of the differential cross section

This appendix is dedicated to the calculation of the CGLN amplitudes and the differential cross section for the photoproduction process $p\gamma \rightarrow p\eta$ described in the chapters 3 and 4. The evaluation given here is in analogy to [39]. The Mandelstam variables are given as usual by

$$s = (p_1 + k)^2, \quad u = (p_1 - q)^2, \quad t = (p_2 - p_1)^2$$

where k is the momentum of the incoming photon, q is the momentum of the outgoing η , and p_1 and p_2 are the momenta of the incoming and outgoing proton, respectively. A photoproduction amplitude $\mathcal{M} = \epsilon_\mu \mathcal{M}^\mu$ can be decomposed as

$$\mathcal{M} = i\epsilon_\mu \bar{u}_2 \sum_{k=1}^8 B_k \mathcal{N}_k^\mu u_1,$$

where u_1 and \bar{u}_2 the spinors and the operator basis is given by

$$\begin{aligned} \mathcal{N}_1^\mu &= \gamma_5 \gamma^\mu \not{k}, & \mathcal{N}_2^\mu &= \gamma_5 p^\mu, \\ \mathcal{N}_3^\mu &= 2\gamma_5 q^\mu, & \mathcal{N}_4^\mu &= 2\gamma_5 k^\mu, \\ \mathcal{N}_5^\mu &= \gamma_5 \gamma^\mu, & \mathcal{N}_6^\mu &= \frac{1}{2} \gamma_5 \not{k} p^\mu, \\ \mathcal{N}_7^\mu &= \gamma_5 \not{k} k^\mu, & \mathcal{N}_8^\mu &= \gamma_5 \not{k} q^\mu. \end{aligned}$$

The total four-momentum is denoted by $p = p_1 + k = p_2 + q$. The coefficients B_k can be expressed in terms of the coefficients of the Dirac structures of the photoproduction amplitude \mathcal{M}^μ as in eq. (D.1):

$$\begin{aligned} B_1 &= -\mathcal{M}_5 - \mathcal{M}_6 + m_p \mathcal{M}_7, \\ B_2 &= \frac{1}{2} \mathcal{M}_3 + \frac{1}{2} \mathcal{M}_4 + \mathcal{M}_5 + \mathcal{M}_6 - m_p \mathcal{M}_7 - m_p \mathcal{M}_{10} - \frac{1}{2} m_p \mathcal{M}_{11}, \end{aligned}$$

$$\begin{aligned}
& + \frac{1}{2}(s + m_p^2)\mathcal{M}_{12} - m_p\mathcal{M}_{13} - \frac{1}{2}m_p\mathcal{M}_{14} + \frac{1}{2}(s + m_p^2)\mathcal{M}_{15}, \\
B_3 = & \frac{1}{2}\mathcal{M}_2 + \frac{1}{4}\mathcal{M}_3 + \frac{1}{4}\mathcal{M}_4 + \frac{1}{2}\mathcal{M}_5 + \frac{1}{2}\mathcal{M}_6 - \frac{1}{2}m_p\mathcal{M}_7 - m_p\mathcal{M}_8 \\
& - \frac{1}{2}m_p\mathcal{M}_9 - \frac{1}{2}m_p\mathcal{M}_{10} - \frac{1}{4}m_p\mathcal{M}_{11} + \frac{1}{4}(s + m_p^2)\mathcal{M}_{12} \\
& - \frac{1}{2}m_p\mathcal{M}_{13} - \frac{1}{4}m_p\mathcal{M}_{14} + \frac{1}{4}(s + m_p^2)\mathcal{M}_{15}, \\
B_4 = & \frac{1}{4}\mathcal{M}_3 - \frac{1}{4}\mathcal{M}_4 + \frac{1}{2}\mathcal{M}_5 + \frac{1}{2}\mathcal{M}_6 - \frac{1}{2}m_p\mathcal{M}_7 - \frac{1}{2}m_p\mathcal{M}_{10} \\
& - \frac{1}{4}m_p\mathcal{M}_{11} + \frac{1}{4}(s + m_p^2)\mathcal{M}_{12} + \frac{1}{2}m_p\mathcal{M}_{13} + \frac{1}{4}m_p\mathcal{M}_{14} \\
& - \frac{1}{4}(s + m_p^2)\mathcal{M}_{15}, \\
B_5 = & -\mathcal{M}_1 - m_p\mathcal{M}_6 - (s - m_p^2)\mathcal{M}_7, \\
B_6 = & -\mathcal{M}_{10} - \mathcal{M}_{11} + m_p\mathcal{M}_{12} - \mathcal{M}_{13} - \mathcal{M}_{14} + m_p\mathcal{M}_{15}, \\
B_7 = & -\frac{1}{2}\mathcal{M}_{10} - \frac{1}{2}\mathcal{M}_{11} + \frac{1}{2}m_p\mathcal{M}_{12} + \frac{1}{2}\mathcal{M}_{13} + \frac{1}{2}\mathcal{M}_{14} - \frac{1}{2}m_p\mathcal{M}_{15}, \\
B_8 = & -\mathcal{M}_8 - \mathcal{M}_9 - \frac{1}{2}\mathcal{M}_{10} - \frac{1}{2}\mathcal{M}_{11} + \frac{1}{2}m_p\mathcal{M}_{12} - \frac{1}{2}\mathcal{M}_{13} - \frac{1}{2}\mathcal{M}_{14} \\
& + \frac{1}{2}m_p\mathcal{M}_{15},
\end{aligned}$$

where m_p denotes the mass of the proton. For gauge invariant amplitudes two constraints on the coefficients B_k can be derived:

$$\begin{aligned}
k^2 B_1 + k_\mu p^\mu B_2 + 2k_\mu q^\mu B_3 + 2k^2 B_4 &= 0, \\
B_5 + \frac{1}{2}k_\mu p^\mu B_6 + k^2 B_7 + k_\mu q^\mu B_8 &= 0.
\end{aligned}$$

These constraints can be used to eliminate two coefficients of the B_k , which are chosen to be B_3 and B_5 . Hence the total amplitude can be rewritten in a manifestly gauge invariant form:

$$\mathcal{M} = i\bar{u}_2 \sum_{k=1}^6 A_k M_k u_1$$

where the operator basis reads

$$\begin{aligned}
M_1 &= \frac{1}{2}\gamma_5\gamma_\mu\gamma_\nu F^{\mu\nu}, & M_2 &= \gamma_5 p_\mu (q_\nu - \frac{1}{2}k_\nu) F^{\mu\nu} \\
M_3 &= \gamma_5\gamma_\mu q_\nu F^{\mu\nu}, & M_4 &= \gamma_5\gamma_\mu p_\nu F^{\mu\nu} - 2m_p M_1, \\
M_5 &= \gamma_5 k_\mu q_\nu F^{\mu\nu}, & M_6 &= \gamma_5 k_\mu \gamma_\nu F^{\mu\nu},
\end{aligned}$$

with $F^{\mu\nu} = \epsilon^\mu k^\nu - \epsilon^\nu k^\mu$. The coefficients A_k are given by

$$A_1 = B_1 - m_p B_6,$$

$$\begin{aligned}
A_2 &= \frac{2}{M_\eta^2 - t} B_2, \\
A_3 &= -B_8, \\
A_4 &= -\frac{1}{2} B_6, \\
A_5 &= \frac{2}{s + u - 2m_p^2} \left(B_1 - \frac{s - u}{2(M_\eta^2 - t)} B_2 + 2B_4 \right), \\
A_6 &= B_7,
\end{aligned}$$

where M_η is the mass of the η meson.

For an evaluation of the Chew, Goldberger, Low and Nambu (CGLN) amplitudes, the following decompositions will make use of the conventions in [39, 40]. The total amplitude can be rewritten once again, using the standard representation of the Dirac matrices:

$$\frac{1}{8\pi\sqrt{s}} i\bar{u}_2 \sum_{k=1}^6 A_k M_k u_1 = \chi_2^\dagger \mathbf{F} \chi_1, \quad (\text{E.1})$$

where the χ_i are Pauli spinors and the matrix \mathbf{F} is given by

$$\begin{aligned}
\mathbf{F} &= i(\sigma \cdot \mathbf{b})\mathcal{F}_1 + (\sigma \cdot \hat{\mathbf{q}})(\sigma \cdot (\hat{\mathbf{k}} \times \mathbf{b}))\mathcal{F}_2 + i(\sigma \cdot \hat{\mathbf{k}})(\hat{\mathbf{q}} \cdot \mathbf{b})\mathcal{F}_3 \\
&\quad + i(\sigma \cdot \hat{\mathbf{q}})(\hat{\mathbf{q}} \cdot \mathbf{b})\mathcal{F}_4 - i(\sigma \cdot \hat{\mathbf{q}})b_0\mathcal{F}_7 - i(\sigma \cdot \hat{\mathbf{k}})b_0\mathcal{F}_8.
\end{aligned}$$

Here, σ is a three-vector containing the Pauli matrices in the standard representation as its components, $\hat{\mathbf{q}}$ and $\hat{\mathbf{k}}$ are the three-vector components of q and k normalized to a unit vector and the four-vector $b = (b_0, \mathbf{b})$ is defined by

$$b_\mu = \epsilon_\mu - \frac{\boldsymbol{\epsilon} \cdot \hat{\mathbf{k}}}{|\mathbf{k}|} k_\mu,$$

where $\boldsymbol{\epsilon}$ is the three-vector part of the four-vector ϵ . The CGLN-amplitudes \mathcal{F}_i can be evaluated in terms of the A_i by substituting the standard representation of Dirac spinors and matrices on the l.h.s. of eq. E.1:

$$\begin{aligned}
\mathcal{F}_1 &= (\sqrt{s} - m_p) \frac{\sqrt{E_1 + m_p} \sqrt{E_2 + m_p}}{8\pi\sqrt{s}} \left[A_1 + \frac{k_\mu q^\mu}{\sqrt{s} - m_p} A_3 \right. \\
&\quad \left. + \left(\sqrt{s} - m_p - \frac{k_\mu q^\mu}{\sqrt{s} - m_p} \right) A_4 - \frac{k^2}{\sqrt{s} - m_p} A_6 \right], \\
\mathcal{F}_2 &= (\sqrt{s} + m_p) \frac{\sqrt{E_1 + m_p} \sqrt{E_2 + m_p}}{8\pi\sqrt{s}} \frac{|\mathbf{q}||\mathbf{k}|}{(E_1 + m_p)(E_2 + m_p)} \left[-A_1 \right. \\
&\quad \left. + \frac{k_\mu q^\mu}{\sqrt{s} + m_p} A_3 + \left(\sqrt{s} + m_p - \frac{k_\mu q^\mu}{\sqrt{s} + m_p} \right) A_4 - \frac{k^2}{\sqrt{s} + m_p} A_6 \right], \\
\mathcal{F}_3 &= (\sqrt{s} + m_p) \frac{\sqrt{E_1 + m_p} \sqrt{E_2 + m_p}}{8\pi\sqrt{s}} \frac{|\mathbf{q}||\mathbf{k}|}{E_1 + m_p} \left[\frac{m_p^2 - s + \frac{1}{2}k^2}{\sqrt{s} + m_p} A_2 + A_3 \right]
\end{aligned}$$

$$\begin{aligned}
& - A_4 - \frac{k^2}{\sqrt{s} + m_p} A_5 \Big], \\
\mathcal{F}_4 = & (\sqrt{s} - m_p) \frac{\sqrt{E_1 + m_p} \sqrt{E_2 + m_p}}{8\pi\sqrt{s}} \frac{|\mathbf{q}|^2}{E_2 + m_p} \left[\frac{s - m_p^2 - \frac{1}{2}k^2}{\sqrt{s} - m_p} A_2 + A_3 \right. \\
& \left. - A_4 + \frac{k^2}{\sqrt{s} - m_p} A_5 \right], \\
\mathcal{F}_7 = & \frac{\sqrt{E_1 + m_p} \sqrt{E_2 + m_p}}{8\pi\sqrt{s}} \frac{|\mathbf{q}|}{E_2 + m_p} \left[(m_p - E_1) A_1 \right. \\
& - \left(\frac{|\mathbf{k}|^2}{2k_0} (2k_0\sqrt{s} - 3k_\mu q^\mu) - \frac{\mathbf{q} \cdot \mathbf{k}}{2k_0} (2s - 2m_p^2 - k^2) \right) A_2 \\
& + (q_0(\sqrt{s} - m_p) - k_\mu q^\mu) A_3 \\
& + (k_\mu q^\mu - q_0(\sqrt{s} - m_p) + (E_1 - m_p)(\sqrt{s} + m_p)) A_4 \\
& \left. + (q_0 k^2 - k_0 k_\mu q^\mu) A_5 - (E_1 - m_p)(\sqrt{s} + m_p) A_6 \right], \\
\mathcal{F}_8 = & \frac{\sqrt{E_1 + m_p} \sqrt{E_2 + m_p}}{8\pi\sqrt{s}} \frac{|\mathbf{k}|}{E_1 + m_p} \left[(E_1 + m_1) A_1 \right. \\
& + \left(\frac{|\mathbf{k}|^2}{2k_0} (2k_0\sqrt{s} - 3k_\mu q^\mu) - \frac{\mathbf{q} \cdot \mathbf{k}}{2k_0} (2s - 2m_p^2 - k^2) \right) A_2 \\
& + (q_0(\sqrt{s} + m_p) - k_\mu q^\mu) A_3 \\
& + (k_\mu q^\mu - q_0(\sqrt{s} + m_p) + (E_1 + m_p)(\sqrt{s} - m_p)) A_4 \\
& \left. - (q_0 k^2 - k_0 k_\mu q^\mu) A_5 - (E_1 + m_p)(\sqrt{s} - m_p) A_6 \right],
\end{aligned}$$

where $E_i = \sqrt{\mathbf{p}_i^2 + m_p^2}$ with $i = 1, 2$. Now, the CGLN-amplitudes can be used to calculate the multipoles, when restricted to s - and p -waves:

$$\begin{pmatrix} E_{0+} \\ M_{1+} \\ M_{1-} \\ E_{1+} \end{pmatrix} = \int_{-1}^1 dz \begin{pmatrix} \frac{1}{2}P_0 & -\frac{1}{2}P_1 & 0 & \frac{1}{6}P_{0,2} \\ \frac{1}{4}P_1 & -\frac{1}{4}P_2 & -\frac{1}{12}P_{0,2} & 0 \\ -\frac{1}{2}P_1 & \frac{1}{2}P_0 & \frac{1}{6}P_{0,2} & 0 \\ \frac{1}{4}P_1 & -\frac{1}{4}P_2 & \frac{1}{12}P_{0,2} & \frac{1}{10}P_{1,3} \end{pmatrix} \begin{pmatrix} \mathcal{F}_1 \\ \mathcal{F}_2 \\ \mathcal{F}_3 \\ \mathcal{F}_4 \end{pmatrix}$$

and likewise

$$\begin{pmatrix} L_{0+} \\ L_{1+} \\ L_{1-} \end{pmatrix} = \frac{k_0}{|\mathbf{k}|} \int_{-1}^1 dz \begin{pmatrix} \frac{1}{2}P_1 & \frac{1}{2}P_0 \\ \frac{1}{4}P_2 & \frac{1}{4}P_1 \\ \frac{1}{2}P_0 & \frac{1}{2}P_1 \end{pmatrix} \begin{pmatrix} \mathcal{F}_7 \\ \mathcal{F}_8 \end{pmatrix},$$

where $P_l = P_l(z)$ are the Legendre polynomials, $z = \cos(\theta)$ is the scattering angle and

$$P_{0,2} = P_0 - P_2, \quad P_{1,3} = P_1 - P_3.$$

The unpolarized differential cross sections for the η -photoproduction amplitude off protons can be given in terms of CGLN-amplitudes in agreement with [39]:

$$\begin{aligned} \frac{d\sigma}{d\Omega} = \frac{|\mathbf{q}|}{|\mathbf{k}|} & \left[|\mathcal{F}_1|^2 + |\mathcal{F}_2|^2 + \frac{1}{2}|\mathcal{F}_3|^2 + \frac{1}{2}|\mathcal{F}_4|^2 + \text{Re}(\mathcal{F}_1\mathcal{F}_4^*) + \text{Re}(\mathcal{F}_2\mathcal{F}_3^*) \right. \\ & + (\text{Re}(\mathcal{F}_2\mathcal{F}_4^*) - 2\text{Re}(\mathcal{F}_1\mathcal{F}_2^*))z \\ & \left. - \left(\frac{1}{2}|\mathcal{F}_3|^2 + \frac{1}{2}|\mathcal{F}_4|^2 + \text{Re}(\mathcal{F}_1\mathcal{F}_4^* + \mathcal{F}_2\mathcal{F}_3^*) \right)z^2 - \text{Re}(\mathcal{F}_3\mathcal{F}_4^*)z^3 \right]. \end{aligned}$$

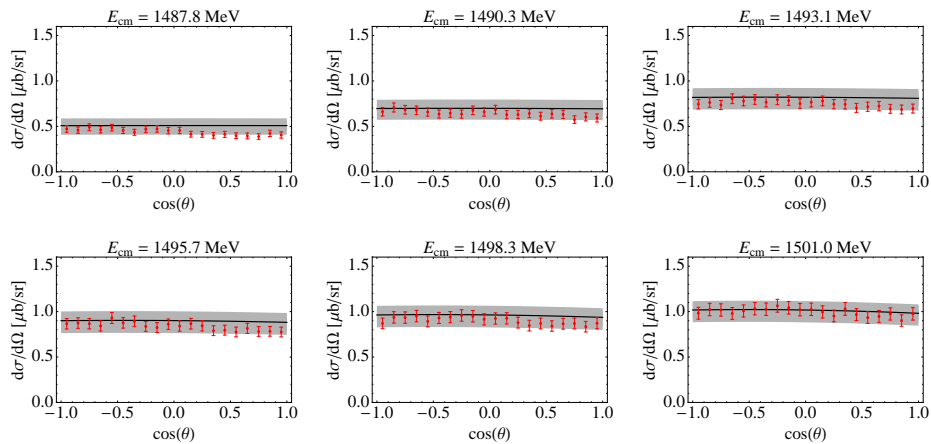
Appendix F

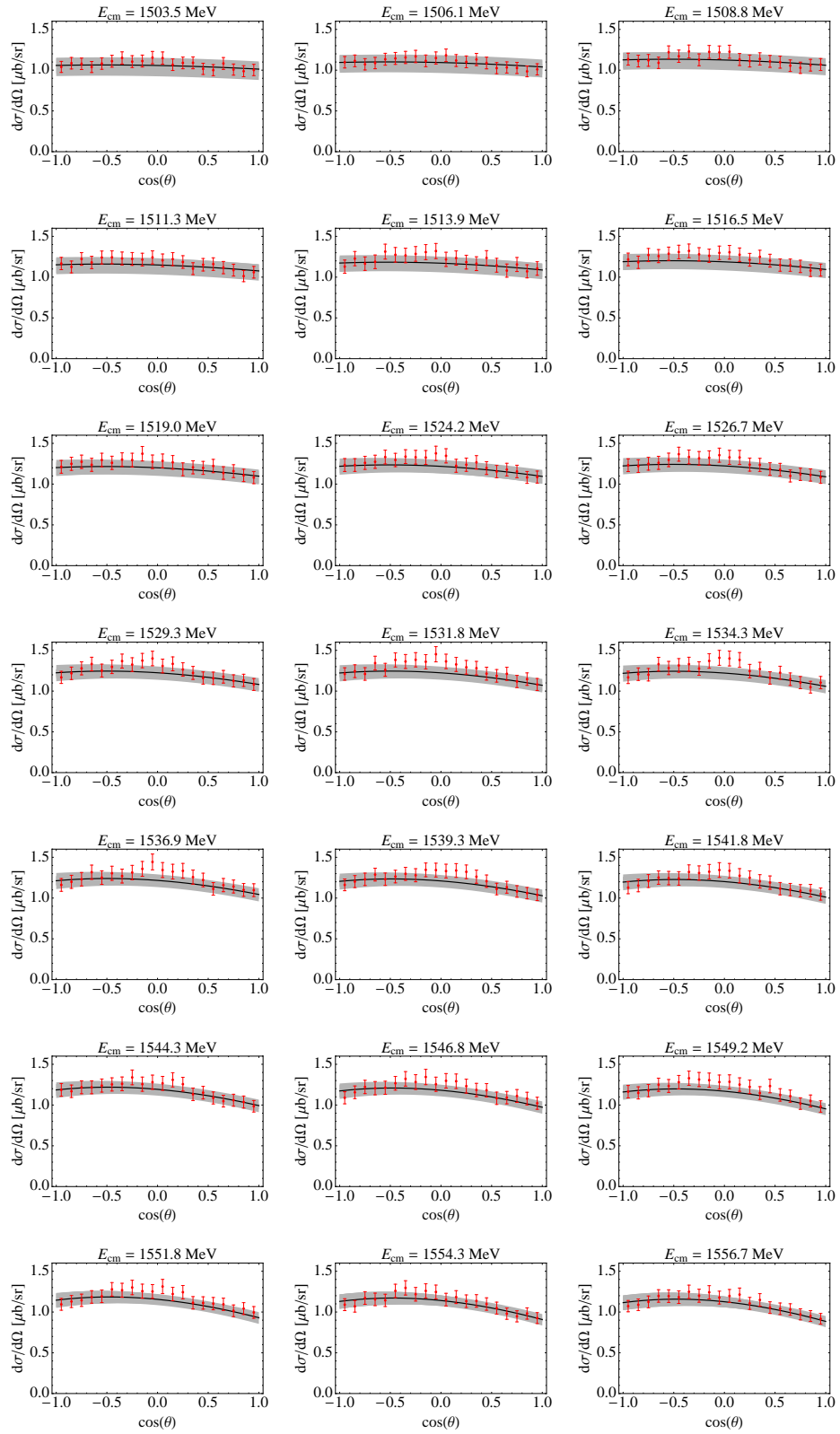
Differential cross section plots

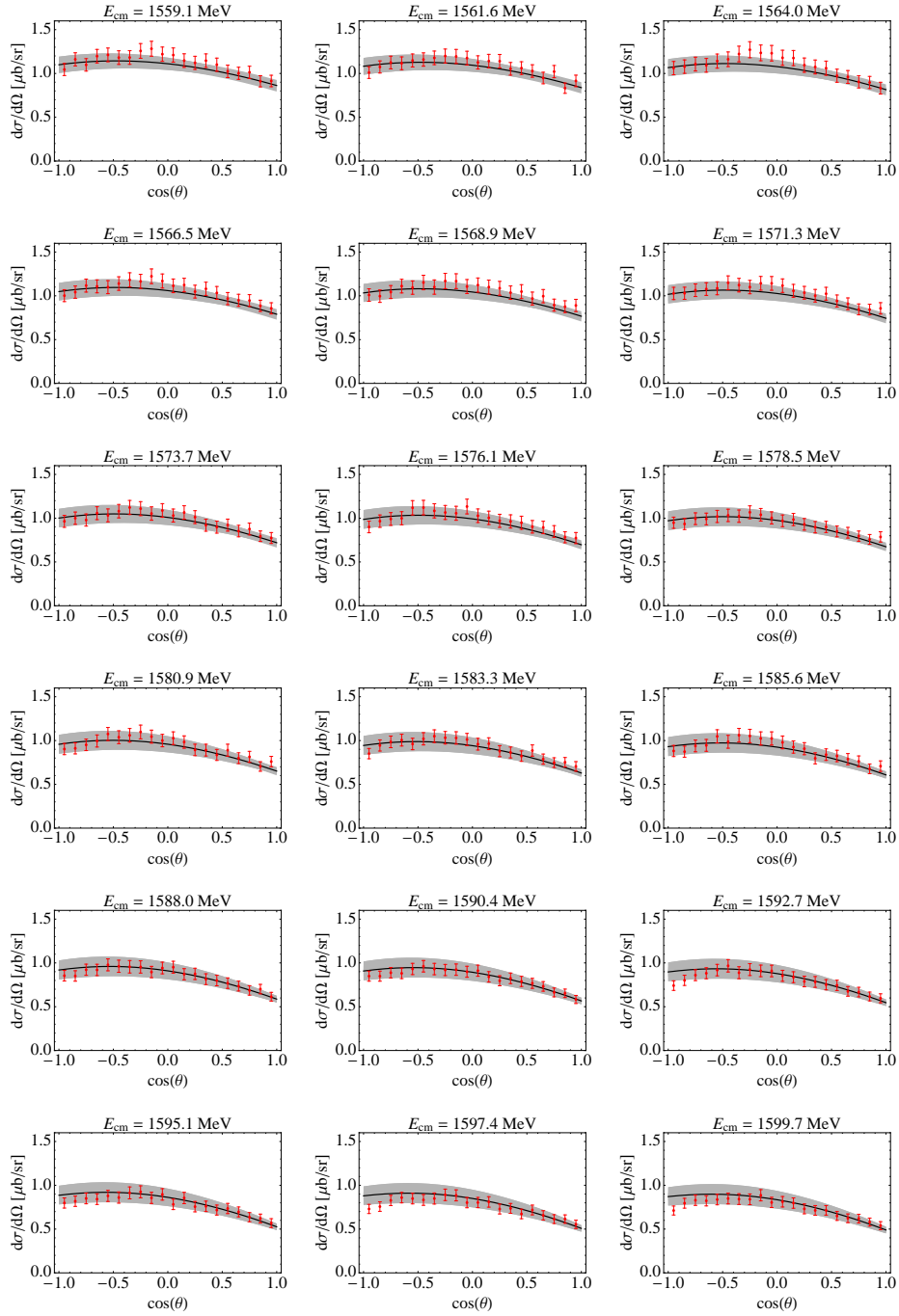
This appendix provides the complete sets of plots from the fit to the differential cross section data in the leading order approach of chapter 3, as well as from the extension of the amplitude of chapter 4.

F.1 Leading order approach

This section contains the full set of differential cross section plots from the leading order approach of chapter 3. Fig. F.1 shows all data points from McNicoll et al. [29] to which the model was fitted and the resulting best fit for the parameters quantified in eq. (3.12). Masses and decay constants are given by eq. (2.15) and eq. (2.3), respectively. The overall $\chi^2/d.o.f.$ for this fit is given by eq. (3.13).







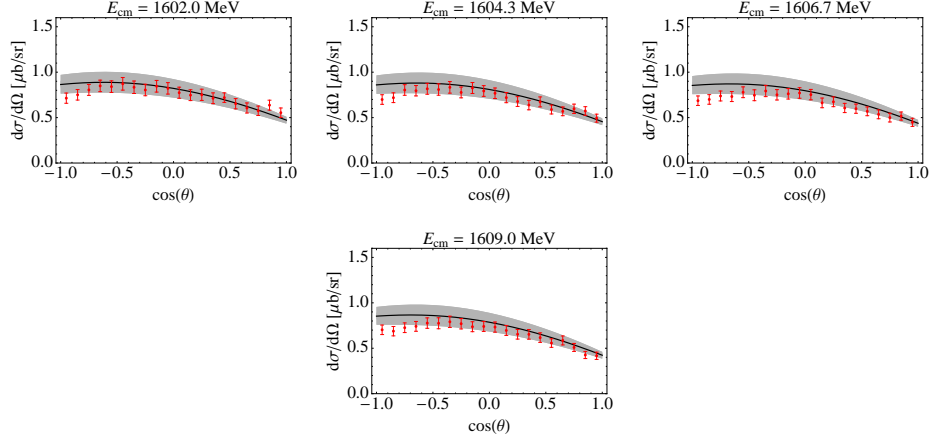
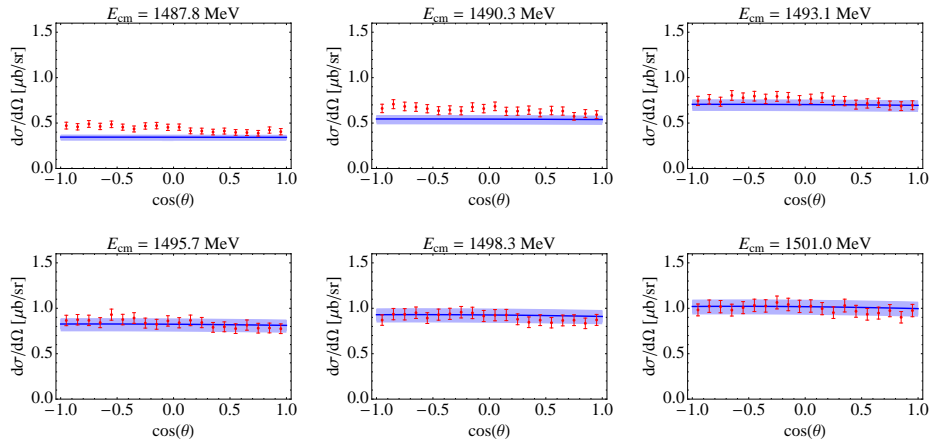


Figure F.1: Differential cross section of the model evaluated in chapter 3 (black line) fitted to the data points taken from McNicoll et al. [29] (red symbols) from threshold up to the center-of-mass energy $E_{\text{cm}} = \sqrt{s} = 1609.0$ MeV. The shaded area represents the error estimate.

F.2 Extended amplitude

This section provides the complete set of differential cross section data of the evaluation of the extended amplitude of chapter 4. Again, the data points are taken from McNicoll et al. [29]. Fig. F.2 shows the best fit of the of the model including NLO potentials, whereas fig. F.3 shows the best fit without NLO potentials. The corresponding parameter sets are given by eq. (4.8) for the amplitude with NLO potentials and by eq. (4.9) for the amplitude without NLO potentials. The overall $\chi^2/\text{d.o.f}$ are given by eq. (4.10).



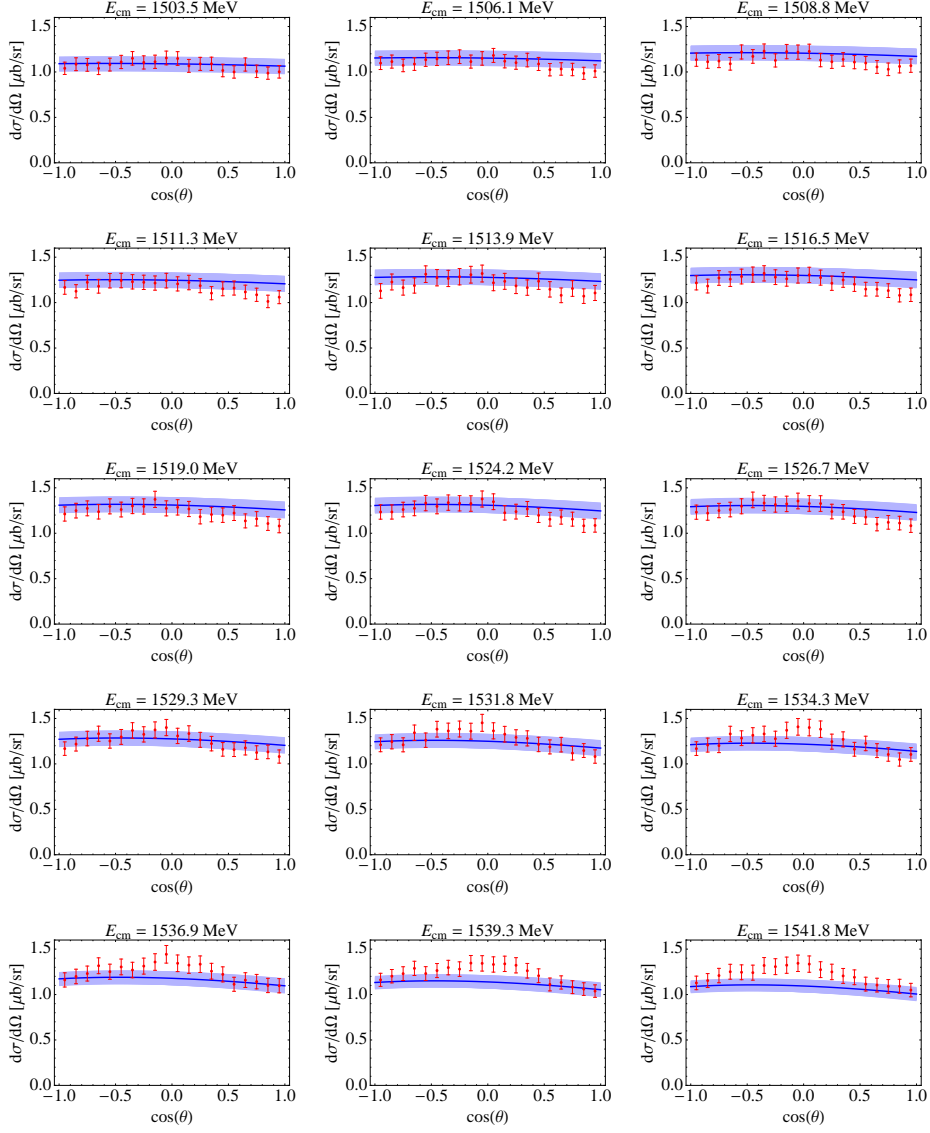
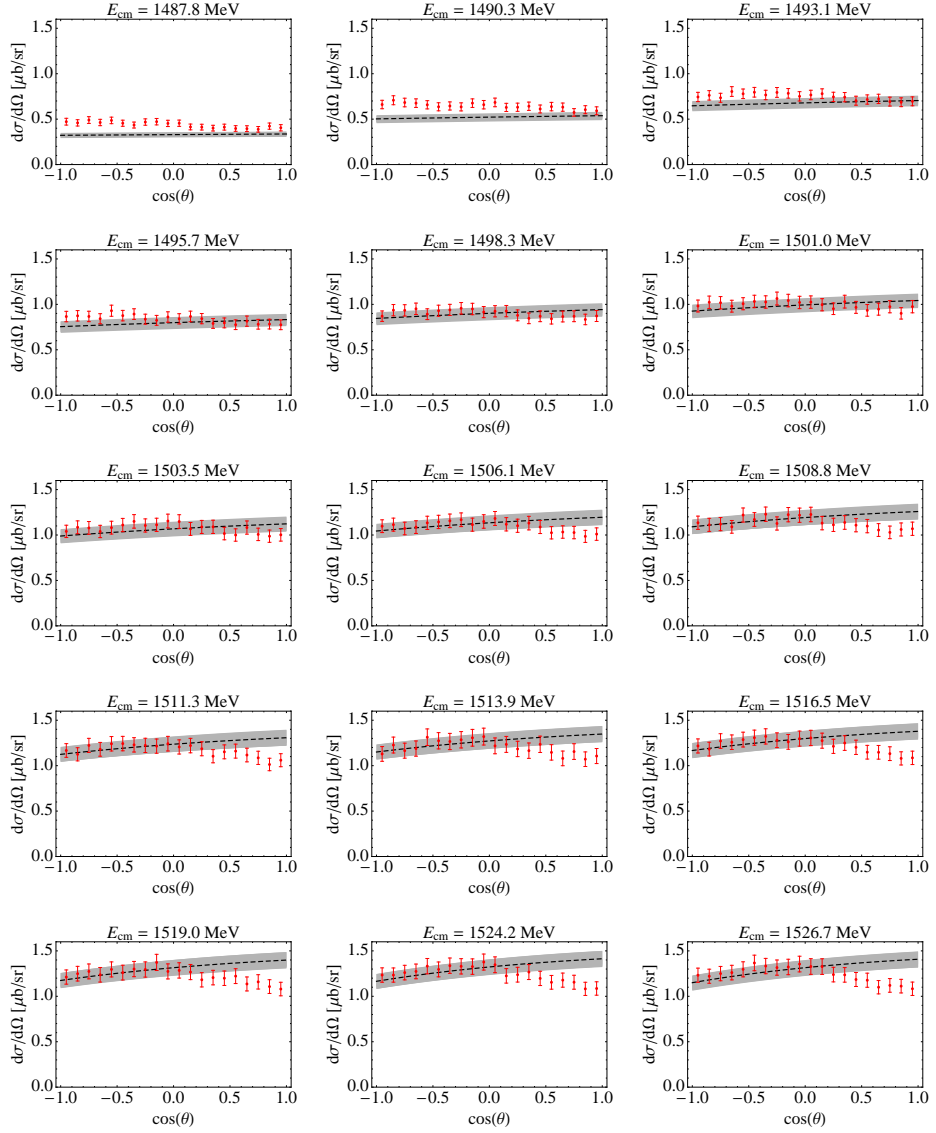


Figure F.2: Differential cross section of the model with NLO potentials evaluated in chapter 4 (blue line) fitted to the data points taken from McNicoll et al. [29] (red symbols) from threshold up to the center-of-mass energy $E_{\text{cm}} = \sqrt{s} = 1541.8$ MeV. The blue shaded area represents the error estimate.



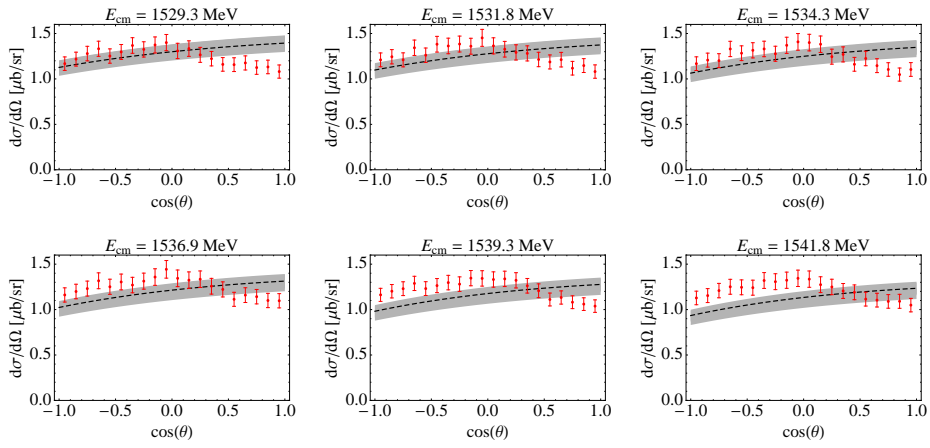


Figure F.3: Differential cross section of the model without NLO potentials evaluated in chapter 4 (black dashed line) fitted to the data points taken from McNicoll et al. [29] (red symbols) from threshold up to the center-of-mass energy $E_{\text{cm}} = \sqrt{s} = 1541.8$ MeV. The shaded area represents the error estimate.

Bibliography

- [1] S. Weinberg, *Physica A* **96** (1979) 327.
- [2] E.P. Wigner, *Phys. Rev.* **70** (1946) 15.
- [3] E.P. Wigner, L. Eisenbud. *Phys. Rev.* **72** (1947) 29.
- [4] Tran N. Truong, *Phys. Rev. Lett.* **61**, (1988) 2526; **67**, (1991) 2260.
- [5] B. Borasoy, P. C. Bruns, U.-G. Meißner, R. Nisler, *Eur. Phys. J. A* **34** (2007) 161.
- [6] W. Heisenberg, *Z. Phys.* **120** (1943), 513.
- [7] W. Heisenberg, *Z. Phys.* **120** (1943), 673.
- [8] S. Weinberg, *'The Quantum Theory of Fields. Vol. I: Foundations'*, Cambridge Univ. Pr. (2005).
- [9] G. F. Chew, *'The analytic S matrix: A basis for Nuclear Democracy'*, W. A. Benjamin Inc. (1966).
- [10] F. Gross, *'Relativistic Quantum Mechanics and Field Theory'*, Wiley-Interscience, 1993.
- [11] M. E. Peskin, D. V. Schroeder, *'An Introduction to Quantum Field Theory'*, Westview Press (1995).
- [12] R. L. Jaffe, *Nucl. Phys. A* **804** (2008) 25.
- [13] G. 't Hooft, *Phys. Rev. D* **14** (1976) 3432.
- [14] E. Witten, *Nucl. Phys. B* **234** (1979) 269.
- [15] J. Nieves, E. Ruiz Arriola, *Nucl. Phys. A* **679** (2000) 57.
- [16] C. Vafa and E. Witten, *Nucl. Phys. B* **234** (1984) 173.
- [17] Y. Nambu, *Phys. Rev. Lett.* **4** (1960) 380.
- [18] J. Goldstone, *Nuovo Cim.* **19** (1961) 154.

- [19] J. Goldstone, A. Salam, S. Weinberg, Phys Rev. **127** (1962) 965.
- [20] S. Scherer, M. R. Schindler, '*A Chiral Perturbation Theory Primer*', arXiv:hep-ph/0505265v1 (2005).
- [21] J. Gasser, H. Leutwyler, Annals Phys. **158** (1984) 142
- [22] M. Gell-Mann, R. J. Oakes and B. Renner, Phys. Rev. **175** (1968) 2195.
- [23] J. Gasser, M. E. Sainio, A. Svarc, Nucl. Phys. B **307** (1988) 779.
- [24] A. Krause, Helv. Phys. Acta **63** (1990) 3.
- [25] M. Frink and U.-G. Meißner, JHEP **0407** (2004) 028 [arXiv:hep-lat/0404018].
- [26] F. E. Close, R. G. Roberts, Phys. Lett. B **316** (1993) 165.
- [27] B. Borasoy, Phys. Rev. D **59** (1999) 054021.
- [28] P. C. Bruns, M. Mai, U.-G. Meißner, Phys. Lett B **697** (2011) 254.
- [29] E. F. McNicoll et al. , Phys. Rev. C **82** (2010) 035208.
- [30] CBELSA, TAPS Collaboration, Phys. Rev. C **80** (2009) 055202.
- [31] P. C. Bruns, '*Multi-scale chiral dynamics*', SVH (2010).
- [32] G. Höhler and H. Schopper, *Landolt-Börnstein, New Series, I/9B2, 501 P.*, Springer (1938)
- [33] R. A. Arndt, W. J. Briscoe, I. I. Strakovsky, R. L. Workman, Phys. Rev. C **74** (2006) 045205.
- [34] K. Nakamura et al. (Particle Data Group), Journal of Physics G **37**, (2010) 075021.
- [35] T. Inoue, E. Oset, M. J. Vicente Vacas, Phys. Rev. C **65** (2002) 035204.
- [36] J. Nieves, E. Ruiz Arriola, Phys. Rev. D **64** (2001) 116008.
- [37] T. Becher, H. Leutwyler, Eur. Phys. J. C **9** (1999) 643.
- [38] B. Kubis, U.-G. Meißner, Eur. Phys. J. C **18** (2001) 747.
- [39] F. A. Berends, A. Donnachie, D. L. Weaver, Nucl. Phys. B **4** (1967) 1.
- [40] G. F. Chew, M. L. Goldberger, F. E. Low, Y. Nambu, Phys. Rev. **106** (1957) 1345.